Hydrolysis of Amides and Phenylamide Pesticides at the Mineral-Water Interface

Dissertation

der Mathematisch-Naturwissenschaftlichen Fakultät

der Eberhard Karls Universität Tübingen

zur Erlangung des Grades eines

Doktors der Naturwissenschaften

(Dr. rer. nat.)

vorgelegt von

M.Sc. Tingting Chen

aus Shandong, China

Tübingen

2014

Tag der mündlichen Qualifikation:	26.11.2014
Dekan:	Prof. Dr. Wolfgang Rosenstiel
1. Berichterstatter:	Prof. Dr. Stefan B. Haderlein
2. Berichterstatter:	Prof. Dr. Christian Zwiener

Acknowledgements

First and foremost I would like to thank my supervisor, Prof. Dr. Stefan Haderlein, for giving me the chance of doing a Ph.D., and for his guidance, support, and great encouragements. Besides the academic adviser, he has also been a great mentor of my life. Thank Prof. Dr. Christian Zwiener, Prof. Dr. Olaf Cirpka and Prof. Dr. Peter Grathwohl for being on the defense committee. I am also very grateful to Prof. Dr. Olaf Cirpka and Dr. Chuanhe Lu for their help with the modeling setup in Chapter 3. Also thank Prof. Dr. Christian Zwiener for the insightful discussions about HPLC.

Then I would like to express my gratitude to Monika Hertel, Ellen Struve, Wolfgang Kürner and Dr. Thomas Wendel for experimental materials preparation, instrument maintenance, and a lot of practical support and help in the laboratory. I also sincerely thankful to Marion Schäffling, Eva Wolf, Dr. Wolfgang Bott, Dr. Peter Merkel for all their administrative help. In addition, thank Manuela Hoch and Willi Kappler for their computer technology support.

Many group members in Environmental Mineralogy & Chemistry have helped me immensely throughout my Ph.D. work. Thank Dr. Christine Laskov for showing me the laboratory in the beginning as well as many helpful discussions. I am also deeply grateful to my colleagues Satoshi, Phil, Anke, Michaela, Dijie, Chun-Chi, Dafina, Karin, Daniel, Katharina, Silvia, Tutrinh, Zhengrong, Shaojian…… and all other past and present group members, working with them made my Ph.D. experience meaningful and inspiring. Specially thank Yago Haußmann for the German version of abstract. My great acknowledgement also goes to many Ph.D. students of other groups, including Jie, Juanjuan, Ke, Zijie, Ronnie, Dennis and Dominik…… Besides, thank all my friends in Tübingen for much fun and good time we had.

Finally, I would like to thank my family for their unconditional love and constant support.

Sincere acknowledgement goes to German Research Foundation (DFG), which supported and funded this study as a part of project: SPP1315-Biogeochemical Interfaces in Soil.

Table of Contents

Abstract

In this study, batch experiments on the hydrolysis of pesticides or pesticide-like amides were performed at the mineral-water interface. The main goal is to elucidate the influence of minerals on surface mediated hydrolytic reactions of amides. First, the results show that hydrolysis of 4'- and 2'-nitrophthalanilic acid is intramolecular catalyzed reaction in acidic solutions (pH < 4.3). The neutral species are the active forms for the intramolecular catalysis. The mass loss was observed during the hydrolysis, and a by-product *N*-phenylphthalimide may be yielded. For all selected mineral suspensions of SiO_2, Al_2O_3, goethite, kaolinite, hectorite or Na-rich montmorillonite, the observed rate constants of 4'- and 2'-nitrophthalanilic acid at certain pH are of the same order of magnitude as those in the corresponding aqueous solution. Therefore, the investigated minerals have an insignificant effect on the intramolecular catalyzed hydrolysis of 4'- and 2'-nitrophthalanilic acid. In addition, no measurable adsorption was observed on mineral surfaces for 4'- and 2'-nitrophthalanilic acid as well as the hydrolysis products, 4- and 2-nitroaniline. Second, hydrolysis of *N*-methyl-*N*-(4-nitrophenyl)-2-pyridinecarboxamide (N-Me-PCA) in mineral suspensions as well as aqueous solutions is general base-catalyzed reaction throughout pH 9.5-11. Mineral surfaces have no strong effects on the hydrolysis of N-Me-PCA, the observed rate constants are only slightly lower in hectorite and Na-montmorillonite suspensions compared with aqueous solution and the other mineral suspensions. N-Me-PCA can adsorb on hectorite and Na-montmorillonite to different extent depending on suspension pH. Third, the hydrolysis of racemic metalaxyl and enantiopure metalaxyl-M in mineral suspensions was also investigated. The reaction kinetics and enantiomeric ratios of *R*- and *S*-enantiomer of metalaxyl were measured by enantioselective high performance liquid chromatography (HPLC). For racemic metalaxyl, the hydrolysis of *R*- and *S*-metalaxyl follows pseudo-first-order kinetics and is completely base-catalyzed reaction over pH 9.5-12 in aqueous solutions and mineral suspensions. Furthermore, hydrolysis of *R*- and *S*-metalaxyl occurs with retention of configuration. Although hydrolysis of *R*-metalaxyl is slightly faster than that of *S*-metalaxyl, the chemically mediated hydrolysis is basically nonenantioselective. Hydrolysis rate constants in mineral suspensions are similar to those in the corresponding aqueous solutions, suggesting an insignificant effect of minerals on metalaxyl hydrolysis. In the case of enantiopure metalaxyl-M, a computer model was developed using MATLAB® to describe different processes observed in the hydrolysis

experiments. The results show that in mineral suspensions and aqueous solutions over pH 9.5-11 the enantiopure *R*-metalaxyl is configurationally unstable and readily enantiomerizes to its antipode,*S*-metalaxyl, while the hydrolysis products, *R*- and *S*-MX-acid, are configurationally stable and do not interconvert to each other. The enantiomerization of *R*- and *S*-metalaxyl also follows first-order kinetics and is base-catalyzed reaction over pH 9.5-11. The rate constants for enantiomerization are in the range of 22-32% of those for hydrolysis. In addition, there is not much difference in rate constants of enantiomerization between aqueous solutions and mineral suspensions at the same pH, indicating unimportant influence of minerals on chiral conversion of metalaxyl enantiomers.

Zusammenfassung

In der vorliegenden Arbeit wurden Batch-Experimente durchgeführt um das Hydrolyseverhalten einer Reihe von Pestiziden oder pestizid-ähnlichen Amiden an der Wasser-Mineral-Grenzschicht zu untersuchen. Ziel war es, den Einfluss verschiedener Minerale auf die oberflächen-katalysierten hydrolytischen Reaktionen der Amide zu klären. Die Ergebnisse zeigen, dass die Hydrolyse von 4'- und 2'-Nitroanilin Phtalsäureamid in sauren Lösungen (pH < 4,3) intramolekular katalysiert wird und die neutralen Spezies die aktive Form für die intramolekulare Katalyse darstellen. Während der Reaktion wurde die Abnahme der Edukts sowie die Bildung von *N*-Phenylphthalimid als Nebenprodukt festgestellt. In allen ausgewählten Mineral-Suspensionen von SiO_2, Al_2O_3, Goethit, Kaolinit, Hektorit und Na-Montmorillionit sank die beobachtete Geschwindigkeitskonstante der Hydrolyse von 4'- und 2'-Nitroanilin Phtalsäureamid mit steigenden pH-Werten. Alle so beobachteten Geschwindigkeitskonstanten unterscheiden sich somit nur unwesentlich von der Geschwindigkeitskonstante der Hydrolyse in reiner Lösung. Demnach haben die untersuchten Minerale keinen signifikanten Effekt auf die intramolekular katalysierte Hydrolyse von 4'- und 2'-Nitroanilin Phtalsäureamid. Außerdem konnte keine messbare Adsorption beobachtet werden, weder für 4'- und 2'-Nitroanilin Phtalsäureamid, noch für die Hydrolyseprodukte 4'- und 2'-Nitroanilin. Die Hydrolyse von *N*-methyl-*N*-(4-nitrophenyl)-2-pyridinecarboxamide (N-Me-PCA) hingegen ist sowohl in Anwesenheit der Minerale, als auch in homogenen Lösungen eine basisch katalysierte Reaktion zwischen pH 9,5-11. Auch in diesem Fall konnte nur ein minimaler Einfluss der Minerale auf die Hydrolyse von N-Me-PCA festgestellt werden. Die beobachteten Geschwindigkeitskonstanten in Anwesenheit von Hektorit und Na-Montmorillionit waren nur geringfügig kleiner als in den anderen Mineral-Suspensionen oder wässrigen Lösungen. N-Me-PCA adsorbiert an Hektorit und Na-Montmorillionit in unterschiedlichem Ausmaß, abhängig vom pH-Wert der Lösung. Schließlich wurde auch die Hydrolyse von razemischen Metalaxyl und seinem reinen R-Enantiomer in Mineral-Suspensionen untersucht. Dabei wurde die Reaktionskinetik und die enantiomerischen Anteile von *R*- und *S*-Enantiomeren des Metalaxyl mit enantioselektiver HPLC (High Performance Liquid Chromatography) gemessen. Bei dem razemischen Metalaxyl folgte die Hydrolyse von R- und S-Metalaxyl einer Kinetik pseudo-erster Ordnung und ist über einen pH-Wert von 9,5-12 vollständig basisch katalysiert, sowohl in wässriger Lösung als auch in den Mineral-Suspensionen. Beide

Enantiomere ändern ihre Konfiguration während der Hydrolyse nicht. Auch wenn die Hydrolyse des *R*-Metalaxyl über einen pH-Wert zwischen 9,5-12 minimal schneller ist als die Hydrolyse des *S*-Metalaxyl, kann von einer nicht-enantioselektiven chemischen Hydrolyse gesprochen werden. Die Geschwindigkeitskonstanten von wässriger Lösung und Mineral-Suspension sind bei gleichem pH-Wert kaum unterschiedlich, was einen insignifikanten Einfluss des Minerals auf die Hydrolyse vermuten lässt. Für das enantiomerenreine *R*-Metalaxyl wurde ein Reaktionsmodell mit MATLAB® aufgestellt, um verschiedene beobachtete Prozesse während des Experiments zu beschreiben. Die Ergebnisse zeigen, dass das reine *R*-Metalaxyl in Mineral-Suspensionen bei pH-Werten zwischen 9,5-11 strukturell instabil wird und zu *S*-Metalaxyl enantiomerisiert, während die Hydrolyse-Produkte *R*- und *S*-MX-Säure strukturell stabil bleiben und sich nicht ineinander wandeln. Die Enantiomerisierung des *R*- und *S*-Metalaxyl ist eine Reaktion erster Ordnung und basisch katalysiert. Die Geschwindigkeitskonstanten der Enantiomerisierung liegen bei 22-32% der Geschwindigkeitskonstante der Hydrolyse. Zudem gibt es keine signifikanten Unterschiede in der Rate der Enantiomerisierung zwischen der wässrigen Lösung und der Mineral-Suspensionen bei gleichem pH, was auf einen geringen Einfluss der Minerale auf die chirale Umwandlung der Metalaxyl-Enantiomere schließen lässt.

1. Introduction

1.1 Pesticides

Pesticides are defined in many different ways depending on some specific features. One widely accepted definition is given by the Food and Agriculture Organization (FAO) as:

Pesticide means any substance or mixture of substances intended for preventing, destroying or controlling any pest, including vectors of human or animal disease, unwanted species of plants or animals causing harm during or otherwise interfering with the production, processing, storage, transport, or marketing of food, agricultural commodities, wood and wood products or animal feedstuffs, or substances which may be administered to animals for the control of insects, arachnids or other pests in or on their bodies. The term includes substances intended for use as a plant growth regulator, defoliant, desiccant, or agent for thinning fruit or preventing the premature fall of fruit, and substances applied to crops either before or after harvest to protect the commodity from deterioration during storage and transport (FAO 2002).

Pesticides can be classified in many different ways. According to the type of pest they control, pesticides can be classified as insecticides, fungicides, herbicides, algicides, fumigants, nematicides, rodenticides, repellents, etc., and based on the production method or source, pesticides can be referred to as chemical pesticides, biopesticides, antimicrobials and pest control devices (EPA). Some widely used chemically-related pesticides include organophosphate pesticides, carbamate pesticides, organochlorine insecticides, pyrethroid pesticides and sulfonylurea pesticides (EPA). In addition, the products can be grouped into liquids, solids, or gases according to their formulation (Pleština 2003). There are a large number of pesticides currently in use, e.g., in both 2006 and 2007, there are approximately 5.2 billion pounds of pesticides used in the world, with herbicides accounted for the largest part (40% of total use), followed by other pesticides (33%), insecticides (17%), and fungicides (10%) (Grube, Donaldson et al. 2011).

Pesticides have made substantial contributions to the modern agricultural production system, e.g., improving yields and quality of crops, reducing the contamination of food by toxic fungi and controlling insects that spread diseases (Craven, Garratt et al. 2007).

On the other hand, pesticide use has caused growing concern over the environment, natural resources, and human health (Rosenfeld and Feng 2011). It is reported that instead of their intended target species over 98% of insecticides and 95% of herbicides reach other destinations including non-target species, air, water and soil (Miller 2004). Applied pesticides can reach surface water (e.g., rivers, lakes and reservoirs) and ground water through runoff and leaching from treated fields (Rosenfeld and Feng 2011). For example, pesticide contamination of water is widespread in the US, the results of the National Water-Quality Assessment (NAWQA) Program implemented by the U.S. Geological Survey (USGS) show that one or more pesticides or their degradation products are detected in water more than 90% of the time during the year in streams for agricultural or urban land and 65% of the time in undeveloped streams (Gilliom, Barbash et al. 2006). Pesticides are also frequently detected in ground water. The reports by USGS indicate that pesticides are detected in more than 50% of the shallow wells sampled in agricultural and urban areas (Gilliom, Barbash et al. 2006). In addition, some pesticides (e.g., organochlorine insecticides including aldrin, chlordane, DDT, dieldrin, heptachlor et al.) are persistent organic pollutants and may cause substantial risk on human, animal and the environment. Therefore, it is important to evaluate the environmental behavior of pesticides before their widespread use or release, to assess the ecological risk they may pose, and to understand the principles of pesticide transport and fate in the environment.

1.2 Minerals

Soils are complex materials consisting of solids, liquids and gases. More than 90% of the soil solid is inorganic component, which includes both primary and secondary minerals with particle size ranging from clay-sized colloids (<0.002 mm) to gravel (>2 mm) and rocks (Sparks 2003). Depending on their particular properties (e.g., particle size, surface area and charge behavior), the inorganic components of soil significantly influence many physical and chemical reactions and processes occurring in soil. Examples of the important primary minerals in soil are quartz and feldspar. They mainly occur in the sand and silt fractions of soils and can also be found in weathered clay fractions. On the other hand, examples of the common secondary minerals in soil are phyllosilicates (e.g., kaolins and smectites) and oxides (e.g., gibbsite and goethite), which occur primarily in the clay fraction of the soil (Sparks 2003).

1.2.1 Oxide Minerals

The oxide minerals present in soils generally include oxides, hydroxides, oxyhydroxides, and hydrated oxides of silicon, iron, aluminum, manganese and titanium (Scheinost 2005). Typically, the oxides have simpler structure than phyllosilicates, containing hexagonal or cubic close-packed O^{2-} and/or OH^- anions with Fe^{3+}, Al^{3+}, Mn^{4+} or Mn^{3+} occupying in octahedral sites (McBride 1994). Some metal oxides, e.g., iron and aluminum oxides, have high specific surface areas and reactivity, which may exhibit significant effects on many processes (e.g. sorption and redox reaction) occurring in soil and therefore influence the availability and mobility of agrochemicals (Sparks 2003, Scheinost 2005).

1.2.1.1 Goethite

Goethite (named after Johann Wolfgang von Goethe), α-FeOOH, occurs in rocks and throughout the various compartments of the global ecosystem. It has a well-defined crystal structure, which is isostructural with diaspora (α-AlOOH) based on hexagonal close packing of anions (O^{2-} and OH^-). Goethite is one of the most thermodynamically stable Fe^{III} oxide phases under ambient conditions and is, therefore, either the first oxide to form or the end member of many transformations. Goethite is dark brown or black in massive crystal aggregates, whereas the powder is yellow and responsible for the vivid colors of many rocks, soils and ochre deposits. Goethite is also an industrially important pigment (Cornell and Schwertmann 2004). In aqueous environment, the surface of iron oxide is covered by hydroxyl groups, which may arise from adsorption of water or from structural hydroxyl groups. The functional groups of iron oxides, i.e. the surface hydroxyl groups, are chemically reactive and can interact with gaseous and soluble species (Cornell and Schwertmann 2004). The available sites (functional groups) per unit mass of iron oxide depend on the nature of the oxide and also on its specific surface area. The surface area can affect reactivity (e.g. dehydroxylation), interaction with sorbents and phase transformations of the iron oxide (Cornell and Schwertmann 2004).

1.2.1.2 Aluminum Oxide

Aluminum, which constitutes approximately 8.8% by mass of crustal rocks, is the most abundant metallic element and the third most abundant element in the crustal regions of the Earth (Büchel, Moretto et al. 2000, Atkins and Overton 2010). In nature, it mainly occurs as oxides in numerous minerals and aluminosilicates. There are several forms

of aluminum oxide: (i) α-alumina (corundum), (ii) activated alumina, e.g., γ-alumina, η-alumina and ρ-alumina, (iii) hydrated alumina such as $Al_2O_3 \cdot H_2O$ and $Al_2O_3 \cdot 3H_2O$ (natural gibbsite) and (iv) acidic, neutral and basic alumina (Patnaik 2003). Alpha-alumina is a very hard and refractory material and its mineral form known as corundum which is used to produce precious gems (e.g. ruby and sapphire). The structure of α-alumina is comprised of hexagonal close packing of O^{2-} ions with Al^{3+} ions occupying two-thirds of the octahedral sites in an ordered array (Atkins and Overton 2010). Activated alumina is extensively used as adsorbent and catalyst because of their large surface area, appropriate pore structure and affinity for water and other polar molecules (Patnaik 2003).

1.2.1.3 Silicon Dioxide

Silicon dioxide, SiO_2, is also known as silica and presents almost everywhere on earth. As one of the most important and abundant oxides on earth, SiO_2 makes up about 60% weight of the earth's crust as silica itself or in association with other metal oxides in silicates (Patnaik 2003). It is available in several structural forms: polymorphic crystalline silica, synthetic quartz crystals, amorphous silica, and vitreous silica (Patnaik 2003). There are three polymorphic forms of crystalline silica occurring at atmospheric pressure, i.e. Quartz, tridymite, and cristobalite, and each is stable within a characteristic temperature range. Quartz is stable below 870°C and has two different atomic arrangements, i.e. alpha and beta quartz. Alpha quartz is the most common type of silica and possesses a high commercial value (Patnaik 2003). Amorphous silica lacks crystal structure and does not form a sharp x-ray diffraction pattern. They are commonly aggregates of small particles with high specific surface area. There are several forms of amorphous silica, e.g. colloidal silica, precipitated silica, silica gels, and fumed silica. The surface of amorphous silica may contain silanol (SiOH) groups or can be anhydrous. In nature, amorphous silica may arise from aquatic organisms occurring in the form of shells, plates, or skeletons. Amorphous silica is also identified in volcanic ash or in precipitated material from the hot supersaturated waters of hot springs (Patnaik 2003). Vitreous silica is a glass form of silica. It can be transparent, translucent, or opaque and exhibits high resistance to chemical attack. At ambient temperature, it is not attacked by any chemicals except hydrofluoric acid. Silica has been extensively used in industry, such as the building materials and raw materials of all types of glasses. Amorphous silica can be used as an abrasive, absorbent and catalyst support, e.g., silica gel, a common desiccant and adsorbent, is used as

packing material in chromatography columns and in clean-up of organic extracts to remove interference (Patnaik 2003).

1.2.2 Clay Minerals

Clay mineral refers to a group of hydrated phyllosilicates that constitute the fine-grained fraction of rocks, sediments and soils (Bergaya and Lagaly 2006). Clay minerals are characterized by their different crystal structures, which give rise to a series of unique physical and chemical properties. The structure of clay mineral is comprised of two basic units, i.e., an octahedral sheet and a tetrahedral sheet. In the tetrahedral layer, four oxygen atoms coordinate with the center silicon atom forming a tetrahedron, which can link to adjacent ones by sharing three corner oxygen atoms to form an infinite two-dimensional hexagonal network. In the octahedral sheet, closely packed oxygen and hydroxyls coordinate with aluminum, iron and magnesium atoms to form an octahedron, which connects the neighboring ones by sharing edges (Brigatti, Galan et al. 2006, Murray 2006). Common cations in tetrahedral sheet are Si^{4+}, Al^{3+}, and Fe^{3+}, and those in octahedral sheet are Al^{3+}, Fe^{3+}, Mg^{2+} and Fe^{2+}, but the cations of other transition elements, e.g., Li^{+}, Mn^{2+}, Co^{2+}, Ni^{2+}, Cu^{2+}, and Zn^{2+} can also occur (Brigatti, Galan et al. 2006). When the octahedral sheet is dominantly occupied by trivalent aluminum cations, only two-thirds of octahedral sites are filled in order to maintain the charge balance, and the resulting mineral is defined as dioctahedral. On the other hand, when divalent magnesium cations are predominant cations, all three positions are occupied to balance the charge and the mineral is accordingly referred to as trioctahedral (Murray 2006, Theng 2012). All apical oxygen atoms of the silica tetrahedrons point to the same direction and form a common plane with the octahedral anions (e.g., OH^{-} and O^{2-}), by which the tetrahedral sheet and the octahedral sheet are joined (Brigatti, Galan et al. 2006). Accordingly, there are two types of clay minerals, 1:1 and 2:1 layer structure, depending on the number of tetrahedral and octahedral sheets in the layer structure (Schulze 2005). The 1:1 layer structure is composed of the repetition of one tetrahedral and one octahedral sheet, while in the 2:1 layer structure one octahedral layer is sandwiched between two tetrahedral layers (Brigatti, Galan et al. 2006). The common 1:1 phyllosilicates are kaolin and serpentine group, while 2:1 phyllosilicates include pyrophyllite, talc, micas, smectites, vermiculite and chlorite (Brigatti, Galan et al. 2006). Due to different arrangement and composition of the tetrahedral and octahedral sheets, each type of clay minerals has its particular physical and chemical properties.

1.2.2.1 Kaolinite

Kaolinite is common in soils and tends to be particularly abundant in more weathered soils (Schulze 2005). It is also the most common clay mineral in the kaolin group, which comprises dioctahedral 1:1 layer structure with a general formula $Al_2Si_2O_5(OH)_4$ (Brigatti, Galan et al. 2006). The 1:1 layer of kaolinite is electrically neutral and stacked above each other. Any two neighboring layers are combined by hydrogen bonding between basal oxygen atoms of the tetrahedral sheet and hydroxyl groups of the exterior plane of the octahedral sheet (Schulze 2005). There is very little isomorphic substitution either for silicon in the tetrahedral sheet or for aluminum in the octahedral sheet, which accounts for some properties of kaolinite, e.g. minimal layer charge, very low cation exchange capacity and relatively low surface area (Murray 2006).

1.2.2.2 Smectite

There are several types of smectite minerals, including sodium montmorillonite, calcium montmorillonite, saponite (magnesium montmorillonite), nontronite (iron montmorillonite), hectorite (lithium montmorillonite), and beidellite (aluminum montmorillonite) (Murray 2006). Smectites are 2:1 layer minerals which consist of two silica tetrahedral sheets, one sandwiched octahedral sheet, and hydrated cations in the interlayer space. The tetrahedral, octahedral and interlayer positions can be occupied by a wide range of cations, for instance, Si^{4+}, Al^{3+}, and Fe^{3+} generally occupy tetrahedral sheet, while Al^{3+}, Fe^{3+}, Fe^{2+}, Mg^{2+}, Ni^{2+}, Zn^{2+}, and Li^{+} are commonly found in octahedral sheet (Brigatti, Galan et al. 2006). If the octahedral sites are dominantly occupied by aluminum, the smectite mineral is beidellite; if occupied by iron, the particular species is nontronite; and if by magnesium, the species is saponite (Murray 2006). Montmorillonite is a dominantly dioctahedral smectite. Hectorite is a rare clay but it is predominantly trioctahedral with Mg^{2+} and Li^{+} occupying the octahedral sites (Huggett 2005). In smectites, there is considerable substitution of Fe^{3+}, Fe^{2+}, and Mg^{2+} for Al^{3+} in octahedral sites and some substitution of Al^{3+} for Si^{4+} in tetrahedral sites, which both create an excess of negative charge (Brigatti, Galan et al. 2006, Murray 2006). This net negative layer charge is balanced by the interlayer cations, e.g., Ca^{2+}, Mg^{2+}, Na^{+}, or K^{+}. If the interlayer cation is calcium, the corresponding smectite mineral is calcium montmorillonite; if it is sodium, the mineral is sodium montmorillonite (Murray 2006). Sodium montmorillonite has one water layer in the interlayer position, however, calcium montmorillonite generally has two water layers. This gives rise to the basal

spacing of sodium montmorillonite being about 12.3 Å and that of calcium montmorillonite being about 15 Å (Grim and Güven 1978, Murray 2006). An important characteristic of smectites is their swelling capacity, i.e., expand and shrink with the addition or loss (through heating) of water and some organic molecules (Huggett 2005). The characteristics of each specific smectite are different depending on their structure and composition. Sodium montmorillonite and hectorite have high cation exchange capacity, which normally ranges from 80 to 130 meq/100 g; whereas calcium montmorillonite has medium cation exchange capacity ranging from 40 to 70 meq/100 g (Murray 2006). Basically, smectites have very fine particle size and high surface area, e.g., the surface area of sodium montmorillonite normally being about 150-200 m^2/g. The high layer charge and high surface area also account for the high sorptive capacity and high viscosity of sodium montmorillonite. Additionally, sodium montmorillonite and hectorite are excellent suspending agents due to a unique property, thixotropy, which is the ability to become fluid when stirred or shaken and return to a gel upon standing (Huggett 2005).

1.3 Interactions of Pesticides with Minerals

Pesticides have been playing an important role in the development of modern agriculture. By controlling pests, plant diseases and other harmful organisms, the uses of pesticides have largely improved crop yields and quality. However, in recent years pesticide residues have been detected in soil, surface and/or ground water, foods and even animal tissues. This phenomenon has raised great environmental concern. As pesticides are still widely used for crop protection, the potential effects on the environment as well as humans and animals should be taken into account.

Soil is the main compartment for disposition of pesticides since most of agrochemicals finally reach the soil once they are applied (Cornejo, Celis et al. 2004). Pesticides present in the soil can proceed a large number of processes such as sorption, hydrolysis, photolysis, redox reaction, microbial degradation and other abiotic or biotic reactions, which mainly depend on characteristics of pesticides, soil properties, and the environmental conditions. Water hydrolysis is a very important transformation process because most pesticides eventually arrive in solution or in the sediments of rivers, lakes, and/or oceans (Bailey, Clark et al. 2002). This process involves a nucleophile (e.g., H_2O or OH^-) attacking a more electron deficient atom (e.g., carbon or phosphorus) of a hydrolysable moiety in organic molecules and inducing the leaving

group exit (Vallero 2004). Many pesticides contain the functional groups that are susceptible to hydrolysis, for example, organic halides, esters, amides, carbamates, urea derivatives, phosphoric acid esters and thioesters (McBride 1994). This partial decomposition of pesticides by hydrolysis often makes the molecule more soluble in water, thus more susceptible to degradation by microorganisms (Bailey, Clark et al. 2002).

Hydrolysis of organic chemicals can be catalyzed by acid or base, dissolved metal species, metals oxides, clay minerals and organic matter (Plastourgou and Hoffmann 1984, Joo, Eberlein et al. 2008). Metal ions may affect hydrolysis of organic chemicals in different ways, particularly three catalysis mechanisms have been proposed in literature: (1) metal ion coordination of the hydrolysable moiety to facilitate the attack of a nucleophile (e.g., H_2O, OH^-); (2) metal ion coordination of water and consequent deprotonation to form a nucleophile; (3) metal ion coordination of the leaving group to promote its dissociation (Smolen and Stone 1997, Schwarzenbach, Gschwend et al. 2005). For example, Smolen and Stone (1997) reported hydrolysis of thionate and oxonate organophosphorus pesticides catalyzed by divalent metal ions, and found that Cu^{II} possesses most suitable properties for all three catalysis mechanisms and acts as a much better catalyst than other divalent metal ions examined (Co^{II}, Ni^{II}, Zn^{II}, Pb^{II}) for thionate esters and oxonate esters, e.g., the hydrolysis of one thionate ester chlorpyrifos-methyl has been enhanced by more than two orders of magnitude in the presence of 1.0 mM Cu^{II} at pH 5-7. Moreover, large rate enhancements have also been observed in metal ion promoted water or hydroxide ion catalyzed hydrolysis of esters and amides (Fife and Squillacote 1978, Przystas and Fife 1990, Tang and Sayre 1993). However, the hydrolytic reaction of a compound may not be always promoted, in some cases, the reaction can also be inhibited. For instance, Huang and Stone (1999) have reported metal ions (Cu^{II} and Zn^{II}) prevent the hydrolysis of pesticide naptalam (N-1-naphthylphthalamic acid). The observed inhibition is attributed to two mechanisms: (1) metal ion coordination of the carbonyl group of naptalam, which results in deprotonation of the amide group and makes the compound less susceptible toward nucleophilic attack; (2) metal ion coordination of the free carboxylate group of naptalam, which prevents the intramolecular nucleophilic attack. Therefore, metal ions can influence both the mechanisms and the rates of organic compounds hydrolysis, and different metals have different catalytic or inhibitory effects on hydrolysis (Schwarzenbach, Gschwend et al. 2005).

Similarly, the hydrolytic reaction may also be catalyzed or in some cases inhibited due to lattice-bound metal atoms coordination with organic molecules at mineral surface (Schwarzenbach, Gschwend et al. 2005). As a good example, Torrents and Stone (1991) have reported hydrolysis of phenyl picolinate at the mineral-water interface. Significant enhancement of the rate of phenyl picolinate hydrolysis has been observed in goethite (FeOOH) and anatase (TiO_2) suspensions. However, no surface catalyzed hydrolysis occurs in silica (SiO_2), γ-aluminum oxide (γ-Al_2O_3) and hematite (Fe_2O_3) suspensions. The catalytic effect is attributed to surface-bound metal coordination with the carbonyl oxygen via a chelate formation, which involves the two ligand donor groups (carboxyl oxygen and pyridinal nitrogen) of phenyl picolinate and surface metal centers. Such a complex can activate the carbonyl carbon toward the nucleophilic attack analogous to the effects of metal ions. The characteristics and relative positions of the donor groups in organic molecule play an important role in surface catalyzed reaction, e.g., hydrolysis of the isomeric phenyl isonicotinate, which cannot form a surface chelate, is not catalyzed by any of the oxide surfaces investigated. Furthermore, Torrents and Stone (1994) have also reported carboxylate esters, which possess an auxiliary oxygen ligand, are subjected to oxide surface-catalyzed hydrolysis. Analogous to the above-mentioned nitrogen ligand in phenyl picolinate, the auxiliary oxygen ligand as well as the carbonyl oxygen group in esters can form a chelate with surface metal centers and facilitate the reaction, for example, hydrolysis of phenyl salicylate is catalyzed at Al_2O_3, TiO_2, and FeOOH surfaces. In addition, hydrolysis of phosphorothionate pesticides can also be accelerated by metal oxide surface (Torrents and Stone 1994), e.g., methyl chlorpyrifos possessing an auxiliary nitrogen ligand is more susceptible to surface-catalyzed hydrolysis compared with methyl parathion and ronnel which do not possess an appropriate auxiliary donor group. However, methyl parathion and ronnel are also subjected to surface-catalyzed hydrolysis, indicating that chelate formation may not be necessary for surface catalysis. Moreover, Smolen and Stone (1998) reported TiO_2 is more effective than Al_2O_3 and α-FeOOH with regard to surface-catalyzed hydrolysis of chlorpyrifos-methyl thionate and oxonate esters.

In addition to metal oxides, clay minerals are also important catalysts for surface-catalyzed reaction of pesticides in soil. First, clay minerals play an important role in sorption of pesticides in soil due to their particular physical and chemical properties. Because of the isomorphic substitutions involving cations of lower positive charge (e.g., Al^{3+} for Si^{4+}, Fe^{2+} or Mg^{2+} for Al^{3+}) in the internal structure, clay minerals exhibit a

negative surface charge to the surrounding aqueous solution (Schwarzenbach, Gschwend et al. 2005). Therefore, organic cations can be adsorbed to clay minerals through ion exchange processes (Cornejo, Celis et al. 2004). For example, sorption of triorganotin biocides (TOTs, e.g. organotin pesticides triphenyltin and tributyltin) onto mineral surfaces is attributed to cation exchange of the TOT^+ species with negatively charged surface sites (Weidenhaupt, Arnold et al. 1997). On the other hand, clay minerals only weakly retain organic anions through anion exchange, which usually takes place on the edges of aluminosilicate layers (Churchman, Gates et al. 2006). Owing to the hydrophilic characteristics caused by hydration water of exchangeable cations, sorption of nonionic organic compounds to clay minerals is often considered to be reduced (Cornejo, Celis et al. 2004). However, high surface areas and large pore volumes may enable clay minerals to adsorb nonionic organic chemicals significantly under certain conditions (Churchman, Gates et al. 2006). Sorption of nonionic substances to mineral surfaces has been observed in many studies (Schwarzenbach and Westall 1981, Estes 1988, Haderlein and Schwarzenbach 1993, Schlautman and Morgan 1994, Haderlein, Weissmahr et al. 1996, Mader, Uwe-Goss et al. 1997, Hundal, Thompson et al. 2001). For example, Hundal et al. (2001) found the reference smectites can adsorb considerable phenanthrene(a polycyclic aromatic hydrocarbon) from water. A possible mechanism was proposed that the small platelets of smectites can form a network of quasicrystals with nano- or micropores to retain phenanthrene. They have also suggested the nature of apolar phenanthrene binding to smectites is mainly a physical process which is not related to charge characteristics or hydration of minerals. Nevertheless, some nonionic organic chemicals have a strong specific interaction with clay mineral surfaces (Schwarzenbach, Gschwend et al. 2005), e.g., electron donor-acceptor (EDA) complex formation with oxygens at the external siloxane surface of clay mineral is considered to account for the specific adsorption of nitroaromatic compounds (NACs) (Haderlein and Schwarzenbach 1993, Haderlein, Weissmahr et al. 1996).

Layer structures and surface characteristics of clay minerals greatly influence the sorption of organic chemicals. A wide variety of interactions occur between organic substances and 2:1 clay minerals: polar organic compounds can displace interlayer water molecules of hydrated smectites and vermiculites; cationic organic chemicals exchange with the interlayer cations; and neutral organic molecules can interact with mineral surface by hydrogen bonds, coordination bonds, acid-base reactions, charge

transfer, and van der Waals forces (Lagaly, Ogawa et al. 2006). For example, P. Fusi et al. (1988) reported herbicide Fluazifop-butyl penetrates into the interlayer space of smectites and is adsorbed by direct coordination or through a water bridge between its C=O group and the exchangeable cation. The herbicide alachlor is also showed to be adsorbed onto Na-montmorillonite by replacing the interlayer water of clay minerals (Nasser, Gal et al. 1997). Compared with expandable 2:1 clay minerals, 1:1 clay minerals generally show a lower affinity for organic compounds, e.g. intercalation of organic molecules only occurring for kaolin species (Lagaly, Ogawa et al. 2006). In addition, the surface cations of clay minerals play an important role in the sorption of organic molecules. For instance, the strength of NACs adsorption on kaolinite is dependent upon the type of cations adsorbed to the siloxane surface: only very weak specific adsorption is observed in the presence of strongly hydrated cations (e.g., Li^+, Na^+, Ca^{2+}, Mg^{2+} or Al^{3+}), while kaolinites saturated with more weakly hydrated cations (e.g., NH_4^+, K^+, Rb^+, Cs^+) show a larger affinity for NACs (Haderlein and Schwarzenbach 1993). Similar results are found for other clay minerals such as illite and montmorillonite (Haderlein, Weissmahr et al. 1996). U. Herwig et al. (2001) reported hydrolysis constant of the exchangeable cation determines adsorption constant of herbicide atrazine, and the adsorption capacity of Fe^{3+} -montmorillonite is considerably higher than that of Cu^{2+}, Ni^{2+}, Ca^{2+} or Na^+ -montmorillonite.

Interaction with mineral surfaces has an important effect on the rate and pathway of organic compounds transformation, e.g. surface catalyzed hydrolysis of phenyl picolinate at metal oxide surface (Torrents and Stone 1991). Similarly, sorption on clay minerals may also influence the hydrolytic reaction of organic chemicals. For instance, depending on the exchangeable cations, hydrolysis of herbicide fenoxaprop-ethyl in montmorillonite suspensions occurs by different mechanisms (Pusino, Petretto et al. 1996): on the one hand, coordination of carbonyl oxygen of fenoxaprop-ethyl to the surface metal ions facilitates the ester bond hydrolysis in Ca^{2+} or Na^+ saturating montmorillonite; on the other hand, at Fe^{3+}- or Al^{3+}-montmorillonite surface the ether group cleavage of fenoxaprop-ethyl is favored by protonation of the benzoxazole ring nitrogen. Wei et al. (2001) also reported the influence of clay minerals on carbamate pesticides hydrolysis. Their results show that montmorillonite plays a more important role in the hydrolysis of carbamate pesticides than beidellite, illite, or vermiculite, e.g., the strong sorption of chlorpropham on montmorillonite significantly prevents the hydrolysis, while the hydrolysis of carbosulfan is promoted by montmorillonite due to

surface acidity and/or surface chelate mechanism. Nevertheless, significant sorption is not necessary for surface catalysis, for example, the hydrolysis of aldicarb is accelerated by montmorillonite although the sorption of that on mineral is insignificant (less than 5%).

1.4 Scope of the Study

Depending on the physical and chemical characteristics of mineral, the properties of pesticides and the environmental conditions, mineral surfaces may substantially affect both kinetics and mechanisms of pesticides hydrolysis in soil. Therefore, we are going to address the following questions in this work: (i) can the large rate enhancements for hydrolysis of some amides by dissolved metal ions also occur at mineral surfaces, (ii) how do the functional groups of organic compounds affect the surface mediated reaction, (iii) is the hydrolysis of chiral pesticides at mineral surfaces stereo-selective, and (iv) does the adsorption on minerals play an important role in surface-catalyzed (or inhibited) hydrolysis. Answering these questions will improve the understanding of pesticides abiotic transformation in soil.

To address the above open questions, batch experiments with a series of pesticides or pesticide-like amides (see Table 1.1) are performed at the mineral-water interface. The overall goal of this study is to elucidate the effects of minerals on surface mediated hydrolytic reactions of amide pesticides. The selected minerals are representative oxides and clay minerals present in A and B horizons of natural soils, including amorphous silica, aluminum oxide, goethite, kaolinite, hectorite and Na-rich montmorillonite. More specifically, the main objectives are (i) to qualify and quantify the model amides as well as their hydrolysis products in homogeneous and heterogeneous conditions, (ii) to investigate the kinetics and mechanisms of amide hydrolysis in aqueous solutions and mineral suspensions, (iii) to evaluate how sorption and other interactions with mineral surface affect the rate, mechanism, and product spectrum of amide hydrolysis, and (iv) to study the stereo-selectivity of chiral pesticides hydrolysis at mineral surface.

Table 1.1. Properties of the Investigated Amides and Pesticides [a]

CA Index Name	Molecular Formula	Molecular Weight	CAS Registry Number	Density (g/cm^3)	Mass Solubility (g/L, at pH 7 & 25 ℃)	pK_a
Benzoic acid, 2-[[(4-nitrophenyl)amino]carbonyl]-	$C_{14}H_{10}N_2O_5$	286.24	6307-10-4	1.485	240	3.39
Benzoic acid, 2-[[(2-nitrophenyl)amino]carbonyl]-	$C_{14}H_{10}N_2O_5$	286.24	6307-12-6	1.485	210	3.41
2-Pyridinecarboxamide, N-methyl-N-(4-nitrophenyl)-	$C_{13}H_{11}N_3O_3$	257.24	134847-69-1	1.340	0.36	1.62
Alanine, N-(2,6-dimethylphenyl)-N-(2-methoxyacetyl)-, methyl ester	$C_{15}H_{21}NO_4$	279.33	57837-19-1	1.117	0.31	1.41
D-Alanine, N-(2,6-dimethylphenyl)-N-(2-methoxyacetyl)-, methyl ester	$C_{15}H_{21}NO_4$	279.33	70630-17-0	1.117	0.31	1.41

[a] All the property values are from SciFinder® of CAS.

1.5 Thesis Outline

This dissertation consists of the following chapters:

- Chapter 1 presents a general introduction about the background of this study, the objectives and structures of the thesis.
- In Chapter 2, hydrolysis of a series of amides with functionalized ligand at the mineral-water interface is investigated by batch experiments. The selected amides are 4'-nitrophthalanilic acid, 2'-nitrophthalanilic acid and *N*-methyl-*N*-(4-nitrophenyl)-2-pyridinecarboxamide. The concentrations of model amides as well as their hydrolysis products are measured by HPLC. Reaction rates and mechanisms are assessed in homogenous and heterogeneous conditions respectively. The effects of different functional ligands on hydrolytic reaction are compared. Moreover, adsorption of amides on mineral as well as its influence on hydrolysis are discussed.
- The hydrolysis of chiral pesticides (metalaxyl and metalaxyl-M) in mineral suspensions is discussed in Chapter 3. The enantiomers of metalaxyl and their respective hydrolytic products are determined by chiral HPLC. Hydrolysis kinetics and mechanisms are evaluated for *R*- and *S*-enantiomer in racemic mixture and also for pure *R*-enantiomer. The configurational stability and hydrolysis enantioselectivity of metalaxyl are identified. In the case of enantiopure metalaxyl-M, a computer model is developed using MATLAB® to elucidate different reaction processes occurring concurrently with hydrolysis.
- The conclusions of this study and suggestions for future research are given in Chapter 4.

References

Atkins, P. and T. Overton (2010). Shriver and Atkins' Inorganic Chemistry, OUP Oxford.

Bailey, R. A., et al. (2002). 8 - Haloorganics and pesticides. Chemistry of the Environment (Second Edition). R. A. Bailey, H. M. Clark, J. P. Ferris, S. Krause and R. L. Strong. San Diego, Academic Press**:** 223-293.

Bergaya, F. and G. Lagaly (2006). Chapter 1 General Introduction: Clays, Clay Minerals, and Clay Science. Developments in Clay Science. B. K. G. T. Faïza Bergaya and L. Gerhard, Elsevier. **Volume 1:** 1-18.

Brigatti, M. F., et al. (2006). Chapter 2 Structures and Mineralogy of Clay Minerals. Developments in Clay Science. B. K. G. T. Faïza Bergaya and L. Gerhard, Elsevier. **Volume 1:** 19-86.

Büchel, K. H., et al. (2000). Industrial Inorganic Chemistry, 2nd Completely Revised Edition, WILEY-VCH Verlag GmbH.

Churchman, G. J., et al. (2006). Chapter 11.1 Clays and Clay Minerals for Pollution Control. Developments in Clay Science. B. K. G. T. Faïza Bergaya and L. Gerhard, Elsevier. **Volume 1:** 625-675.

Cornejo, J., et al. (2004). Pesticide-clay interactions and formulations. Interface Science and Technology. W. Fernando and S. Kestur Gundappa, Elsevier. **Volume 1:** 247-266.

Cornell, R. M. and U. Schwertmann (2004). Introduction to the Iron Oxides. The Iron Oxides, Wiley-VCH Verlag GmbH & Co. KGaA**:** 1-7.

Cornell, R. M. and U. Schwertmann (2004). Surface Area and Porosity. The Iron Oxides, Wiley-VCH Verlag GmbH & Co. KGaA**:** 95-110.

Cornell, R. M. and U. Schwertmann (2004). Surface Chemistry and Colloidal Stability. The Iron Oxides, Wiley-VCH Verlag GmbH & Co. KGaA**:** 221-252.

Craven, A., et al. (2007). Chapter 2 - Regulatory Aspects of Pesticide Risk Assessment. Pesticide Risk Assessment in Rice Paddies. C. Ettore and K. Dimitrios. Amsterdam, Elsevier**:** 25-253.

EPA. "Types of Pesticides." from http://www.epa.gov/pesticides/about/types.htm.

Estes, T. J. (1988). "Adsorption of low molecular weight halocarbons by montmorillonite." Environmental Science and Technology **22**(4): 377-381.

FAO (2002). International Code of Conduct on the Distribution and Use of Pesticides. Rome, Food and Agriculture Organization of the United Nations.

Fife, T. H. and V. L. Squillacote (1978). "Metal ion effects on intramolecular nucleophilic carboxyl group participation in amide and ester hydrolysis. Hydrolysis of N-(8-quinolyl)phthalamic acid and 8-quinolyl hydrogen glutarate." Journal of the American Chemical Society **100**(15): 4787-4793.

Fusi, P., et al. (1988). "Interaction of Fluazifop-butyl and Fluazifop with smectites." Applied Clay Science **3**(1): 63-73.

Gilliom, R. J., et al. (2006). The Quality of Our Nation's Waters-Pesticides in the Nation's Streams and Ground Water, 1992-2001, U.S. Geological Survey Circular 1291.

Grim, R. E. and N. Güven (1978). Bentonites Geology, Mineralogy, Properties and Uses. Developments in Sedimentology. R. E. Grim and N. Güven, Elsevier. **Volume 24:** 1-256.

Grube, A., et al. (2011). "Pesticides Industry Sales and Usage 2006 and 2007 Market Estimates." from http://www.epa.gov/pesticides/pestsales/07pestsales/market_estimates2007.pdf.

Haderlein, S. B. and R. P. Schwarzenbach (1993). "Adsorption of substituted nitrobenzenes and nitrophenols to mineral surfaces." Environmental Science and Technology **27**(2): 316-326.

Haderlein, S. B., et al. (1996). "Specific adsorption of nitroaromatic explosives and pesticides to clay minerals." Environmental Science and Technology **30**(2): 612-622.

Herwig, U., et al. (2001). "Physicochemical interactions between atrazine and clay minerals." Applied Clay Science **18**(5–6): 211-222.

Huang, C. H. and A. T. Stone (1999). "Hydrolysis of naptalam and structurally related amides: Inhibition by dissolved metal ions and metal (hydr)oxide surfaces." Journal of Agricultural and Food Chemistry **47**(10): 4425-4434.

Huggett, J. M. (2005). CLAY MINERALS. Encyclopedia of Geology. R. C. Selley, L. R. M. Cocks and I. R. Plimer. Oxford, Elsevier**:** 358-365.

Hundal, L. S., et al. (2001). "Sorption of Phenanthrene by Reference Smectites." Environmental Science & Technology **35**(17): 3456-3461.

Joo, J. H., et al. (2008). "Imazamethabenz hydrolysis on oxide surfaces at several pH." Journal of Pesticide Science **33**(4): 376-382.

Lagaly, G., et al. (2006). Chapter 7.3 Clay Mineral Organic Interactions. Developments in Clay Science. B. K. G. T. Faïza Bergaya and L. Gerhard, Elsevier. **Volume 1:** 309-377.

Mader, B. T., et al. (1997). "Sorption of nonionic, hydrophobic organic chemicals to mineral surfaces." Environmental Science and Technology **31**(4): 1079-1086.

McBride, M. B. (1994). Environmental Chemistry of Soils, Oxford University Press, Incorporated.

Miller, G. T. (2004). Sustaining the Earth, 6th edition, Thompson Learning, Inc. Pacific Grove, California.

Murray, H. H. (2006). Chapter 2 Structure and Composition of the Clay Minerals and their Physical and Chemical Properties. Developments in Clay Science. H. M. Haydn, Elsevier. **Volume 2:** 7-31.

Nasser, A., et al. (1997). "Adsorption of alachlor by montmorillonites." Journal of Thermal Analysis **50**(1-2): 257-268.

Patnaik, P. (2003). Handbook of Inorganic Chemicals, McGraw-Hill.

Plastourgou, M. and M. R. Hoffmann (1984). "Transformation and fate of organic esters in layered-flow systems: The role of trace metal catalysis." Environmental Science and Technology **18**(10): 756-764.

Pleština, R. (2003). PESTICIDES AND HERBICIDES | Types of Pesticide. Encyclopedia of Food Sciences and Nutrition (Second Edition). C. Editor-in-Chief: Benjamin. Oxford, Academic Press**:** 4473-4483.

Przystas, T. J. and T. H. Fife (1990). "The metal-ion-promoted water- and hydroxide-ion-catalysed hydrolysis of amides." Journal of the Chemical Society, Perkin Transactions 2(3): 393-399.

Pusino, A., et al. (1996). "Montmorillonite Surface-Catalyzed Hydrolysis of Fenoxaprop-ethyl." Journal of Agricultural and Food Chemistry **44**(4): 1150-1154.

Rosenfeld, P. E. and L. G. H. Feng (2011). 11 - Pesticides. Risks of Hazardous Wastes. Boston, William Andrew Publishing**:** 127-154.

Scheinost, A. C. (2005). METAL OXIDES. Encyclopedia of Soils in the Environment. H. Editor-in-Chief: Daniel. Oxford, Elsevier**:** 428-438.

Schlautman, M. A. and J. J. Morgan (1994). "Sorption of perylene on a nonporous inorganic silica surface: Effects of aqueous chemistry on sorption rates." Environmental Science and Technology **28**(12): 2184-2190.

Schulze, D. G. (2005). CLAY MINERALS. Encyclopedia of Soils in the Environment. H. Editor-in-Chief: Daniel. Oxford, Elsevier**:** 246-254.

Schwarzenbach, R. P., et al. (2005). Chemical Transformations I: Hydrolysis and Reactions Involving Other Nucleophilic Species. Environmental Organic Chemistry, John Wiley & Sons, Inc.**:** 489-554.

Schwarzenbach, R. P., et al. (2005). Sorption III: Sorption Processes Involving Inorganic Surfaces. Environmental Organic Chemistry, John Wiley & Sons, Inc.**:** 387-458.

Schwarzenbach, R. P. and J. Westall (1981). "Transport of nonpolar organic compounds from surface water to groundwater. Laboratory sorption studies." Environmental Science and Technology **15**(11): 1360-1367.

Smolen, J. M. and A. T. Stone (1997). "Divalent metal ion-catalyzed hydrolysis of phosphorothionate ester pesticides and their corresponding oxonates." Environmental Science and Technology **31**(6): 1664-1673.

Smolen, J. M. and A. T. Stone (1998). "Metal (hydr)oxide surface-catalyzed hydrolysis of chlorpyrifos-methyl, chlorpyrifos-methyl oxon, and paraoxon." Soil Science Society of America Journal **62**(3): 636-643.

Sparks, D. L. (2003). 2 - Inorganic Soil Components. Environmental Soil Chemistry (Second Edition). Burlington, Academic Press**:** 43-73.

Tang, W. and L. M. Sayre (1993). "Divalent metal ion catalyzed hydrolysis of N-methyl-4′-nitro-6-carboxypicolinanilide. pH-Rate profile transitions and buffer inhibition." Inorganic Chemistry **32**(25): 5785-5791.

Theng, B. K. G. (2012). Chapter 1 - The Clay Minerals. Developments in Clay Science. B. K. G. Theng, Elsevier. **Volume 4:** 3-45.

Torrents, A. and A. T. Stone (1991). "Hydrolysis of phenyl picolinate at the mineral/water interface." Environmental Science and Technology **25**(1): 143-149.

Torrents, A. and A. T. Stone (1994). "Oxide surface-catalyzed hydrolysis of carboxylate esters and phosphorothioate esters." Soil Science Society of America Journal **58**(3): 738-745.

Vallero, D. A. (2004). Chapter 7 - Chemical Reactions in the Environment. Environmental Contaminants. Burlington, Academic Press**:** 333-388.

Wei, J., et al. (2001). "Influence of Clay Minerals on the Hydrolysis of Carbamate Pesticides." Environmental Science & Technology **35**(11): 2226-2232.

Weidenhaupt, A., et al. (1997). "Sorption of Organotin Biocides to Mineral Surfaces." Environmental Science & Technology **31**(9): 2603-2609.

2. Hydrolysis of Amide Model Compounds at the Mineral-Water Interface

2.1 Introduction

Mineral is an important fraction of soil and may interact with some polar or weakly polar pesticides due to its specific surface properties. Mineral surface-catalyzed hydrolysis has been found for some organic chemicals (Torrents and Stone 1991, Torrents and Stone 1993, Pusino, Petretto et al. 1996, Smolen and Stone 1998, Huang and Stone 1999, Wei, Furrer et al. 2001, Shin and Cheney 2004). For example, Torrents and Stone (1991) has observed anatase (TiO_2) and goethite (FeOOH) promote the hydrolysis of phenyl picolinate compared with homogeneous solution, however, silica (SiO_2), γ-aluminum oxide (γ-Al_2O_3) and hematite (Fe_2O_3) have no surface-catalyzed effect on hydrolysis. In addition, Wei et al. (2001) reported that montmorillonite plays a more important role in the hydrolysis of carbamate pesticides than beidellite, illite, or vermiculite. For example, the hydrolysis of carbosulfan is promoted by montmorillonite due to surface acidity and/or surface chelate mechanism, however, the hydrolysis of chlorpropham is significantly inhibited due to its strong sorption on montmorillonite.

Moreover, *N*-methylpicolinanilides are susceptible to metal ion-catalyzed hydrolysis since metal ion can coordinate to the pyridine nitrogen and then facilitate the reaction by carbonyl-activation or metal-hydroxide mechanism. Besides, the *N*-methyl group is not subjected to the chelation induced NH deprotonation which inhibits the reaction. Large rate enhancement (10^4-10^5) has been observed for *N*-methyl-*N*-(4-nitrophenyl)picolinamide at the presence of Cu^{II} (Reddy, Jacobson et al. 1991). Tang and Sayre (1993) also reported that metal ion catalyzed alkaline hydrolysis is dominant at pH 5-7 for *N*-methyl-4'-nitro-6-carboxypicolinanilide and the catalytic effectiveness of metal ions at saturation is Cu^{II} (1×10^6) > Zn^{II} (7×10^5) > Co^{II} (4×10^4) > Ni^{II} (2×10^4). Except for anilides, hydrolysis of amides bearing aliphatic amine groups can also be catalyzed by metal ions, for example, picolinylsarcosine, *N*-(6-carboxypicolinyl)sarcosine and two 8-hydroxyquinoline tertiary amides are subjected to Cu^{II} catalyzed hydrolysis, and the largest rate enhancement factors (10^5-10^7) are obtained for picolinylsarcosine (Sayre, Reddy et al. 1992). Since surface sites and interlayer positions are occupied by a wide range of metal ions, which have analogous properties with dissolved metal ions, metal oxides and clay minerals may also have

strong influence on amide hydrolysis depending on their particular characteristics, e.g., surface area, charge behavior and interlayer cations.

In this study, hydrolysis of a series of amides with functionalized ligand at the mineral-water interface was investigated by batch experiments. The selected model amides are 4'-nitrophthalanilic acid, 2'-nitrophthalanilic acid and *N*-methyl-*N*-(4-nitrophenyl)-2-pyridinecarboxamide (see Figure 2.1). The minerals used include silica, aluminum oxide, goethite, hectorite, kaolinite and Na-rich montmorillonite.

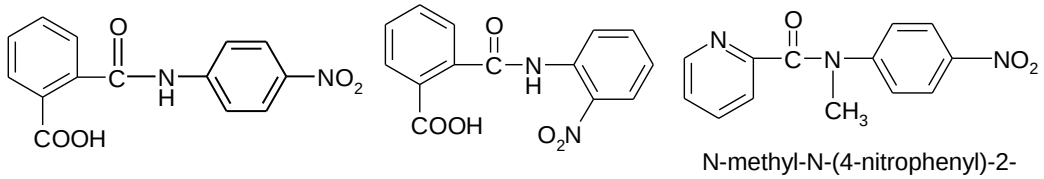

FIGURE 2.1. Structure of model amides.

2.2 Experimental Section

2.2.1 Chemicals

Three model amides, 2'-nitrophthalanilic acid (2-[[(2-nitrophenyl)amino]carbonyl]-benzoic acid), 4'-nitrophthalanilic acid (2-[[(4-nitrophenyl)amino]carbonyl]-benzoic acid) and *N*-methyl-*N*-(4-nitrophenyl)-2-pyridinecarboxamide, were obtained from AKos Consulting & Solutions GmbH (Steinen, Germany). One of the hydrolysis products, *N*-methyl-4-nitroaniline (purity >97%), was purchased from Alfa Aesar (Germany), the others including phthalic acid (1, 2-benzenedicarboxylic acid, purity ≥99.5%), 4-nitroaniline (purity ≥99.0%), 2-nitroaniline (purity >98%) and picolinic acid (2-pyridinecarboxylic acid, purity >99%) were purchased from Sigma-Aldrich (Germany). All compounds were used without further purification.

2.2.2 Minerals

To study the effects of mineral surfaces on amide hydrolysis, some oxides and clay minerals were applied. Oxides include amorphous fumed silica (SiO_2,), highly dispersed fumed aluminum oxide (Al_2O_3, AEROXIDE® Alu C) and goethite (α-FeOOH, Bayferrox® 920 Z). Three types of clay minerals, hectorite (SHCa-1), Na-rich montmorillonite (SWy-2) and well crystallized kaolinite (KGa-1), were obtained from the Source Clays Repository of The Clay Minerals Society (Chantilly VA, USA). All minerals were used without further treatment or purification. Some physical and

chemical properties are listed in Table 2.1.

TABLE 2.1. Physical and Chemical Properties of the Minerals

Mineral	Source	CEC[a] (meq/100g)	Surface Area (m^2/g)
SiO_2	Alfa Aesar	n.d.[b]	350 – 410
Al_2O_3	Evonik Degussa	n.d.	100 ± 15
Hectorite (SHCa-1)	San Bernardino County, California	43.9	63.19 ± 0.50
Na-Montmorillonite (SWy-2)	Crook County, Wyoming	76.4	31.82 ± 0.22
Kaolinite (KGa-1)	Washington County, Georgia	2.0	10.05 ± 0.02
α-FeOOH	LANXESS	n.d.	9.214

[a] cation exchange capacity. [b] n.d., not determined.

2.2.3 Hydrolysis Experiments

To investigate the acid- and base-catalyzed hydrolysis of 4'-nitrophthalanilic acid (4'-NPTA), 2'-nitrophthalanilic acid (2'-NPTA) and *N*-methyl-*N*-(4-nitrophenyl)-2-pyridinecarboxamide (N-Me-PCA), batch experiments were performed in acidic and alkaline aqueous solutions at ambient temperature. The solution pH was selected at pH 0.19-4.29 and 12.01-13.22 for 4'-NPTA, pH 0.43-4.31 and 12.67-13.38 for 2'-NPTA, and pH 0.50-2.51 and 11.05-12.28 for N-Me-PCA. The reaction solutions were initially prepared with 10 mM NaCl in 50 mL brown serum bottles. At pH ≤ 3.0 or pH ≥ 12, concentrated HCl or NaOH solution were used to adjust and control the solution pH, while 3.0 <pH <4.5, formate buffer (5 mM) was used to control the solution pH. Each amide stock solution (≈0.5 mM) was prepared by dissolving a certain amount of 4'-NPTA, 2'-NPTA or N-Me-PCA in 10 mM NaCl solution. To start the reaction, 5 mL freshly prepared stock solution was added to 45 mL buffered electrolyte solution. The reaction solution was completely mixed using a magnetic stir bar, and duplicate samples were taken immediately (as t = 0) and measured by HPLC. Then equal aliquots of reaction solution were transferred to 2 mL borosilicate glass vials sealing with screw caps (PTFE/rubber septa included). The vials were stored in dark under ambient temperature. The solution pH was measured during the experiments and

adjusted using 0.1-1 M HCl or NaOH if necessary. At appropriate intervals, duplicate samples were analyzed by HPLC to determine the concentrations of amides as well as the hydrolysis products.

To investigate the influence of metal oxides and clay minerals on amide hydrolysis, batch experiments were conducted in mineral suspensions. At first, 45 mL of mineral suspensions were prepared in 50 mL brown glass bottles. To prepare the suspension, each mineral was suspended in 10 mM NaCl solutions at a surface area concentration of 200 m^2 L^{-1} (the corresponding mass concentration amounted to 0.57, 2.00, 21.71, 19.90, 3.17 and 6.29 g L^{-1} for SiO_2, Al_2O_3, goethite, kaolinite, hectorite and Na-montmorillonite respectively). The suspension pH was adjusted by adding a small amount of 1-5 M HCl or NaOH to reach different values, and buffered with suitable salts (10 mM formate or acetate buffer for 2'-NPTA and 4'-NPTA over pH 3-5.5, 10 mM carbonate buffer for N-Me-PCA over pH 9.5-11). Then the mineral suspensions were continuously stirred using magnetic stir bars. After 12 h equilibration, 5 mL freshly prepared amide stock solution (model amides dissolved in 10 mM NaCl solutions) was added into mineral suspensions to initiate the reaction. As a control, hydrolysis experiments were concurrently carried out in aqueous solutions (only electrolyte solution without mineral), with the same amide concentration and pH as mineral suspensions. Under vigorous stirring, equal aliquots of reaction suspension or solution were transferred to 2 mL borosilicate glass vials and sealed with screw caps (PTFE/rubber septa included). These vials were collected in a box wrapped with aluminum foil (avoiding the photolysis) and shaken on a rotator at a speed of 15 rpm. The suspension or solution pH was monitored during the reaction and adjusted using 0.1-1 M HCl or NaOH if necessary. Periodically, two vials of each type of suspension or solution were taken for analysis. For experiments conducted in aqueous solutions, samples were directly analyzed by HPLC. However, for mineral suspensions, samples were first centrifuged for 10 min at 4000 rpm (Hermle Z320, Berthold Hermle, Gosheim, Germany), and then the supernatant was used for analysis. The hydrolysis reaction was followed by determining the concentrations of amides and their hydrolytic products in aqueous or supernatant solutions using reversed-phase HPLC.

2.2.4 Adsorption Experiments

In the experiments with mineral suspensions, N-Me-PCA adsorption was found to occur on two clay minerals, hectorite and Na-montmorillonite. To evaluate the sorption

in detail, batch experiments with N-Me-PCA and one of its hydrolytic products, 2-picolinic acid, were performed in hectorite and Na-montmorillonite suspensions. The same conditions (e.g., same pH, ionic strength and buffer concentration) as N-Me-PCA hydrolysis experiments were applied. The detailed procedure for preparing hectorite and Na-montmorillonite suspensions refers to 2.2.3 hydrolysis experiments. A series of stock solutions were prepared by dissolving a certain amount of N-Me-PCA or 2-picolinic acid in 10 mM NaCl solutions, making the concentration of N-Me-PCA or 2-picolinic acid be about 0.5, 1.25 and 2 mM. To initiate sorption, 1 mL freshly prepared stock solution of N-Me-PCA or 2-picolinic acid was added into 49 mL mineral suspension. Hence, the initial concentrations of N-Me-PCA or 2-picolinic acid were approximately 10, 25 or 40 µM. The experiment was also concurrently performed in aqueous solution as a control. Once the suspensions or solutions were fully mixed by stirring, duplicate samples were taken immediately and measured by HPLC. Samples were directly analyzed by HPLC for aqueous solution. However, in the case of hectorite and Na-montmorillonite suspensions, samples were firstly centrifuged for 10 min at 4000 rpm, and then the supernatant was used for HPLC analysis. The mineral suspensions and aqueous solutions were continuously stirred during the sorption. Suspension or solution pH was monitored and adjusted using 0.1-1 M HCl or NaOH if necessary. Periodically, duplicate samples were taken and measured for the sorption of N-Me-PCA and 2-picolinic acid.

2.2.5 HPLC Analysis

The hydrolysis processes of model amides were monitored by a Shimadzu HPLC system, including a system controller (CBA-20A), two pumps (LC-20AD), an online degasser (DGU-20A3), an auto-sampler (SIL-20ACHT) and a photodiode array detector (SPD-M20A). All the amides and their hydrolytic products were eluted using a Restek Allure® C18 column configured with an integral guard cartridge (Allure® C18 column: 150 × 3.2 mm, 5 µm; Allure® C18 guard cartridge: 10 × 2.1 mm). The eluting parameters for 4'- and 2'- NPTA as well as their hydrolysis products were: 0.5 mL/min flow rate; mobile phase A: 90% methanol and 10% pure water, B: 25 mM phosphate buffer (pH 2.5), A : B = 60 : 40 for 4'-NPTA and 4-nitroaniline, A : B = 55 : 45 for 2'-NPTA and 2-nitroaniline; wavelength: 320 nm for 4'-NPTA, 380 nm for 4-NA, 262 nm for 2'-NPTA and 280 nm for 2-NA. While the measuring parameters for N-Me-PCA and its two hydrolytic products (N-methyl-4-nitroaniline and 2-picolinic acid) were: 0.5 mL/min flow rate; mobile phase A: 90% methanol and 10% pure water, B: 25 mM

phosphate buffer (pH 7.5) and 5mM Tetrabutylammonium hydrogensulfate (TBAHS) as ion pair chromatography (IPC) reagent, A : B = 50 : 50; wavelength: 264nm for 2-picolinic acid, 297 nm for N-Me-PCA and 402 nm for N-methyl-4-nitroaniline.

2.2.6 Hydrolysis Kinetics Evaluation

The amide hydrolysis was presumed to follow pseudo-first-order kinetics, which can be described by:

$$\ln (C_t / C_0) = - k_{obs} t$$

where C_0 and C_t are the concentrations of model amides at time zero and t respectively. The observed rate constant (k_{obs}) can be derived by linear regression analysis of plot "ln (C_t / C_0) versus t". Then the hydrolysis half-life ($t_{1/2}$) was calculated by:

$$t_{1/2} = \ln 2 / k_{obs}$$

2.3 Results and Discussion

2.3.1 Hydrolysis of 4'- and 2'-nitrophthalanilic Acid in Aqueous Solutions

2.3.1.1 Results

Hydrolysis experiments for 4'-NPTA and 2'-NPTA were performed in buffered aqueous solution respectively (pH 0.19-4.29 and 12.01-13.22 for 4'-NPTA, pH 0.43-4.31and 12.67-13.38 for 2'-NPTA). The results showed that both 4'-NPTA and 2'-NPTA readily hydrolyzed over the above pH ranges and the respective products, 4-nitroaniline (4-NA) and 2-nitroaniline (2-NA), were obtained. For instance, the reaction profiles at two different pH were present in Figure 2.2 for each amide. The mass balances were also calculated following the reaction and the mass loss was observed to different extent depending on the reactant and solution pH. For example, the mass loss was much more significant at pH ~3 (11.67% for 4'-NPTA and 22.08% for 2'-NPTA, Figure 2.2a and c), while the mass loss was only 3.42% for 4'-NPTA at pH 12.50 and 6.16% for 2'-NPTA at pH 12.67 (Figure 2.2b and d). The mass loss in each amide reaction was plotted as a function of pH. As shown in Figure 2.3, much more mass losses were obtained in the reaction of 2'-NPTA compared with 4'-NPTA, while for both amides there were more significant losses in acidic solutions than in alkaline solutions. The amount of mass loss was quite stable when pH ≥12, less than 3.42% for 4'-NPTA and slightly more than 6% for 2'-NPTA. However, at pH ≤4.31 the mass loss was dependent on solution pH to a large extent. For 4'-NPTA in acidic solutions, the mass loss slightly

increased from 9.02% to 11.67% as pH increased from 0.48 to 3.01, then it reduced as pH continued increasing and reached 6.41% at pH 4.29. In the case of 2'-NPTA, the mass loss first decreased slowly when pH < 2.96 and then reduced dramatically from 22.08% to 8.98% as pH increased from 2.96 to 4.31. Since the predicted pK_a values of 4'- and 2'-nitrophthalanilic acid are 3.39 and 3.41 respectively (provided by SciFinder®), the mass loss-pH plot (Figure 2.3) was shown to curve at pH value close to the acidity constant of amides, which may imply that the species of model amides (neutral or ionized) played an important role in hydrolysis.

Referring to reaction kinetics of model amides hydrolysis, ln (C_t / C_0) was plotted against reaction time (t), which show good linearity, e.g. 4'-NPTA at pH 3.01 and 2'-NPTA at pH 2.96 (Figure 2.4). It is illustrated that hydrolysis of 4'- and 2'-NPTA follows pseudo-first-order kinetics in acidic and alkaline aqueous solutions. The observed rate constants were calculated by performing linear regression on the plot of ln (C_t / C_0) versus t. The results showed that 4'-nitrophthalanilic acid hydrolyzed slightly faster than 2'-nitrophthalanilic acid. For both amides, the observed rate constants reduced in acidic solutions and increased in alkaline solutions as a function of pH. In Figure 2.5, common logarithms of the observed rate constants for hydrolysis of 4'- and 2'-nitrophthalanilic acid were plotted versus solution pH, and linear fit was obtained over specific pH ranges. The rate constant-pH profile also curves when pH approximates to the amide pK_a, which illustrates the hydrolysis of 4'- and 2'-nitrophthalanilic acid is influenced by dissociation of carboxylic acid group. The steeper curves at higher pH indicate that solution pH has a much stronger effect on hydrolysis of the dissociated species. In alkaline solutions, the unit slope at pH ≥ 12 (Figure 2.5a) indicates general base-catalyzed hydrolysis occurred for 4'-nitrophthalanilic acid, however, in the case of 2'-nitrophthalanilic acid (Figure 2.5b), other factors may participate and even play a more important role in the hydrolysis.

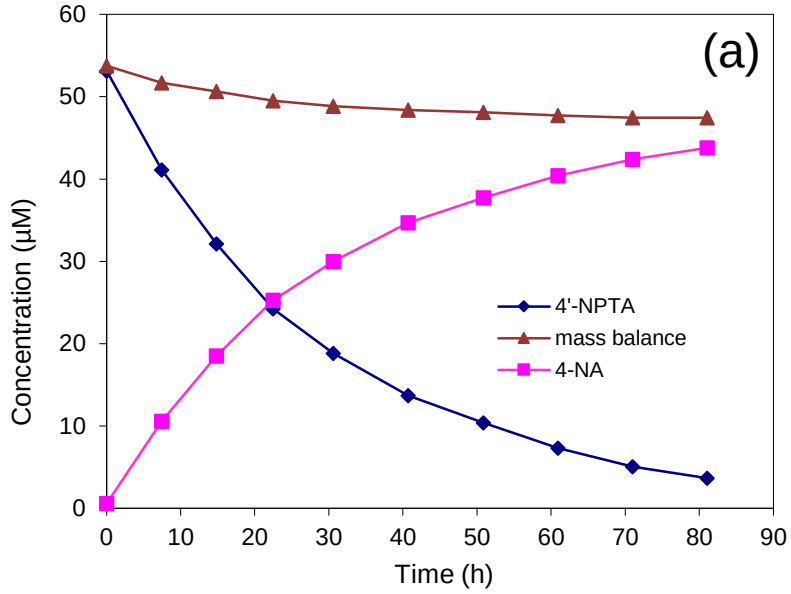
(a)
Concentration (µM)
Time (h)
4'-NPTA
mass balance
4-NA
0
10
20
30
40
50
60
70
80
90

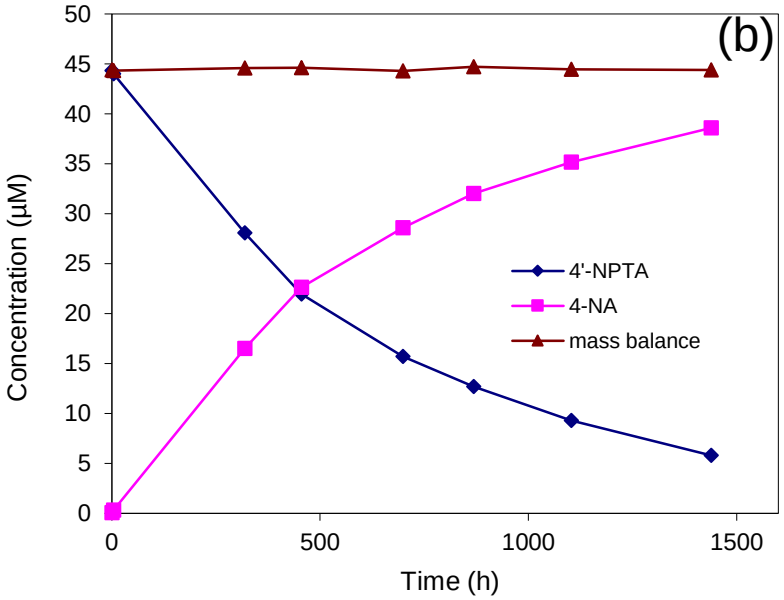
(b)
Concentration (µM)
Time (h)
4'-NPTA
4-NA
mass balance
0
5
10
15
20
25
30
35
40
45
50
500
1000
1500

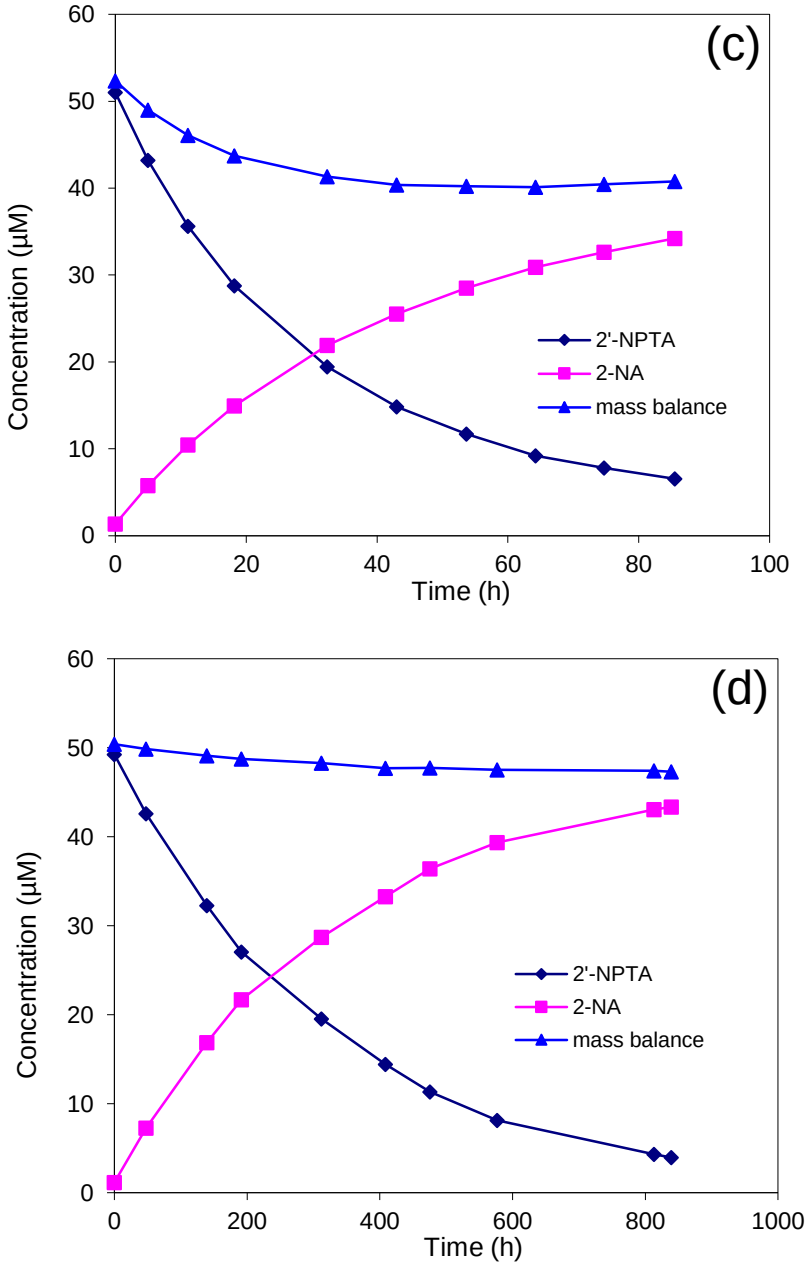

FIGURE 2.2. Hydrolysis of amides in acidic or alkaline aqueous solutions: (a) 4'-NPTA at pH 3.01, (b) 4'-NPTA at pH 12.50, (c) 2'-NPTA at pH 2.96 and (d) 2'-NPTA at pH 12.67.

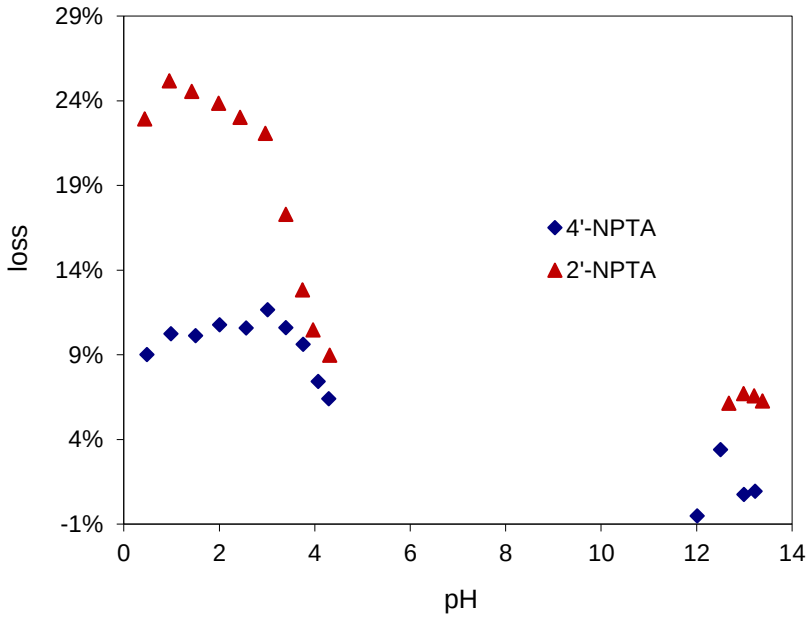

FIGURE 2.3. The mass loss in the hydrolysis of 4'- and 2'- nitrophthalanilic acid.

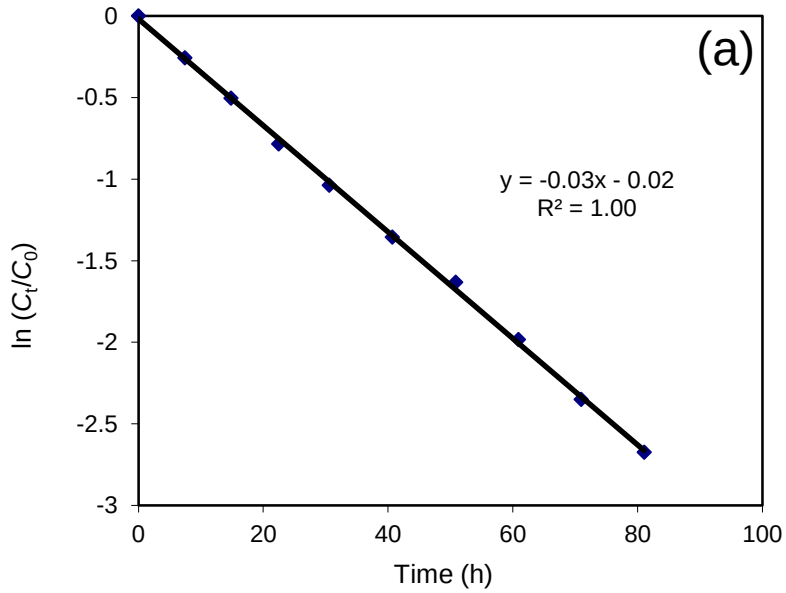

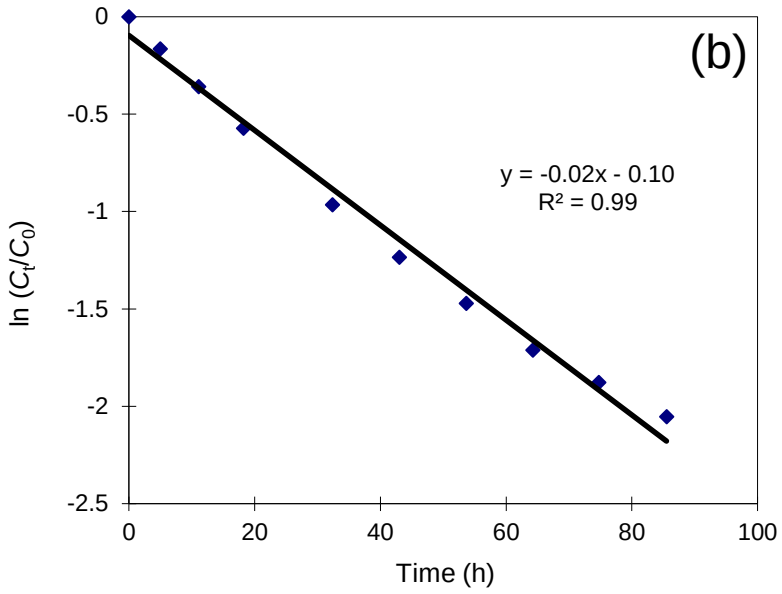

FIGURE 2.4. Plots of ln (C_t /C_0) versus reaction time for amide hydrolysis: (a) 4'-NPTA at pH 3.01 and (b) 2'-NPTA at pH 2.96.

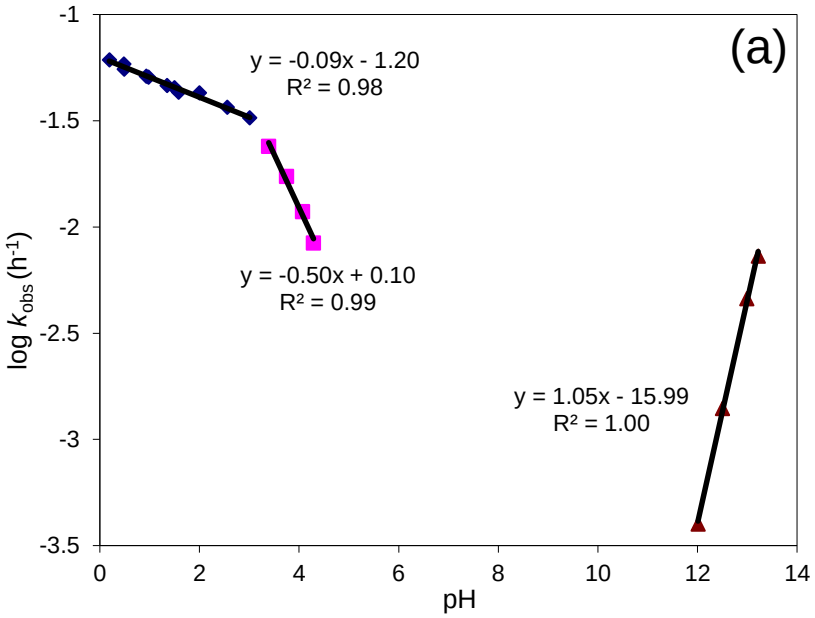

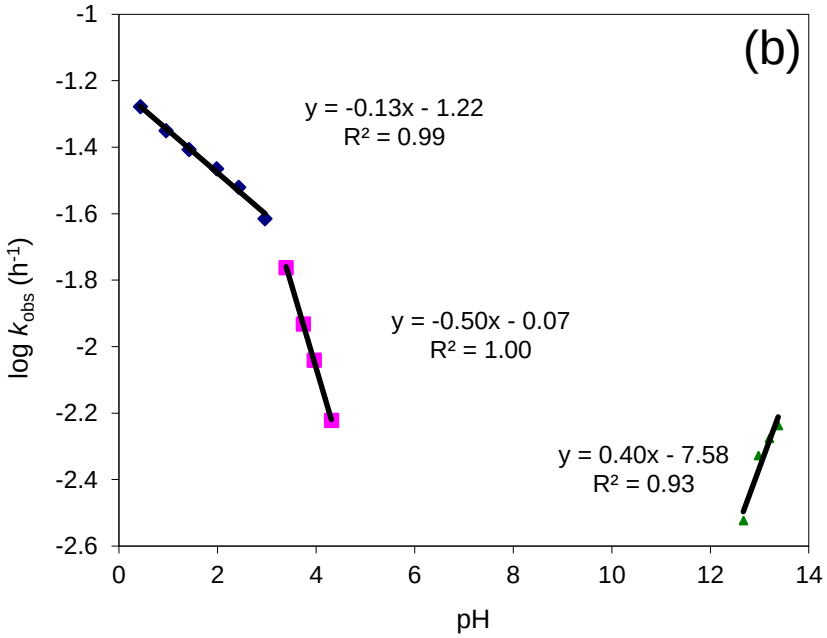

FIGURE 2.5. Plots of log k_{obs} vs pH for amides hydrolysis in buffered aqueous solutions at ambient temperature: (a) 4'-NPTA and (b) 2'-NPTA.

2.3.1.2 Reaction Mechanism

As above mentioned, the plots of log k_{obs} vs pH for 4'- and 2'-NPTA are curved at pH <4.3. In previous studies (Hawkins 1976, Granados, Nassetta et al. 1995) the similar curved rate profiles were also observed for the hydrolysis of some 3'- and 4'-substituted phthalanilic acids and 1-*N*-naphthylphthalamic acid in acidic solutions. A reaction mechanism involving intramolecular catalysis has been proposed for hydrolysis of some phthalamic acid and phthalanilic acid derivatives in acidic conditions (Hawkins 1976, Granados, Nassetta et al. 1995, Huang and Stone 1999). Accordingly, the possible reaction mechanisms for 2'- and 4'-nitrophthalanilic acid at pH <4.3 were postulated similarly. As illustrated in Scheme A (Figure 2.6), the undissociated neighboring carboxylic acid group performs as an intramolecular nucleophile attacking the amide carbonyl carbon to form a tetrahedral intermediate. Then the protonation of leaving group and the cleavage of C-N bond occur, forming the amine product and anhydride which eventually hydrolyzes to phthalic acid. It is shown that the neutral species of 2'- and 4'-nitrophthalanilic acid are the active forms in the intramolecular catalysis. The participation of undissociated carboxyl group in hydrolysis also accounts for the rate profile curving near the amide pK_a.

It was also reported in previous studies (Hawkins 1976, Granados, Nassetta et al. 1995, Huang and Stone 1999) that a side reaction may simultaneously occur with hydrolysis

of substituted phthalanilic acids. As shown in Scheme B (Figure 2.6), the corresponding product, i.e. *N*-phenylphthalimide, is formed by nucleophilic attack of the amide nitrogen on the carboxylic carbonyl carbon followed by water elimination. The formation of *N*-phenylphthalimide also accounts for the mass loss observed for the hydrolysis reaction. Furthermore, the plot of mass loss vs pH in Figure 2.3 shows that solution pH influences the yield of by-product. The amount of *N*-phenylphthalimide keeps stable for 4'-NPTA or decreases slightly for 2'-NPTA at pH <3.01 and then gets much lower from pH 3.01 to 4.31. Hence, it is indicated that the neutral species of 4'- and 2'-nitrophthalanilic acid are also the active forms in the side reaction. In addition, much more phthalimide was produced in the reaction of 2'-NPTA than 4'-NPTA especially at pH < 3.01 (Figure 2.3). The possible reason is that for 2'-NPTA an intramolecular hydrogen bonding can be formed between the *ortho*-nitro group and the hydroxyl group, which stabilizes the tetrahedral intermediate and then promotes the side reaction. While no intramolecular hydrogen bonding is formed for the intermediate of 4'-NPTA (Scheme B in Figure 2.6).

Scheme A:

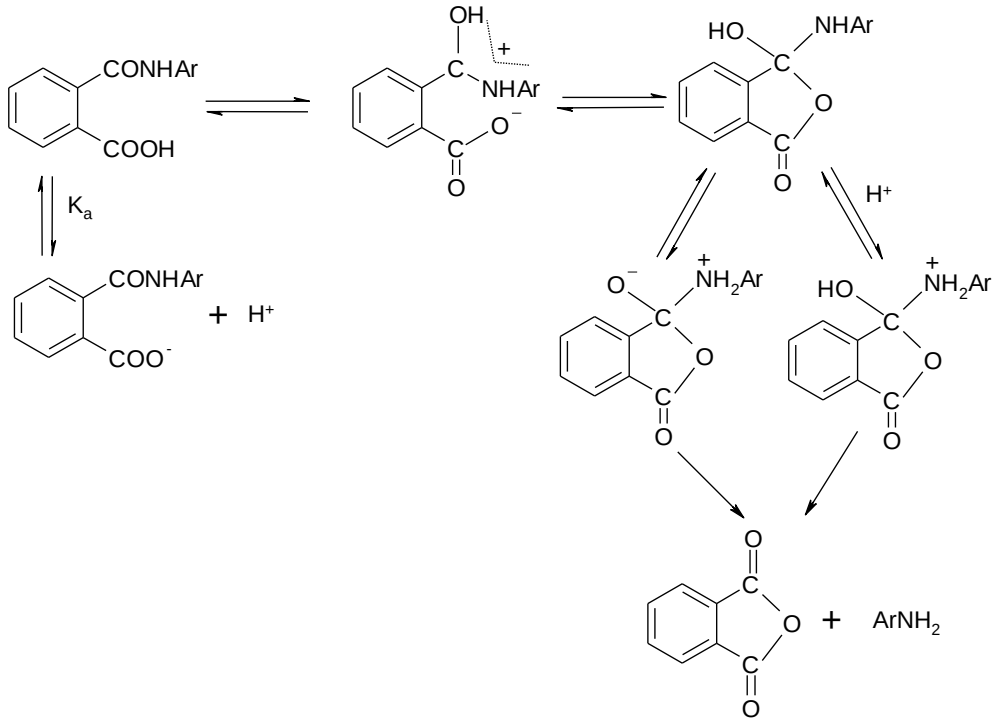

Scheme B:

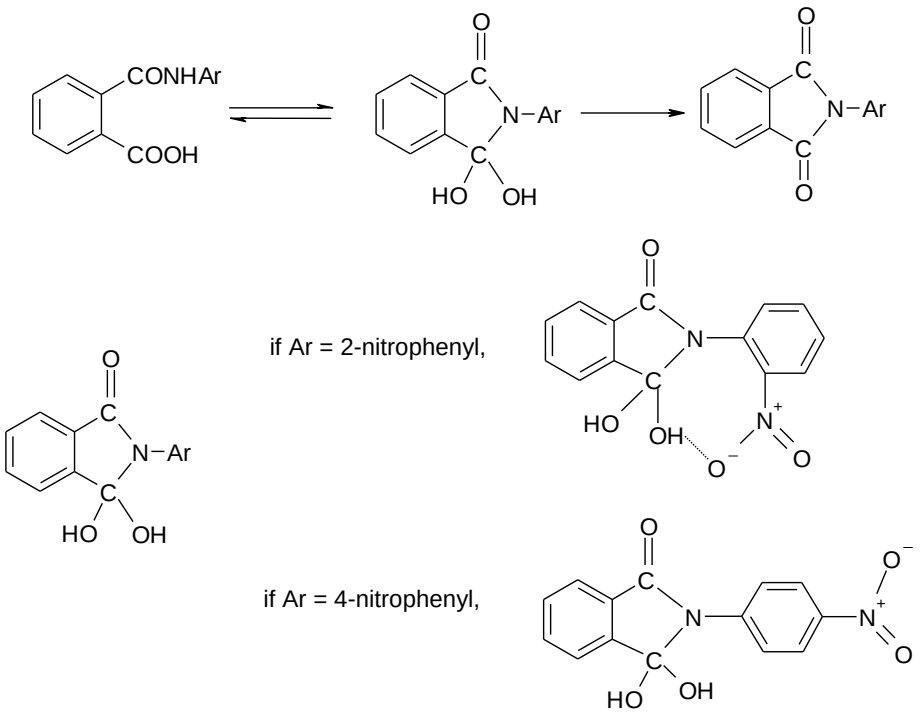

FIGURE 2.6. Hydrolysis pathways proposed for 4'- and 2'-nitrophthalanilic acid in acidic solutions [according to Hawkins (1976); Granados et al. (1995); Huang and Stone (1999)]. Ar represents 4- or 2-nitrophenyl.

2.3.2 Hydrolysis of 4'- and 2'-nitrophthalanilic Acid in Mineral Suspensions

As was stated above, intramolecular catalyzed hydrolysis occurred for 4'- and 2'-nitrophthalanilic acid in acidic solutions. In order to investigate the effects of minerals on the intramolecular catalysis, hydrolysis experiments were conducted in acidic mineral suspensions as well as aqueous solutions (as a control group). The reaction was followed by determining the concentrations of 4'- and 2'-NPTA and their hydrolysis products 4- and 2-nitroaniline in supernatant solutions. When 4'- or 2'-NPTA was added to mineral suspensions, the initial concentration in supernatant was almost equal to that in aqueous solution. Additionally, when the reaction was completed, the concentration of hydrolysis product (4- or 2-NA) in supernatant was nearly the same as that in aqueous solution (data not shown). Hence, in SiO_2, Al_2O_3, goethite, kaolinite, hectorite or Na-montmorillonite suspensions over pH 3-5.5, adsorption of reactant (4'- or 2'-NPTA) and product (4- or 2-NA) is insignificant.

The reaction profile for each mineral suspension was similar to that for aqueous solution and the mass loss also decreased as pH increased. However, plots of ln (C_t / C_0) versus t for the hydrolysis of 4'- and 2'-NPTA in mineral suspensions were not linear when pH <4 (see Figure 2.7 and 2.8). The reason for the decreasing rates is not clear and the curved plots have also been observed in hydrolysis of structurally similar amides, e.g. *N*-(1-naphthyl)phthalamic acid (Huang and Stone 1999). As shown in Figure 2.7a, all examined minerals had an inhibitory effect on 4'-NPTA hydrolysis at pH ~ 3 and this inhibitory effect increased as the reaction proceeded. However, at pH ~ 3.5, the reactions in mineral suspensions were slightly faster during the first two half-lives and then got even slower than those in aqueous solutions due to the inhibition of minerals (Figure 2.7b). At pH ~ 4, except for goethite and SiO_2, the other minerals slightly promoted the hydrolysis of 4'-NPTA (Figure 2.7c). In the case of 2'-NPTA, hydrolysis was more significantly enhanced by Al_2O_3 and kaolinite compared with the other minerals at pH 3-4 (Figure 2.8). Whereas over pH 4.5-5.5 the hydrolysis of 4'- and 2'-NPTA in mineral suspensions followed pseudo-first-order kinetics and the observed rate constants were listed in Table 2.2. The results showed that the hydrolysis rate constants of 4'- and 2'-NPTA in mineral suspensions decreased as pH increased and were of the same order of magnitude as those in the corresponding aqueous solution. In summary, the examined oxides and clay minerals have no significant effect on the hydrolysis of 4'- and 2'-NPTA.

Both 4'- and 2'-NPTA are secondary amides with a neighboring carboxyl group participating as an intramolecular nucleophile. Huang and Stone (1999) have reported hydrolysis of a structurally similar amide, naptalam (N-(1-naphthyl)phthalamic acid), was subjected to inhibition by dissolved metal ions (Cu^{II} and Zn^{II}) and metal oxide surfaces (Al_2O_3 and FeOOH). They proposed that the inhibition by metal oxides should be related to naptalam adsorption onto Al_2O_3 and FeOOH. Moreover, the inhibition mechanism by metal oxides may be similar to that by dissolved metal ions, i.e., the inhibitory effect occurring by (1) metal ion coordination to the carbonyl group of naptalam and inducing deprotonation of the amide nitrogen; and/or (2) metal ion coordination to the carboxyl group of naptalam and hindering the intramolecular nucleophilic attack (Huang and Stone 1999). With regard to 4'- and 2'-NPTA, no measurable adsorption was observed, which may imply that metal ions involved in the oxides and clay minerals could not form complex with amides. Hence, hydrolysis of 4'- and 2'-NPTA is not susceptible to catalysis or inhibition by mineral surfaces.

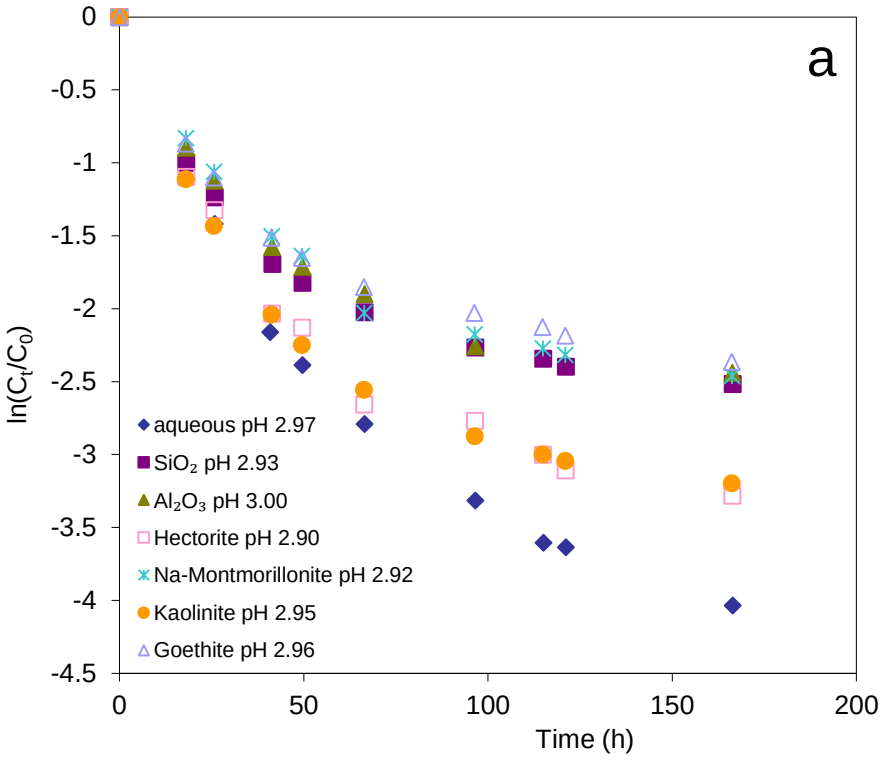
a
ln(Ct/C0)
Time (h)
aqueous pH 2.97
SiO2 pH 2.93
Al2O3 pH 3.00
Hectorite pH 2.90
Na-Montmorillonite pH 2.92
Kaolinite pH 2.95
Goethite pH 2.96

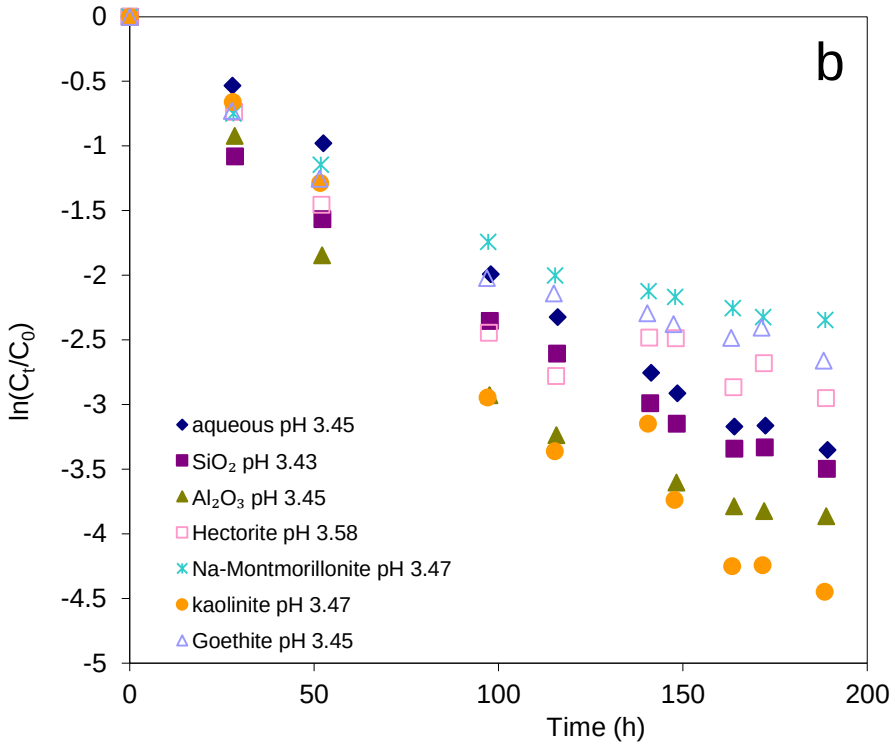
b
ln(Ct/C0)
Time (h)
aqueous pH 3.45
SiO2 pH 3.43
Al2O3 pH 3.45
Hectorite pH 3.58
Na-Montmorillonite pH 3.47
kaolinite pH 3.47
Goethite pH 3.45

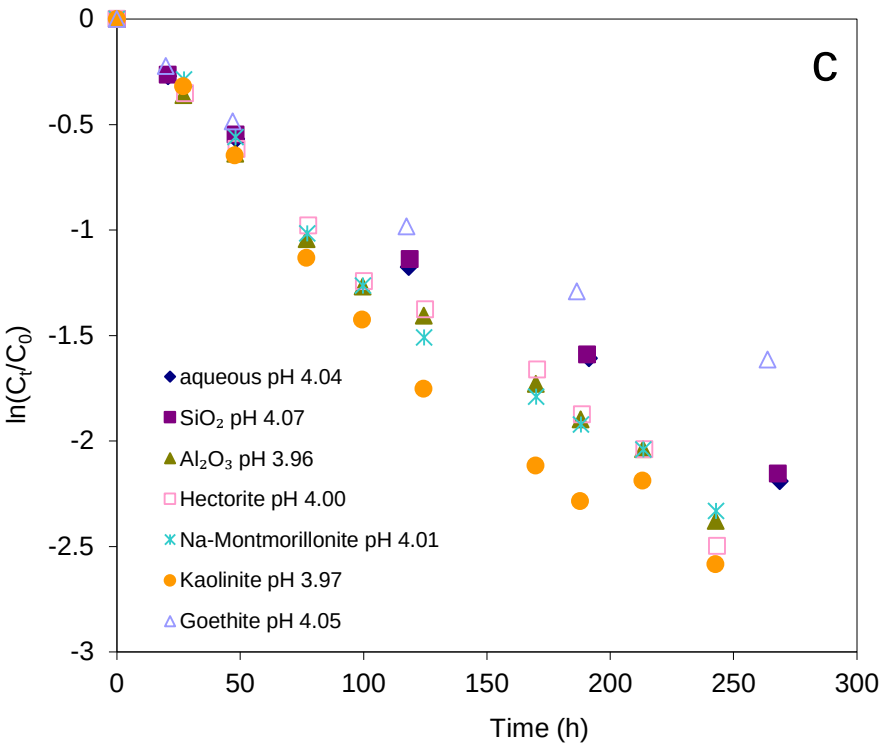

FIGURE 2.7. Plots of ln (C_t /C_0) versus reaction time for 4'-NPTA hydrolysis in mineral suspensions at (a) pH ~ 3, (b) pH ~ 3.5, and (c) pH ~ 4, where C_t is the concentration of 4'-NPTA in supernatant at time *t* and C_0 is the corresponding initial concentration. Reaction conditions: 40-50 μM 4'-NPTA, 200 m^2L^{-1} mineral, 10 mM formate buffer, 10 mM NaCl, ambient temperature.

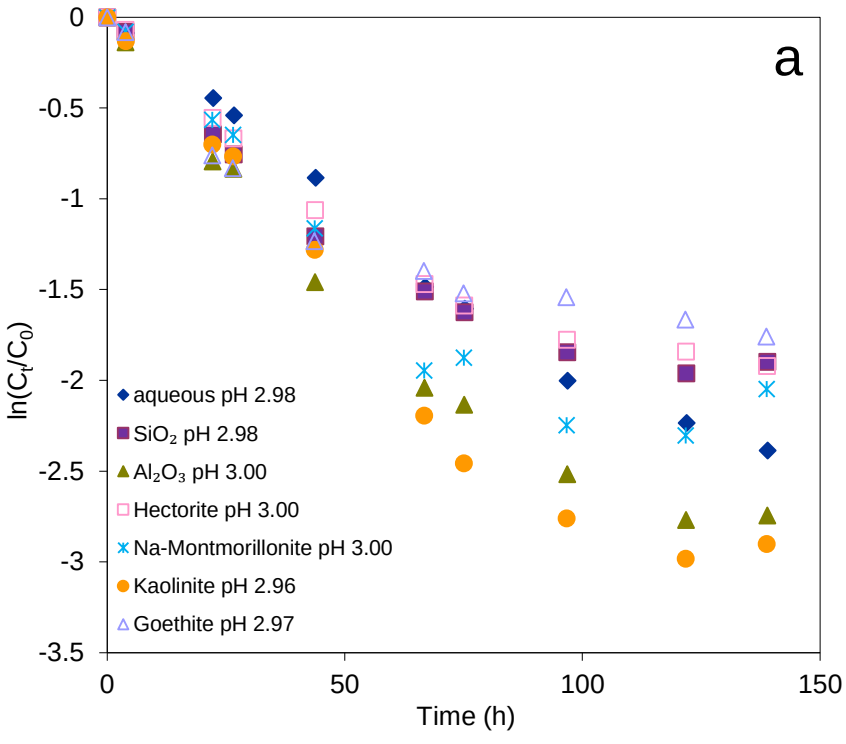

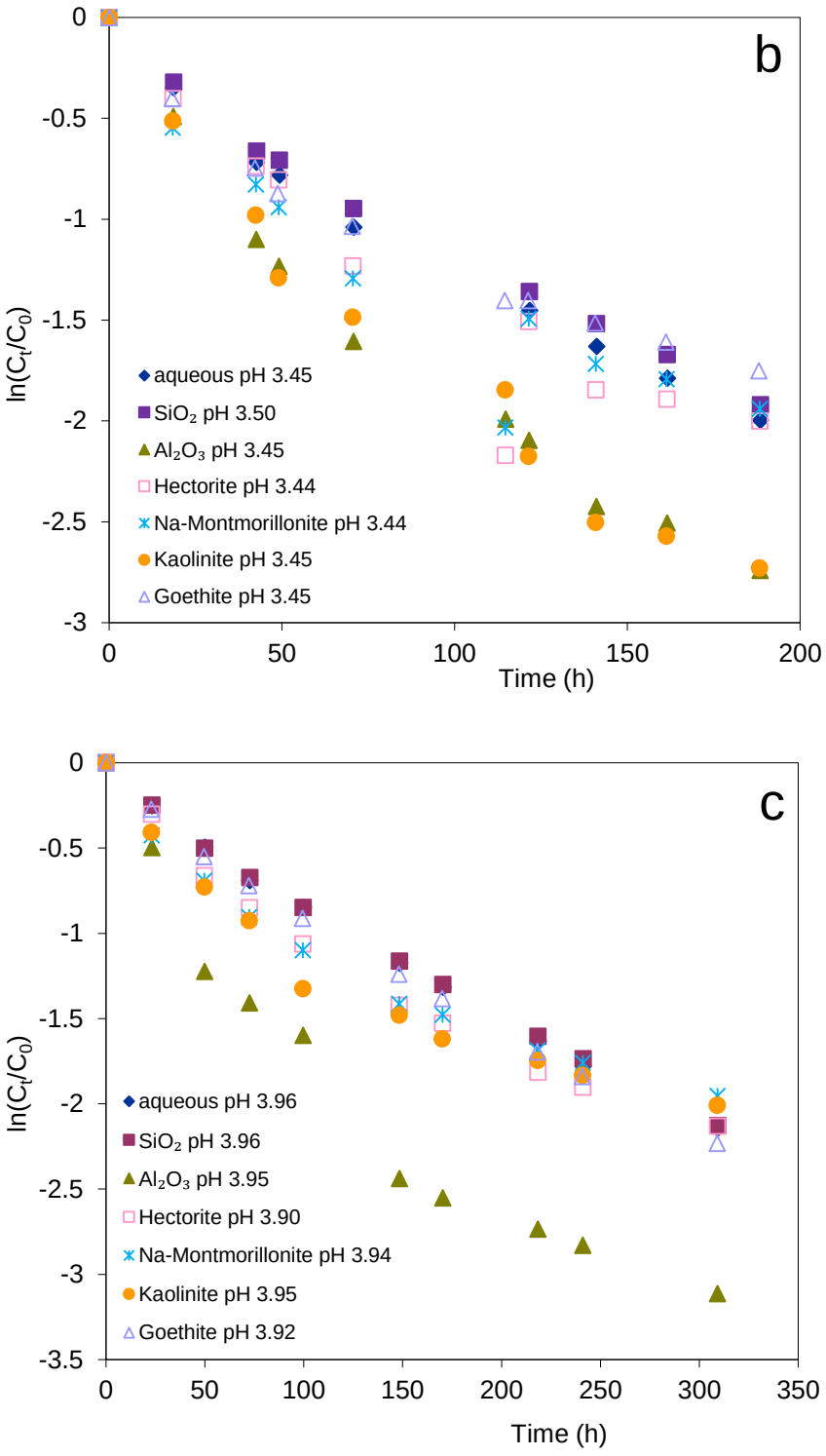

FIGURE 2.8. Plots of ln (C_t /C_0) versus reaction time for 2'-NPTA hydrolysis in mineral suspensions at (a) pH ~ 3, (b) pH ~ 3.5, and (c) pH ~ 4, where C_t is the concentration of 2'-NPTA in supernatant at time *t* and C_0 is the corresponding initial concentration. Reaction conditions: 45-60 µM 2'-NPTA, 200 m^2L^{-1} mineral, 10 mM formate buffer, 10 mM NaCl, ambient temperature.

TABLE 2.2. Hydrolysis Rate Constants for 4'- and 2'-nitrophthalanilic Acid in Different Mineral Suspensions and Aqueous Solutions

Amide	Mineral	pH	k_{obs} (h^{-1})	pH	k_{obs} (h^{-1})	pH	k_{obs} (h^{-1})
4'-NPTA	aqueous	4.63	3.25E-03	5.05	1.36E-03	5.53	4.53E-04
4'-NPTA	SiO_2	4.61	3.55E-03	5.08	1.30E-03	5.56	3.97E-04
4'-NPTA	Al_2O_3	4.65	2.88E-03	5.04	1.38E-03	5.54	4.22E-04
4'-NPTA	hectorite	4.58	3.76E-03	4.90	1.61E-03	5.33	6.91E-04
4'-NPTA	montmorillonite	4.64	2.93E-03	5.11	1.18E-03	5.45	5.29E-04
4'-NPTA	kaolinite	4.58	3.40E-03	5.11	1.22E-03	5.56	4.09E-04
4'-NPTA	goethite	4.63	3.05E-03	5.08	1.22E-03	5.50	4.44E-04
2'-NPTA	aqueous	4.45	3.64E-03	4.95	1.37E-03	5.45	4.80E-04
2'-NPTA	SiO_2	4.47	3.52E-03	4.98	1.31E-03	5.47	4.71E-04
2'-NPTA	Al_2O_3	4.48	3.41E-03	4.92	1.46E-03	5.41	5.21E-04
2'-NPTA	hectorite	4.40	3.70E-03	4.86	1.63E-03	5.50	4.45E-04
2'-NPTA	montmorillonite	4.45	3.52E-03	4.96	1.36E-03	5.49	4.58E-04
2'-NPTA	kaolinite	4.42	3.74E-03	4.91	1.55E-03	5.43	4.93E-04
2'-NPTA	goethite	4.42	3.84E-03	4.95	1.41E-03	5.43	4.90E-04

2.3.3 Hydrolysis of N-Me-PCA in Aqueous Solutions

The hydrolysis of N-Me-PCA (*N*-methyl-*N*-(4-nitrophenyl)-2-pyridinecarboxamide) was performed in aqueous solutions over pH 0.50-2.51 and pH 11.05-12.28 at ambient temperature. The results showed that N-Me-PCA readily hydrolyzed over pH 11.05-12.28 and the hydrolytic product N-methyl-4-nitroaniline (N-Me-NA) was obtained, however, over pH 0.50-2.51 the concentration of N-Me-PCA was stable during a 12-day period and the yield of N-Me-NA was negligible. In strong alkaline solutions, good mass balance was obtained, e.g., the reaction profile of N-Me-PCA at pH 11.05 shown in Figure 2.9. Furthermore, the plots of ln (C_t/C_0) versus time for the hydrolysis of N-Me-PCA in aqueous solutions over pH 11.05-12.28 were linear, for example, the plot for pH 11.05 was presented in Figure 2.10. Accordingly, hydrolysis of N-Me-PCA in alkaline aqueous solutions followed pseudo-first-order kinetics and the observed rate constants were derived from the linear plots. In addition, log k_{obs} was plotted versus solution pH (Figure 2.11). This pH-rate profile is linear over pH 11.05-12.28, indicating that hydrolysis rate constants increase as a function of pH with unit slope. Therefore, the hydrolysis of N-Me-PCA in above pH range is general base-catalyzed reaction.

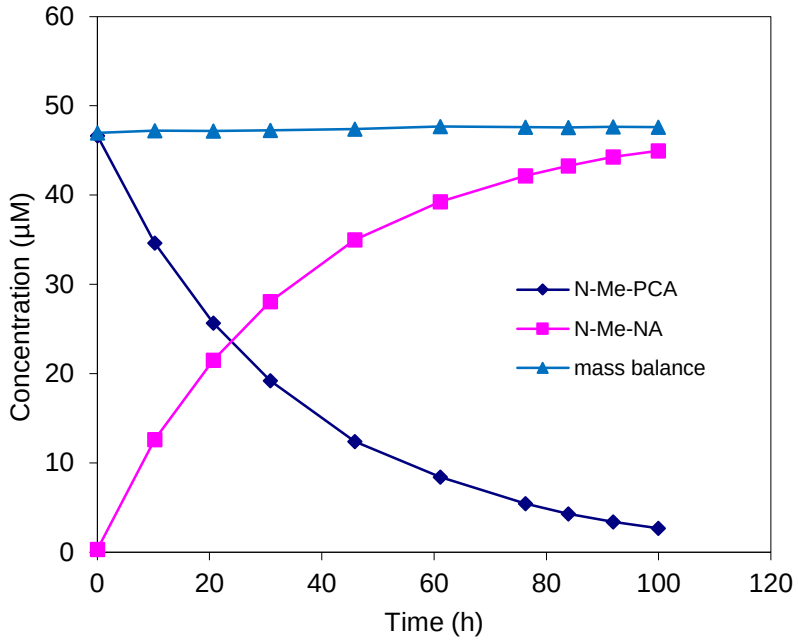

FIGURE 2.9. Hydrolysis of N-Me-PCA in aqueous solution at pH 11.05 under ambient temperature.

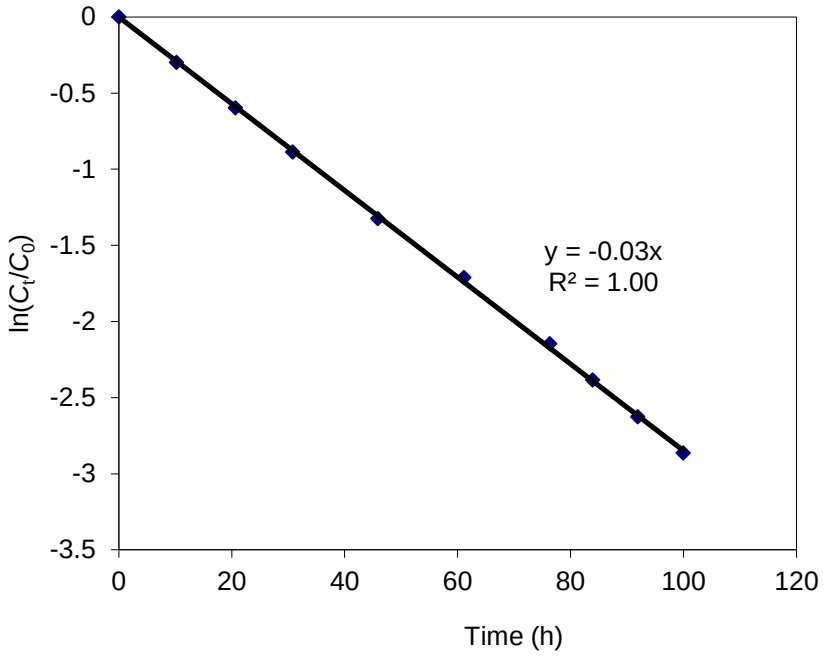

FIGURE 2.10. Plot of ln (C_t /C_0) versus reaction time for N-Me-PCA hydrolysis in aqueous solution at pH 11.05, where C_t and C_0 are the concentrations of N-Me-PCA at time *t* and 0, respectively.

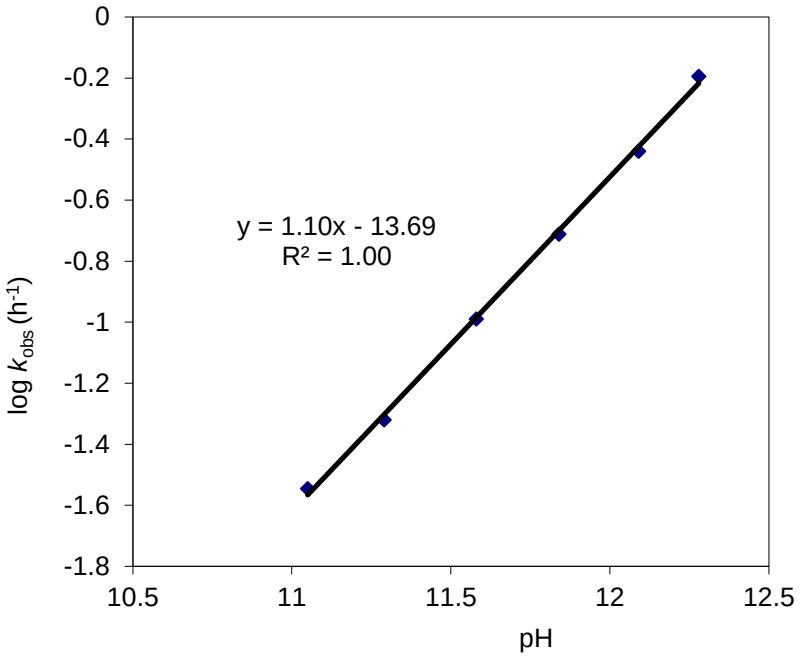

FIGURE 2.11. Plot of log k_{obs} versus pH for the hydrolysis of N-Me-PCA in aqueous solutions.

2.3.4 N-Me-PCA Adsorption

The stoichiometry of hydrolysis reaction illustrated by Figure 2.12 shows that 1 mol of N-Me-PCA can hydrolyze to 1 mol of 2-pyridinecarboxylic acid (2-PA) and 1 mol of N-Me-NA. To examine the mass balance for N-Me-PCA hydrolysis in mineral suspensions and aqueous solutions, the total concentrations of N-Me-PCA and N-Me-NA in supernatant were plotted versus reaction time (see Figure 2.13). The results showed that in SiO_2, Al_2O_3, kaolinite and goethite suspensions as well as aqueous solutions the total concentrations of N-Me-PCA and N-Me-NA were approximately stable at pH 9.5 and slightly decreased following the hydrolysis at pH 10, 10.5 and 11, while in hectorite and Na-montmorillonite suspensions the total concentrations increased as the reaction progressed. Since the total concentrations of N-Me-PCA and N-Me-NA in supernatant of SiO_2, Al_2O_3, kaolinite and goethite suspensions approximate to those in aqueous solutions, the adsorption of N-Me-PCA and N-Me-NA onto these minerals over pH 9.5-11 was insignificant. However, significant differences in the total dissolved concentrations of N-Me-PCA and N-Me-NA were observed between hectorite or Na-montmorillonite suspension and aqueous solution, especially at the beginning of hydrolysis. The less initial dissolved concentration of N-Me-PCA (t = 0, almost no hydrolysis product) in hectorite or Na-montmorillonite suspension than

that in aqueous solution indicated that N-Me-PCA adsorption occurred on those two minerals.

In order to study the influence of sorption on N-Me-PCA hydrolysis, sorption experiments with N-Me-PCA as well as one of its hydrolytic products, picolinic acid, were performed in hectorite and Na-montmorillonite suspensions respectively. The results showed that sorption of picolinic acid was negligible and only N-Me-PCA adsorbed to those clay minerals. Adsorption isotherms of N-Me-PCA on hectorite and Na-montmorillonite were presented in Figure 2.14 and 2.15 respectively. According to classification by Giles (Giles, Smith et al. 1974), when the dissolved concentration of N-Me-PCA < 60 µM, sorption isotherms of N-Me-PCA onto hectorite are C-curve for pH 9.5, S-curve for pH 10 and 10.5, and L-curve for pH 11 (Figure 2.14); whereas sorption isotherms onto Na-montmorillonite are S-curve for pH 9.5, 10 and 10.5, and C-curve for pH 11 (Figure 2.15). It is illustrated that adsorption of N-Me-PCA onto hectorite and Na-montmorillonite is dependent on suspension pH.

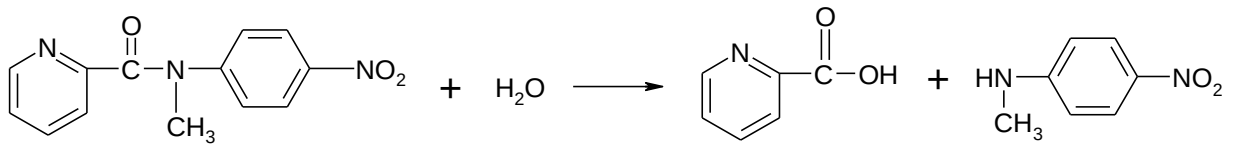

N-methyl-*N*-(4-nitrophenyl)-2-pyridinecarboxamide

2-pyridinecarboxylic acid

N-methyl-4-nitroaniline

FIGURE 2.12. The equation for N-Me-PCA hydrolysis.

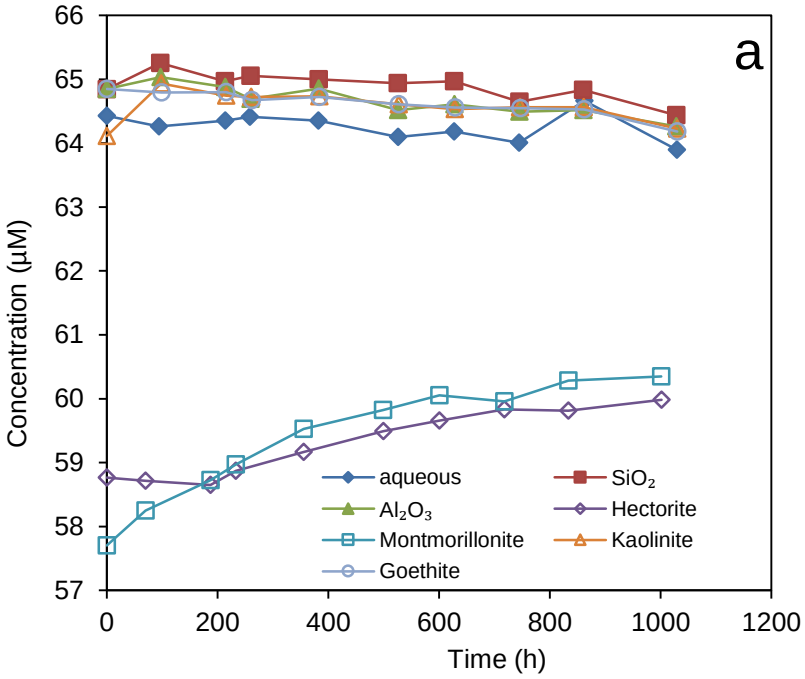

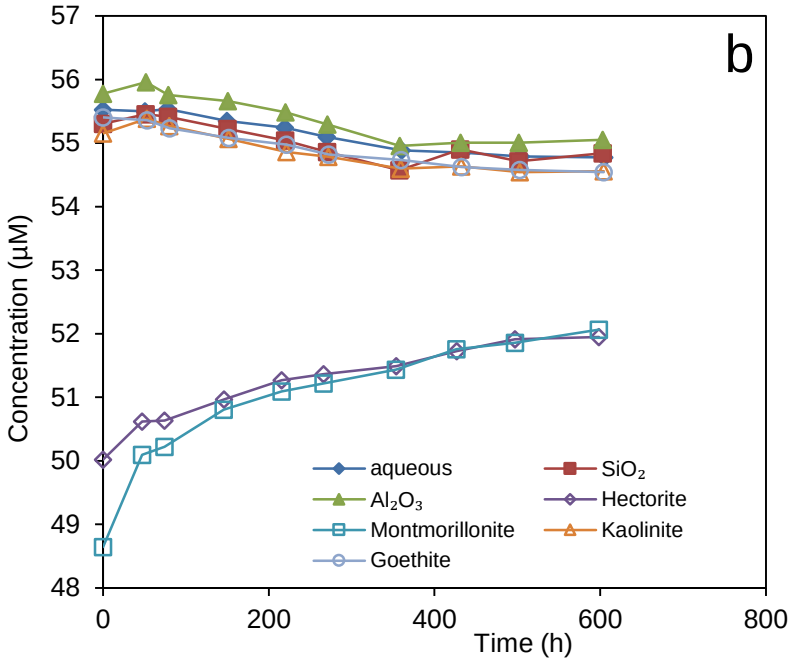
b
Concentration (µM)
Time (h)
aqueous
SiO2
Al2O3
Hectorite
Montmorillonite
Kaolinite
Goethite

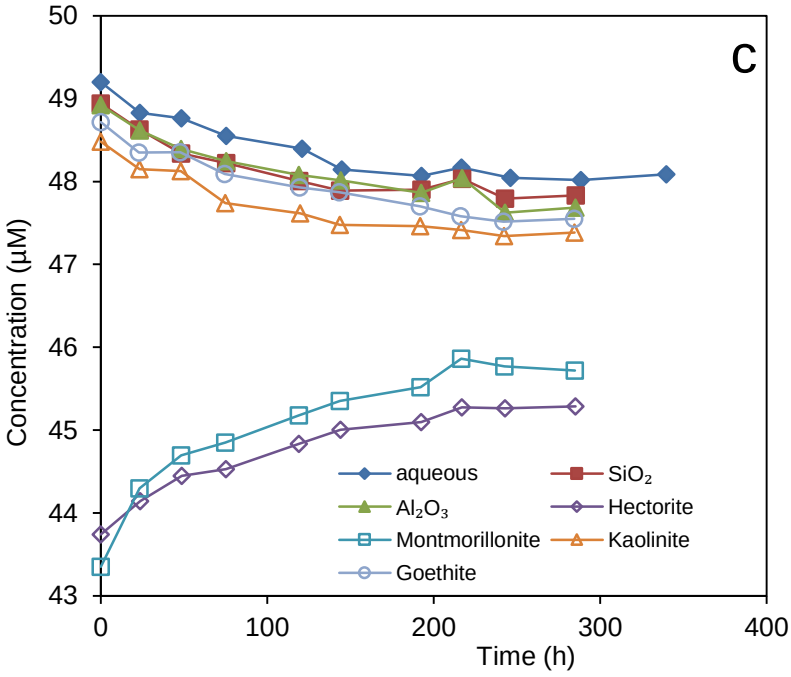
c
Concentration (µM)
Time (h)
aqueous
SiO2
Al2O3
Hectorite
Montmorillonite
Kaolinite
Goethite

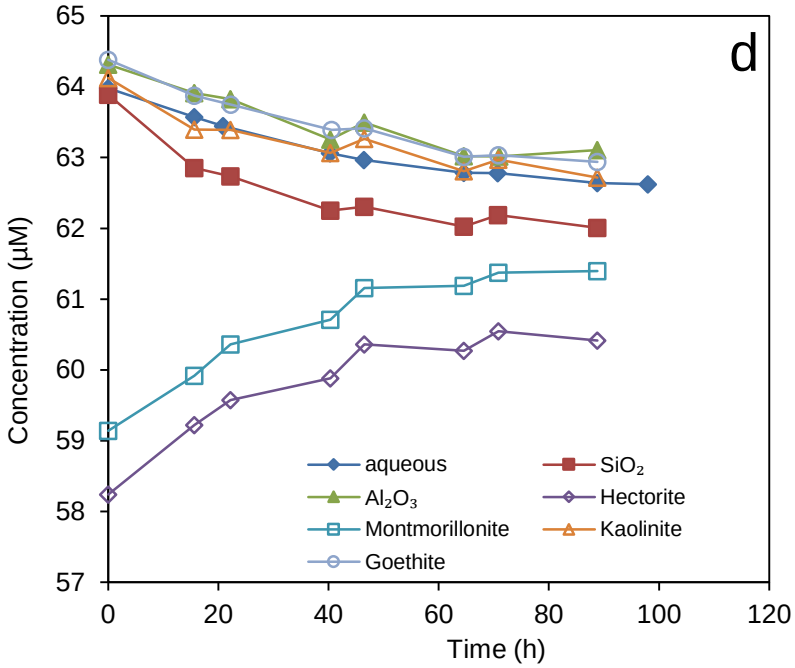

FIGURE 2.13. Mass balance evaluation for N-Me-PCA hydrolysis in a series of mineral suspensions (SiO_2, Al_2O_3, hectorite, Na-montmorillonite, kaolinite, and goethite) as well as aqueous solutions at: (a) pH 9.5, (b) pH 10, (c) pH 10.5, and (d) pH 11. The total concentrations of N-Me-PCA and N-Me-NA in supernatant solutions were plotted versus reaction time.

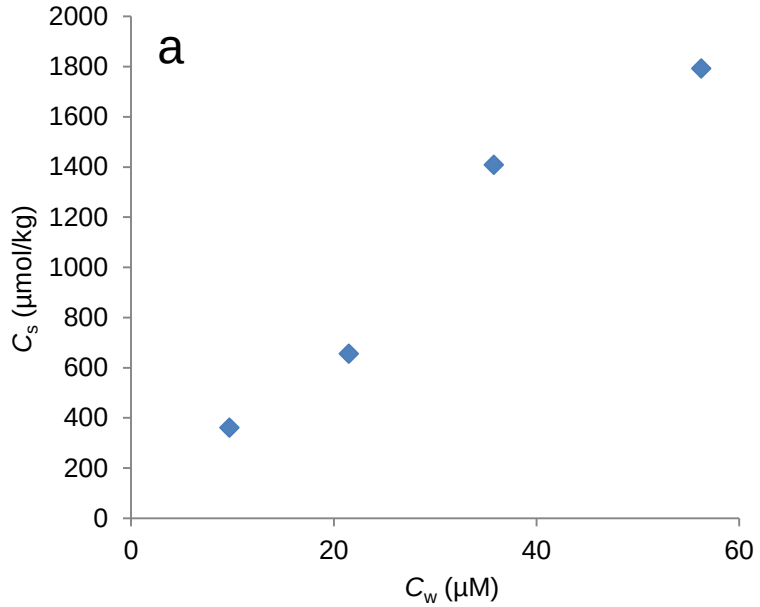

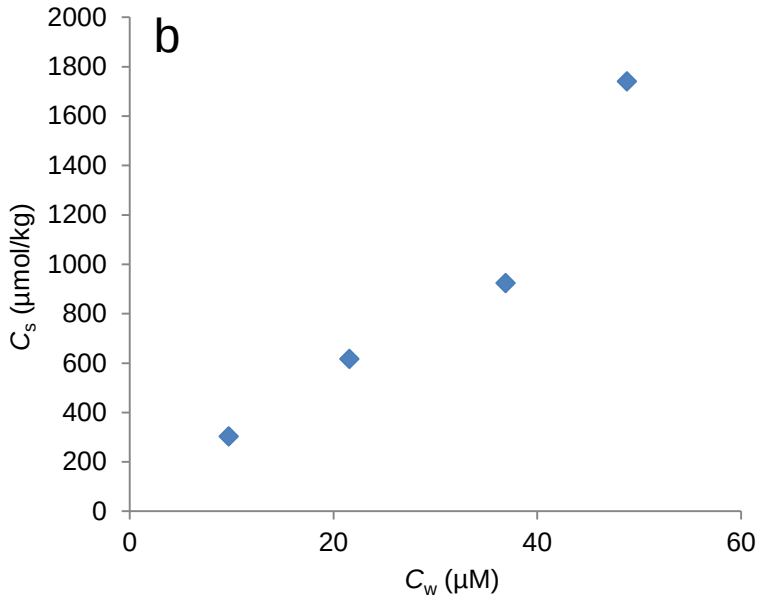
b
2000
1800
1600
1400
1200
1000
800
600
400
200
0
C_s (µmol/kg)
0
20
40
60
C_w (µM)

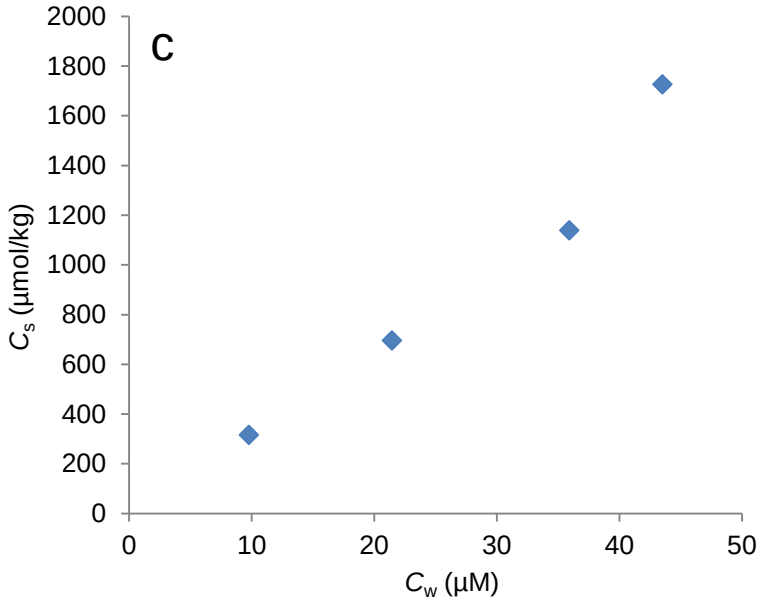
c
2000
1800
1600
1400
1200
1000
800
600
400
200
0
C_s (µmol/kg)
0
10
20
30
40
50
C_w (µM)

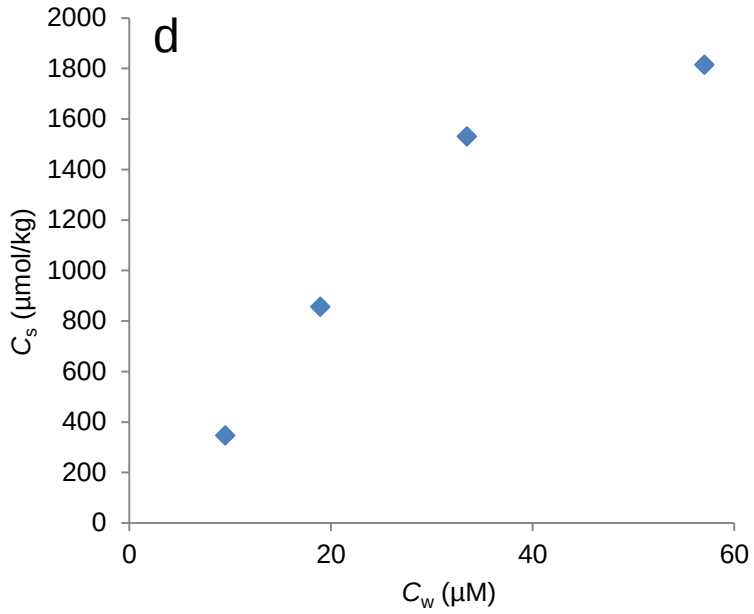

FIGURE 2.14. Adsorption isotherms of N-Me-PCA on hectorite at (a) pH 9.5, (b) pH 10, (c) pH 10.5, and (d) pH 11, where C_s is the concentration of N-Me-PCA in sorbed state and C_w is that in dissolved state.

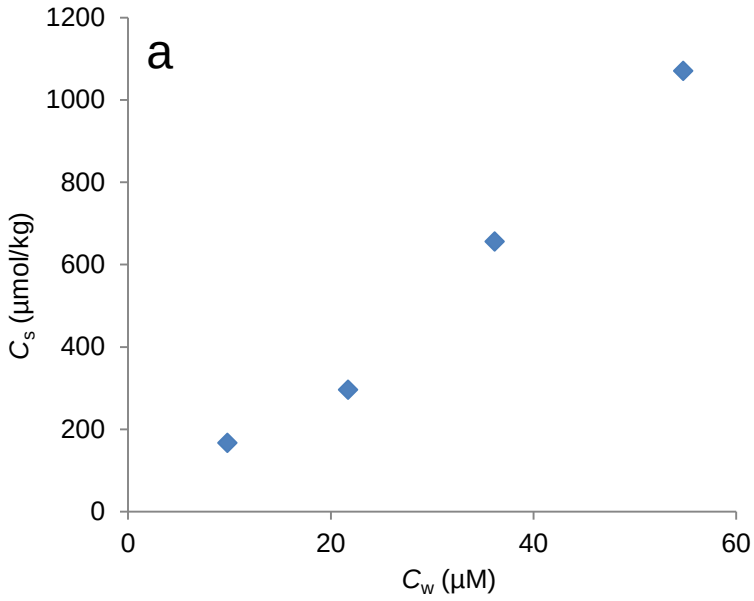

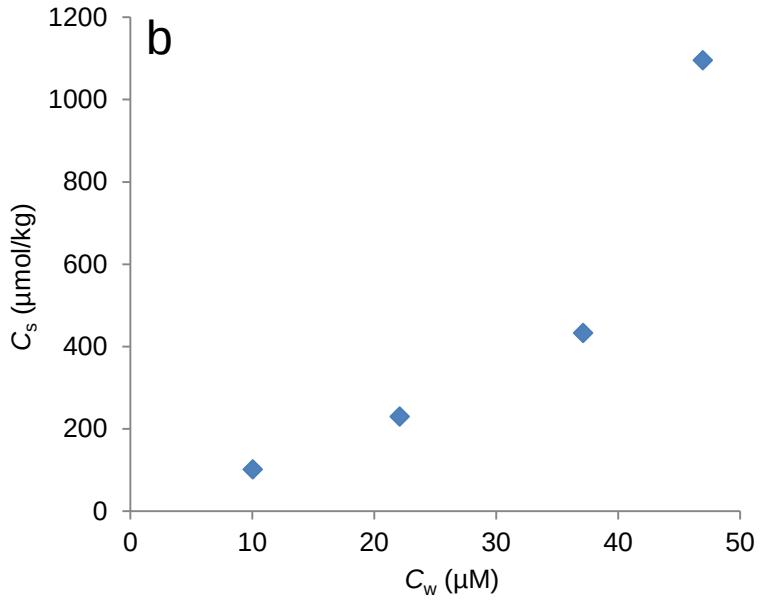
b
1200
1000
800
600
400
200
0
C_s (µmol/kg)
0
10
20
30
40
50
C_w (µM)

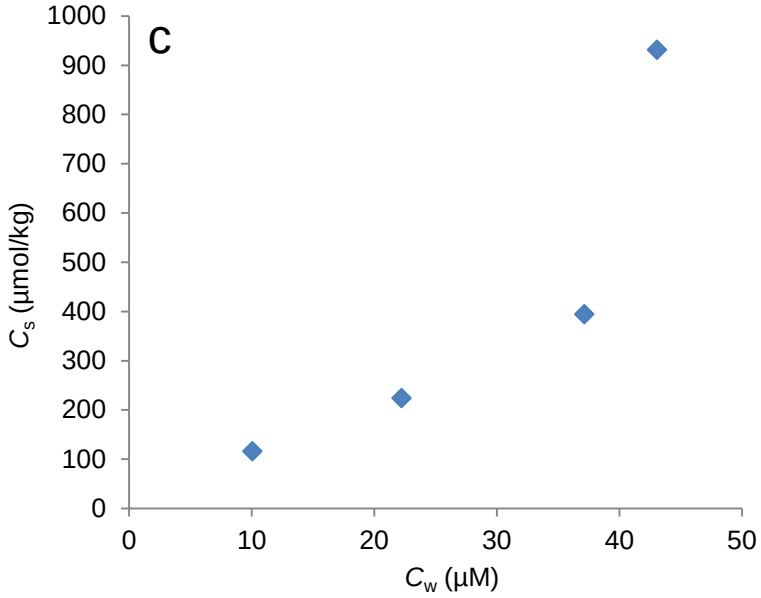
c
1000
900
800
700
600
500
400
300
200
100
0
C_s (µmol/kg)
0
10
20
30
40
50
C_w (µM)

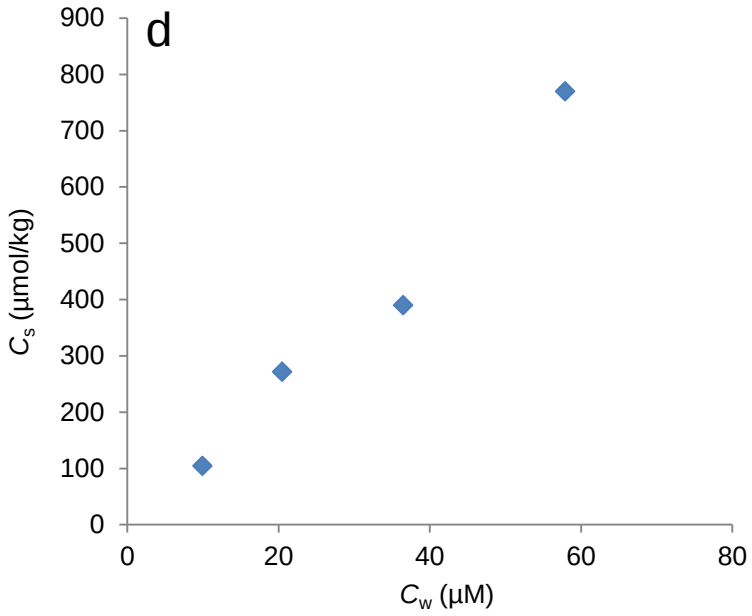

FIGURE 2.15. Adsorption isotherms of N-Me-PCA on Na-montmorillonite at (a) pH 9.5, (b) pH 10, (c) pH 10.5, and (d) pH 11, where C_s is the concentration of N-Me-PCA in sorbed state and C_w is that in dissolved state.

2.3.5 Hydrolysis of N-Me-PCA in Mineral Suspensions

As stated above, measurable reaction kinetics was only obtained for base-catalyzed hydrolysis of N-Me-PCA. Therefore, the influence of minerals on N-Me-PCA hydrolysis was studied at pH 9.5, 10, 10.5, and 11. The results showed that N-Me-PCA also readily hydrolyzed to the products picolinic acid and N-Me-NA in all mineral suspensions. For instance, the reaction profile of N-Me-PCA in kaolinite suspension at pH 10.00 was presented in Figure 2.16, showing that the dissolved concentration of N-Me-PCA decreased gradually and the hydrolysis products picolinic acid and N-Me-NA were obtained correspondingly. Moreover, good mass balance was also observed during the reaction. The hydrolysis kinetics of N-Me-PCA in mineral suspensions can be assessed similarly as in aqueous solutions, in which the pseudo-first-order kinetics has been confirmed. Hence, the observed rate constants can be derived by applying linear regression on the curve of ln (C_t/C_0) versus time. Even though sorption also occurred on hectorite and Na-montmorillonite, the plots of ln (C_t/C_0) versus time are still linear, for example, Figure 2.17 shows good linearity of the curve for N-Me-PCA hydrolysis in hectorite and Na-montmorillonite suspensions at pH 10.

The observed rate constants of N-Me-PCA hydrolysis in different mineral suspensions and aqueous solutions were given in Figure 2.18, illustrating that: (1) the hydrolysis

rate constants of N-Me-PCA are slightly lower in hectorite and Na-montmorillonite suspensions compared with aqueous solution and the other mineral suspensions; (2) the rate constants in mineral suspensions at certain pH are of the same order of magnitude as those in the corresponding aqueous solutions. Therefore the influence of minerals on N-Me-PCA hydrolysis is insignificant over pH 9.5-11. In Figure 2.19, hydrolysis rate constants of N-Me-PCA were plotted against solution/suspension pH on the logarithmic scale. The plots show good linearity and log k_{obs} increases as a function of pH with unit slope for all mineral suspensions, indicating that base-catalyzed hydrolysis is dominant throughout pH 9.5-11.

As possessing chelating functional groups, e.g., carbonyl group and nitrogen ligand donor group, picolinate esters and picolinanilides are susceptible to metal ion and/or mineral surface catalyzed hydrolysis (Przystas and Fife 1990, Torrents and Stone 1991, Sayre, Reddy et al. 1992, Fife and Bembi 1993, Tang and Sayre 1993). For example, in contrast with homogeneous solution, hydrolysis of phenyl picolinate was promoted in TiO_2 and FeOOH suspensions because of a chelate formation involving the carbonyl group and surface bound metal (Torrents and Stone 1991). In addition, significant rate enhancement has been observed for the hydrolysis of N-Me-PCA and its 6-carboxy derivative by divalent metal ions including Cu^{II}, Zn^{II}, Ni^{II} and Co^{II} (Tang and Sayre 1993). However, in this study the examined minerals have no significant influence on N-Me-PCA hydrolysis even though its adsorption onto hectorite and Na-montmorillonite occurred.

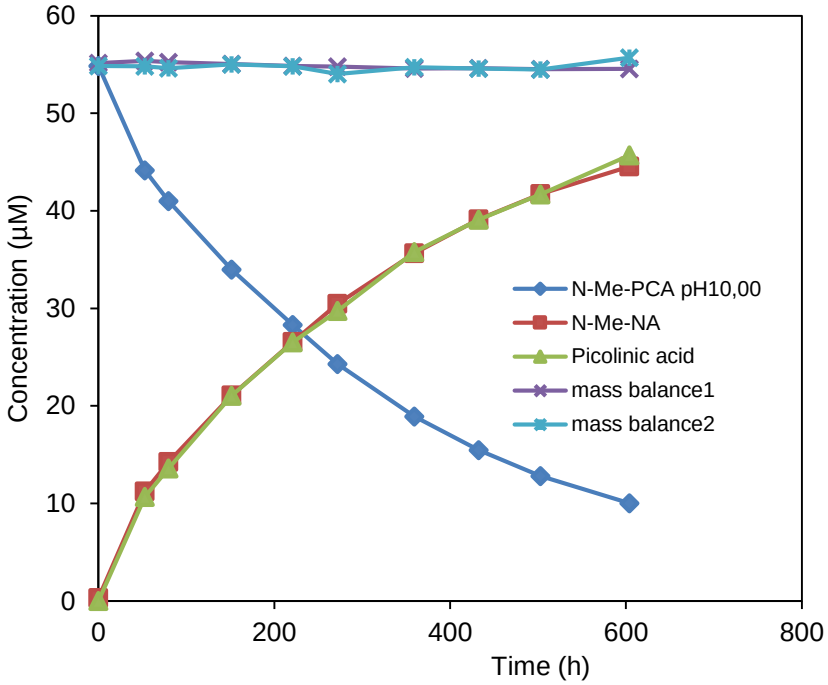

FIGURE 2.16. Hydrolysis of N-Me-PCA in kaolinite suspension at pH 10.00 under ambient temperature. Dissolved concentrations of N-Me-PCA as well as its products N-Me-NA and picolinic acid were plotted versus reaction time. Mass balance 1 involved the total dissolved concentrations of N-Me-PCA and N-Me-NA, while mass balance 2 involved the total dissolved concentrations of N-Me-PCA and picolinic acid.

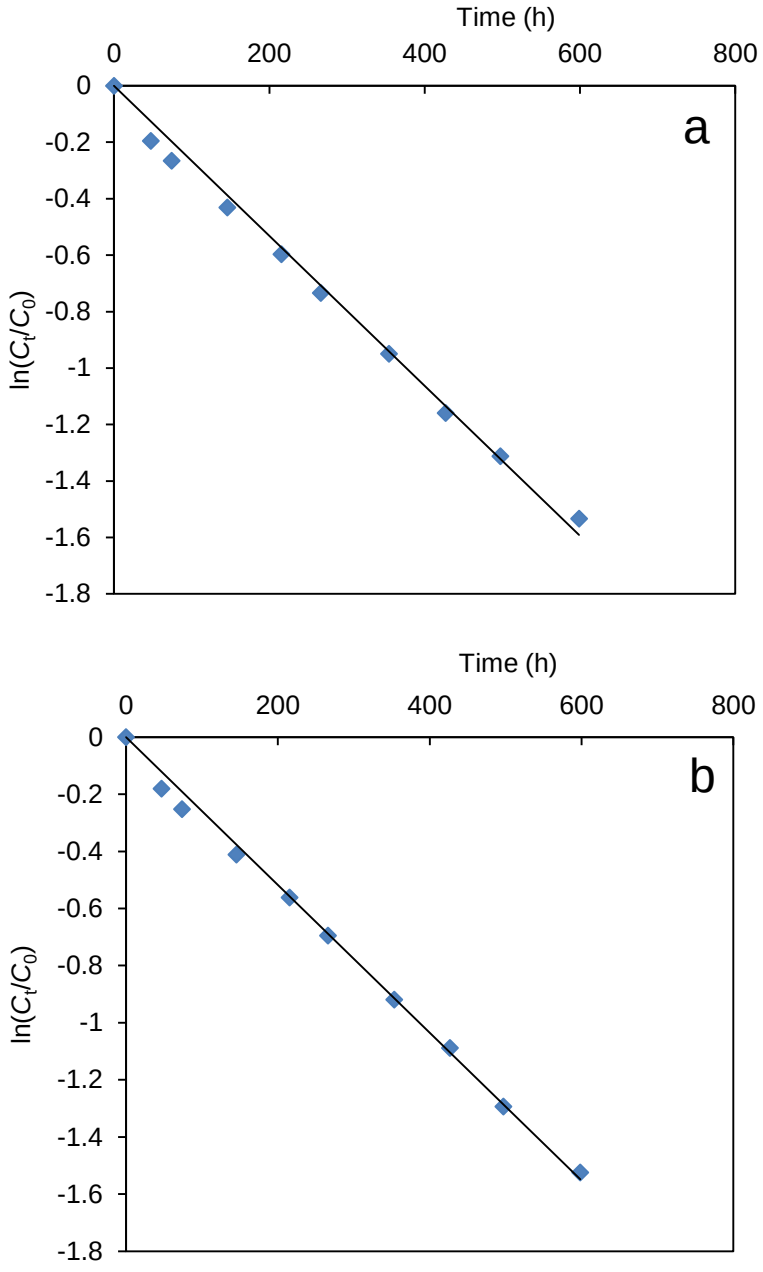

FIGURE 2.17. Plots of ln (C_t /C_0) versus reaction time for N-Me-PCA hydrolysis, where C_t is the dissolved concentration of N-Me-PCA at time *t* and C_0 is the initial dissolved concentration of N-Me-PCA: (a) in hectorite suspension at pH 10.02, (b) in Na-montmorillonite suspension at pH 10.00.

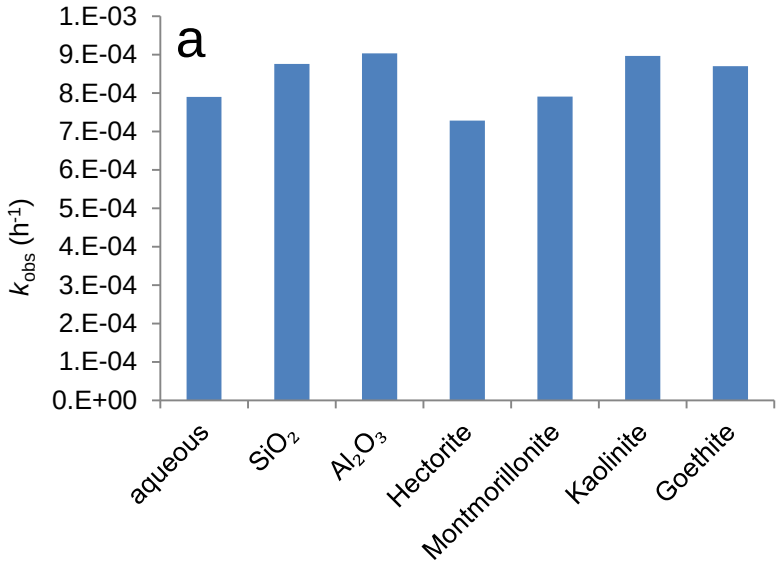
a
1.E-03
9.E-04
8.E-04
7.E-04
6.E-04
5.E-04
4.E-04
3.E-04
2.E-04
1.E-04
0.E+00
k_{obs} (h^{-1})
aqueous
SiO_2
Al_2O_3
Hectorite
Montmorillonite
Kaolinite
Goethite

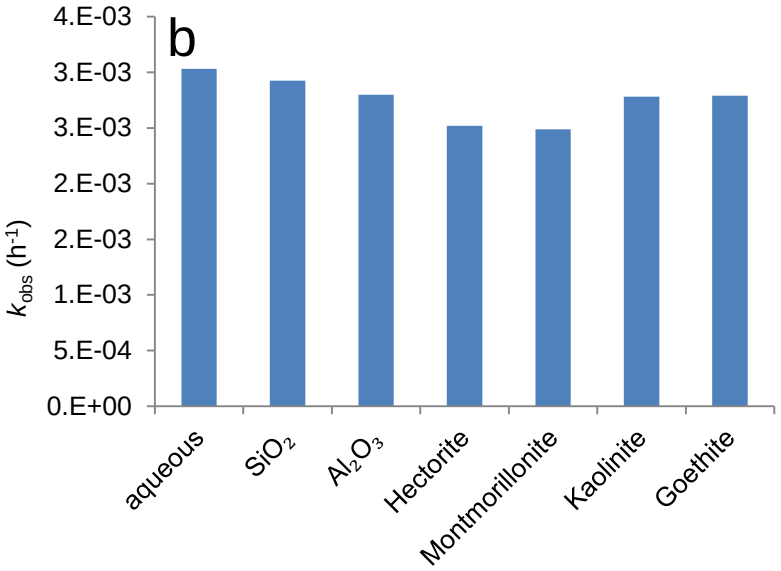
b
4.E-03
3.E-03
3.E-03
2.E-03
2.E-03
1.E-03
5.E-04
0.E+00
k_{obs} (h^{-1})
aqueous
SiO_2
Al_2O_3
Hectorite
Montmorillonite
Kaolinite
Goethite

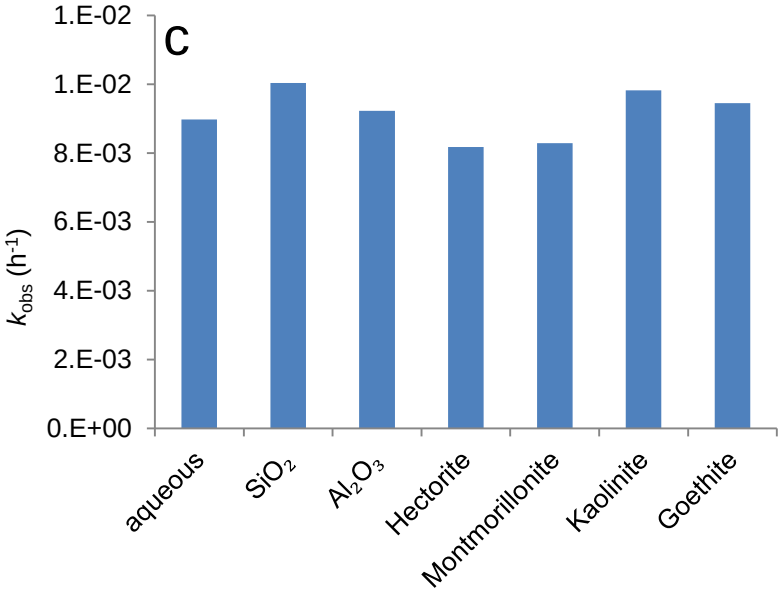
c
1.E-02
1.E-02
8.E-03
6.E-03
4.E-03
2.E-03
0.E+00
k_{obs} (h^{-1})
aqueous
SiO_2
Al_2O_3
Hectorite
Montmorillonite
Kaolinite
Goethite

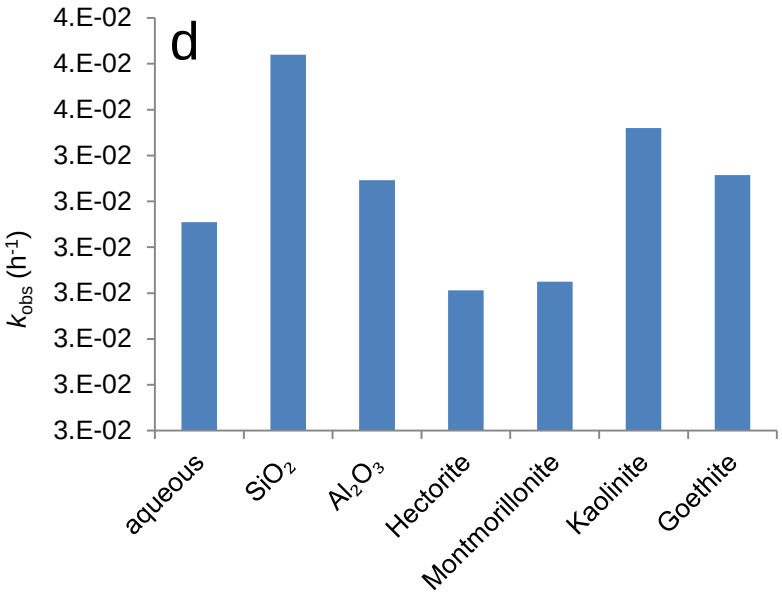

FIGURE 2.18. The observed rate constants of N-Me-PCA hydrolysis in mineral suspensions as well as aqueous solutions at: (a) pH 9.5, (b) pH 10, (c) pH 10.5, and (d) pH 11.

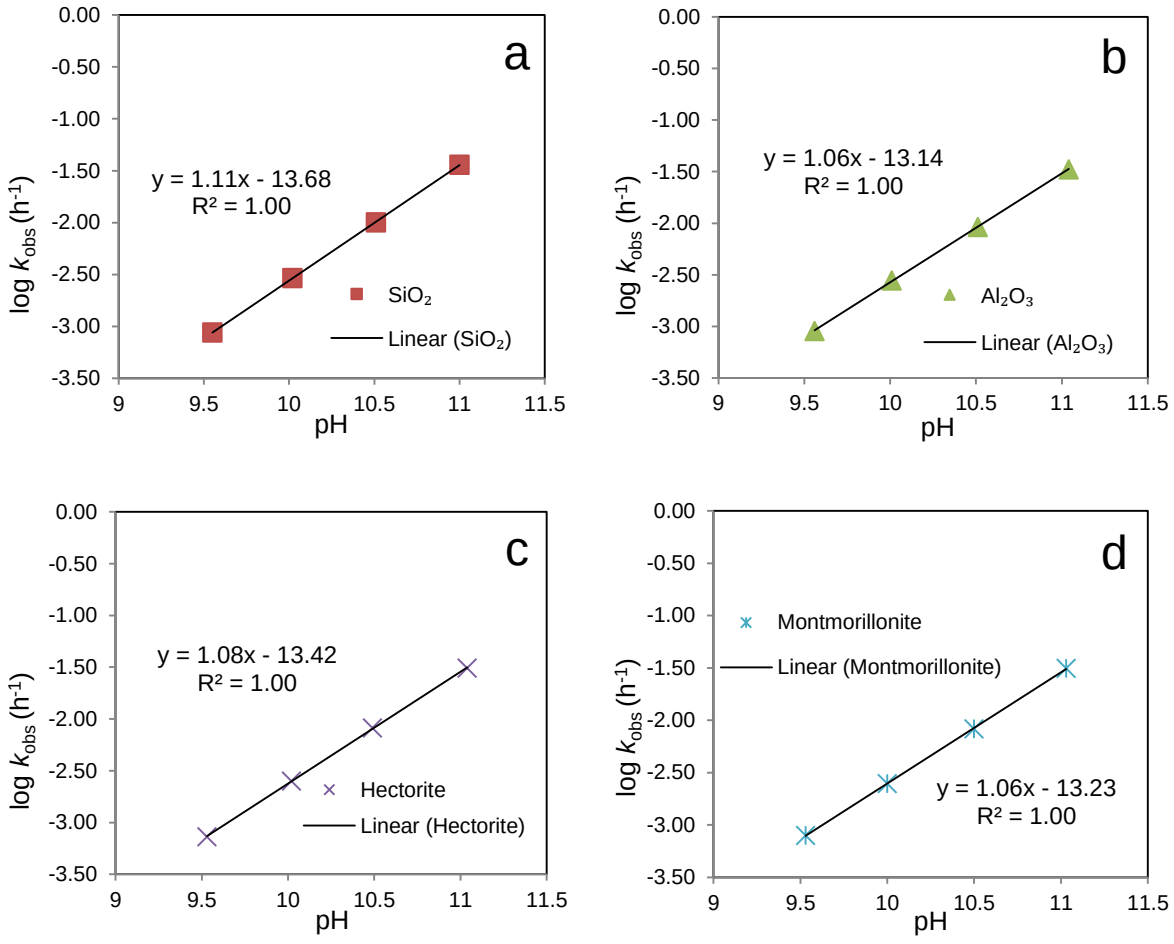

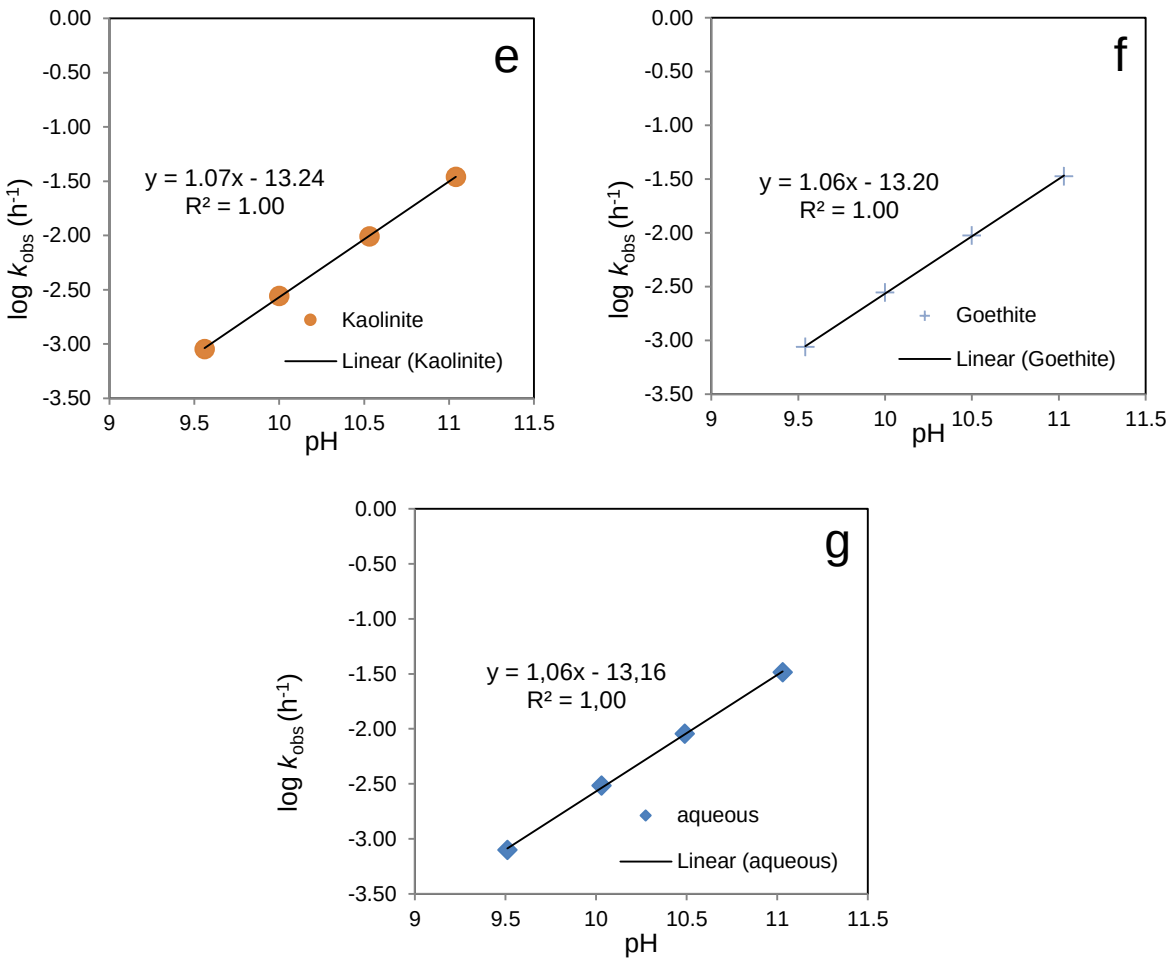

FIGURE 2.19. Plots of log k_{obs} versus pH for N-Me-PCA hydrolysis in (a) SiO_2 suspension, (b) Al_2O_3 suspension, (c) hectorite suspension, (d) Na-montmorillonite suspension, (e) kaolinite suspension, (f) goethite suspension and (g) aqueous solution.

2.4 Conclusions

The objective of the present study was to investigate if the hydrolysis of the amides with adjacent functional groups can be promoted or inhibited by mineral surfaces. The amides hydrolysis was first studied in homogeneous solutions. For 4'- and 2'-NPTA, hydrolysis is intramolecular catalyzed reaction in acidic solutions (pH < 4.3), and the neutral species are the active forms in the intramolecular catalysis. The mass loss was observed in hydrolysis reaction and a by-product *N*-phenylphthalimide may be formed due to the nucleophilic attack of the amide nitrogen on the carboxylic carbonyl carbon followed by water elimination. Furthermore, a series of minerals including SiO_2, Al_2O_3, goethite, kaolinite, hectorite and Na-rich montmorillonite were selected to study the influence on 4'- and 2'-NPTA hydrolysis. The results show that the observed rate

constants of 4'- and 2'-NPTA in acidic mineral suspensions decrease as pH increases and are of the same order of magnitude as those in the corresponding aqueous solutions. Consequently, the investigated minerals have little influence on the intramolecular catalyzed hydrolysis of 4'- and 2'-NPTA. In addition, no measurable adsorption on mineral surfaces was observed for 4'- and 2'-NPTA as well as the products 4- and 2-nitroaniline.

For N-Me-PCA, hydrolysis in aqueous solutions and mineral suspensions is general base-catalyzed reaction over pH 9.5-11. Mineral surfaces have no significant effect on N-Me-PCA hydrolysis, the observed rate constants at certain pH are only slightly lower in hectorite and Na-montmorillonite suspensions compared with aqueous solutions and the other mineral suspensions. Moreover, adsorption of N-Me-PCA occurred on hectorite and Na-montmorillonite to different extent depending on suspension pH.

References

Fife, T. H. and R. Bembi (1993). "Metal ion promoted hydroxide ion and water catalyzed hydrolysis of amides. Effects of the acyl group and the leaving group." Journal of the American Chemical Society **115**(24): 11358-11363.

Giles, C. H., et al. (1974). "A general treatment and classification of the solute adsorption isotherm. I. Theoretical." Journal of Colloid and Interface Science **47**(3): 755-765.

Granados, A., et al. (1995). "Kinetic study on the hydrolysis of 1-N-naphthylphthalamic acid (Naptalam)." Journal of Agricultural and Food Chemistry **43**(9): 2493-2496.

Hawkins, M. D. (1976). "Intramolecular catalysis. Part III.1 hydrolysis of 3′- and 4′-substituted phthalanilic acids [o-(N-Phenylcarbamoyl)benzoic Acids]." Journal of the Chemical Society, Perkin Transactions 2(6): 642-647.

Huang, C. H. and A. T. Stone (1999). "Hydrolysis of naptalam and structurally related amides: Inhibition by dissolved metal ions and metal (hydr)oxide surfaces." Journal of Agricultural and Food Chemistry **47**(10): 4425-4434.

Przystas, T. J. and T. H. Fife (1990). "The metal-ion-promoted water- and hydroxide-ion-catalysed hydrolysis of amides." Journal of the Chemical Society, Perkin Transactions 2(3): 393-399.

Pusino, A., et al. (1996). "Montmorillonite Surface-Catalyzed Hydrolysis of Fenoxaprop-ethyl." Journal of Agricultural and Food Chemistry **44**(4): 1150-1154.

Reddy, K. V., et al. (1991). "Divalent metal ion catalyzed hydrolysis of picolinanilides." Inorganic Chemistry **30**(18): 3520-3525.

Sayre, L. M., et al. (1992). "Metal ion catalysis of amide hydrolysis. Very large rate enhancements by copper(II) in the hydrolysis of simple ligand-functionalized tertiary amides." Inorganic Chemistry **31**(6): 935-937.

Shin, J. Y. and M. A. Cheney (2004). "Abiotic transformation of atrazine in aqueous suspension of four synthetic manganese oxides." Colloids and Surfaces A: Physicochemical and Engineering Aspects **242**(1–3): 85-92.

Smolen, J. M. and A. T. Stone (1998). "Metal (hydr)oxide surface-catalyzed hydrolysis of chlorpyrifos-methyl, chlorpyrifos-methyl oxon, and paraoxon." Soil Science Society of America Journal **62**(3): 636-643.

Tang, W. and L. M. Sayre (1993). "Divalent metal ion catalyzed hydrolysis of N-methyl-4′-nitro-6-carboxypicolinanilide. pH-Rate profile transitions and buffer inhibition." Inorganic Chemistry **32**(25): 5785-5791.

Torrents, A. and A. T. Stone (1991). "Hydrolysis of phenyl picolinate at the mineral/water interface." Environmental Science and Technology **25**(1): 143-149.

Torrents, A. and A. T. Stone (1993). "Catalysis of picolinate ester hydrolysis at the oxide/water interface: Inhibition by coadsorbed species." Environmental Science and Technology **27**(6): 1060-1067.

Wei, J., et al. (2001). "Influence of Clay Minerals on the Hydrolysis of Carbamate Pesticides." Environmental Science & Technology **35**(11): 2226-2232.

3. Hydrolysis of Metalaxyl and Metalaxyl-M at the Mineral-Water Interface

3.1 Introduction

Many pesticides are chiral molecules which have one or more stereogenic centers and give rise to two or more enantiomers/stereoisomers. In general the two enantiomers have the same physical and chemical properties with respect to achiral environments. However, they may react differently in chiral environments (Carey and Sundberg 2007), e.g., at biological systems, each enantiomer may have different biological activity, toxicity, environmental fate and effect on beneficial and nontarget organisms (Buerge, Poiger et al. 2003).

Metalaxyl is a chiral compound due to the presence of an asymmetric carbon in the alkyl moiety and consists of a single pair of enantiomers (*R*-metalaxyl and *S*-metalaxyl, see Figure 3.1 for the absolute configurations). The two enantiomers rotate plane polarized light in opposite directions, where *R*-enantiomer is levorotatory and *S*-enantiomer is dextrorotatory (Zadra, Marucchini et al. 2002). Metalaxyl is a systemic fungicide used to control plant diseases caused by the Oomycetes or water-mold fungi. The mode of action is to interfere with protein synthesis by inhibiting the biosynthesis of ribosomal RNA, especially RNA polymerization (Hutson 1999, Müller and Gisi 2008). It is registered for use on a variety of crops/sites: primarily citrus, cotton, cucurbits, onions, ornamentals, potatoes, soybeans, tobacco, tomatoes and turf (United States. Environmental Protection Agency. Prevention and Substances 1994). Metalaxyl, the first of phenylamide fungicides, was initially introduced into the market in 1977 as the racemic mixture although its fungicidal activity is almost entirely from the *R*-enantiomer (Buser, Müller et al. 2002, Müller and Gisi 2008). In 1996, metalaxyl-M, enriched with biologically active *R*-enantiomer, was introduced to replace the racemic product metalaxyl and started the general use of chiral pesticides (Müller and Gisi 2008). This replacement reduces chemicals dispersed in the environment and is more favorable to environmental profile due to the low application rate of isomer pure products (only half the amounts compared with racemic products).

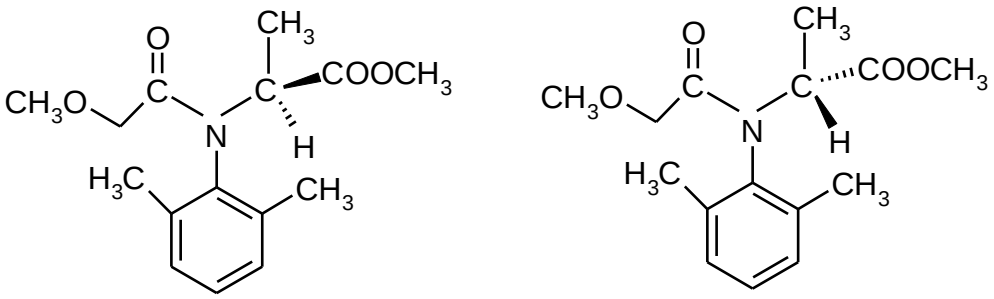

S-(+)-metalaxyl *R*-(-)-metalaxyl

FIGURE 3.1. Chemical structure of *R*- and *S*-metalaxyl.

Metalaxyl is chemically stable, but it is readily biodegraded in soils, plants and animals by hydrolysis, amid bond cleavage, alkyl and aryl hydroxylation and *N*-dealkylation (Hutson 1999). The major metabolite of metalaxyl in soil is the hydrolysis product, i.e. metalaxyl carboxylic acid (MX-acid). Hydrolysis to primary carboxylic acid metabolite accounts for 40-50% of degradation of metalaxyl in soil with the remaining being degraded via other pathways (Hutson 1999, Buser, Müller et al. 2002). Since metalaxyl carboxylic acid is formed by the cleavage of the ester and still contains the asymmetric carbon (stereogenic center), MX-acid also shows C-chirality.

Biological active *R*-metalaxyl and inactive *S*-metalaxyl are expected to behave differently with respect to biotic degradation when *rac*-metalaxyl is released into the environment, resulting in one of enantiomers be enriched. When pure isomer product metalaxyl-M is used, the configurational stability of enantiomers should be taken into account since both the effectiveness of pesticide on plant diseases control and its environmental behavior are concerned. The degradation/dissipation of metalaxyl has been investigated in soils under laboratory conditions. It was shown to be enantioselective with different preferences on soil pH: *R*-metalaxyl degraded faster than its antipode in slightly acidic to alkaline aerobic soils while *S*-metalaxyl degraded more rapidly in acidic aerobic soils and anaerobic soils (Buser, Müller et al. 2002, Buerge, Poiger et al. 2003). The stereo-/enantioselectivity for the degradation of metalaxyl has also been reported in other conditions, for example in sewage sludge (Müller and Buser 1995, Chen and Liu 2009), tropical and temperate soils (Monkiedje, Spiteller et al. 2003), and field conditions (Monkiedje, Zuehlke et al. 2007). In the field, metalaxyl was found to have much shorter half-lives compared with laboratory conditions, and its elimination rates are dependent on formulation with the copper containing formulation being degraded slower (Monkiedje, Zuehlke et al. 2007).

Moreover, both metalaxyl and metalaxyl-M were found to be configurationally stable either in plants or in different types of soils (Buser, Müller et al. 2002, Zadra, Marucchini et al. 2002, Monkiedje, Zuehlke et al. 2007).

Mineral is an important fraction of soil and may interact with some polar or weakly polar pesticides due to the specific surface properties. Catalytic effects of metal oxides and clay minerals on organic chemicals hydrolysis were found by some researchers (Torrents and Stone 1991, Torrents and Stone 1993, Huang and Stone 1999, Wei, Furrer et al. 2001). For example, Torrents and Stone (1991) observed that TiO_2 and FeOOH can promote the hydrolysis of phenyl picolinate comparing with homogeneous solution, however, SiO_2, Al_2O_3 and Fe_2O_3 exhibit no effects on hydrolysis. Furthermore, the influence of clay minerals on hydrolysis of five carbamate pesticides has been studied by Wei et al. (2001), showing that montmorillonite has most significant effects on the carbamates hydrolysis and can either enhance or inhibit hydrolysis with regard to different pesticides.

In this study, hydrolysis experiments for metalaxyl and metalaxyl-M were performed in aqueous solution and mineral suspension to examine: (i) the stereo-selectivity of metalaxyl hydrolysis; (ii) the configurational stability of metalaxyl and metalaxyl-M during the hydrolysis; (iii) the influence of oxides (SiO_2, Al_2O_3 and α-FeOOH) and clay minerals (hectorite, Na-montmorillonite and kaolinite) on the hydrolysis.

3.2 Experimental Section

3.2.1 Chemicals

Analytical standards (purities, >99%) of metalaxyl (*rac*-metalaxyl, 2-[(2,6-dimethylphenyl) methoxyacetylamino] propionic acid methyl ester) and metalaxyl-M (*R*-metalaxyl, (R)-2-[(2,6-dimethylphenyl) methoxyacetylamino] propionic acid methyl ester) were purchased from Sigma-Aldrich (Steinheim, Germany). Racemic metalaxyl fungicide (Tech. Pellets, 96.1%), *R*-enantiomer enriched fungicide metalaxyl-M (Tech., 97.1%), *S*-metalaxyl ((S)-2-[(2,6-dimethylphenyl) methoxyacetylamino] propionic acid methyl ester, 98.3%), metalaxyl carboxylic acid (MX-acid, 2-[(2,6-dimethylphenyl)-methoxyacetyl-amino]-propionic acid, 99%) and *R*-metalaxyl carboxylic acid (*R*-MX-acid, (R)- 2-[(2,6-dimethylphenyl)-methoxyacetyl-amino]-propionic acid, 90%) were obtained from Syngenta (Muenchwilen, Switzerland). All compounds were used without further purification.

3.2.2 Minerals

To study the influence of mineral surfaces on chiral pesticides hydrolysis, some oxides and clay minerals were applied. Oxides include amorphous fumed silica (SiO_2,), highly dispersed fumed aluminum oxide (Al_2O_3, AEROXIDE® Alu C) and goethite (α-FeOOH, Bayferrox® 920 Z). Three types of clay minerals, hectorite (SHCa-1), Na-rich montmorillonite (SWy-2) and well crystallized kaolinite (KGa-1), were obtained from the Source Clays Repository of The Clay Minerals Society (Chantilly VA, USA). Both oxides and clay minerals were used without further treatment or purification. Some physical and chemical properties of the minerals are listed in Table 3.1.

TABLE 3.1. The Properties of Oxides and Clay Minerals Used in this Study

Mineral	Source	CEC[a] (meq/100g)	Surface Area (m^2/g)
SiO_2	Alfa Aesar	n.d.[b]	350 – 410
Al_2O_3	Evonik Degussa	n.d.	100 ± 15
Hectorite (SHCa-1)	San Bernardino County, California	43.9	63.19 ± 0.50
Na-Montmorillonite (SWy-2)	Crook County, Wyoming	76.4	31.82 ± 0.22
Kaolinite (KGa-1)	Washington County, Georgia	2.0	10.05 ± 0.02
α-FeOOH	LANXESS	n.d.	9.214

[a] cation exchange capacity. [b] n.d., not determined.

3.2.3 Hydrolysis Experiments

To study the influence of pH on metalaxyl hydrolysis, preliminary experiments were carried out in aqueous solution over pH 2-5 and pH 9.5-12. The reaction solution was initially prepared with 10 mM NaCl in a 50 mL brown serum bottle. At pH ≤ 2.5 or pH ≥ 11.5, HCl or NaOH was used to buffer the solution, while in the range of pH 3-4, 4.5-5 and 9.5-11, 10 mM formate buffer, acetate buffer and carbonate buffer were applied respectively. The pesticide stock solution (~1 mM) was prepared by dissolving a certain amount of racemic metalaxyl in 10 mM NaCl solution. Then 5 mL freshly prepared stock solution was added to 45 mL buffered NaCl solution, making the initial concentration of *rac*-metalaxyl be ~100 µM (~50 µM for each enantiomer). After the

solution was fully mixed by stirring, duplicate samples were taken immediately (as t = 0) and measured by stereo-selective HPLC. Then equal aliquots of reaction solution were transferred to 2 mL borosilicate glass vials and sealed by screw caps (PTFE/ rubber septa included). The vials were stored in dark under ambient temperature. The solution pH was measured during the experiments and adjusted using 0.1-1 M HCl or NaOH if necessary. At appropriate intervals, two vials for each solution were used for the measurement. The reaction was followed by determining the concentrations of *R*- and *S*-metalaxyl as well as their hydrolysis products, *R*- and *S*-MX-acid.

To investigate the influence of mineral surfaces on the hydrolysis of metalaxyl and metalaxyl-M, batch experiments were conducted in mineral suspensions. Since the above-mentioned preliminary experiments indicated that metalaxyl only hydrolyzed in alkaline solutions within a two-month period, the following batch experiments were performed in the range of pH 9.5-11.5. First, minerals were suspended in 10 mM NaCl solutions at a surface area concentration of 200 m^2 L^{-1} (the corresponding mass concentration amounts to 0.57, 2.00, 21.71, 19.90, 3.17 and 6.29 g L^{-1} for SiO_2, Al_2O_3, goethite, kaolinite, hectorite and Na-montmorillonite respectively). Suspension pH was adjusted by 1-5 M HCl or NaOH and buffered to pH 9.5, 10, 10.5, 11 with 10 mM Na_2CO_3. Then the mineral suspensions were continuously stirred using magnetic stir bars and equilibrated for 12 h. Meanwhile, 1 mM *rac*-metalaxyl and 0.5 mM *R*-metalaxyl stock solutions were prepared by dissolving a certain amount of racemic metalaxyl and metalaxyl-M in 10 mM NaCl solutions respectively. Finally, 5 mL freshly prepared stock solution of *rac*-metalaxyl or *R*-metalaxyl was added into 45 mL mineral suspension to initiate the reaction. As a control, hydrolysis experiments were also concurrently carried out in aqueous solutions, with the same pesticide concentration and pH as mineral suspensions. Under vigorous stirring, equal aliquots of reaction suspension or solution were transferred to 2 mL borosilicate glass vials and sealed by screw caps. The sample vials were collected in a box wrapped with aluminum foil and shaken on a rotator at a speed of 15 rpm. The suspension or solution pH was monitored during the reaction and adjusted using 0.1-1 M HCl or NaOH if necessary. Periodically, two vials for each suspension or solution were taken for analysis. For aqueous solutions, samples were directly analyzed by HPLC. However, in the case of mineral suspensions, samples were first centrifuged for 10 min at 4000 rpm (Hermle Z320, Berthold Hermle, Gosheim, Germany), and then the supernatant was used for analysis. The reactions were monitored by determining the concentrations of *R*- and *S*-metalaxyl

as well as their hydrolysis products in aqueous or supernatant solutions using stereo-selective HPLC.

3.2.4 Adsorption Experiments

During the hydrolysis in mineral suspensions, metalaxyl was found to adsorb on two clay minerals, hectorite and Na-montmorillonite. To learn more about the sorption process, batch experiments were conducted with metalaxyl and its hydrolysis product MX-acid in hectorite and Na-montmorillonite suspensions. The same experimental conditions (e.g., same pH, ionic strength and buffer concentration) were applied as the above-mentioned hydrolysis experiments. The detailed procedure for preparing hectorite and Na-montmorillonite suspensions refers to 3.2.3 hydrolysis experiments. A series of stock solutions were prepared by dissolving a certain amount of racemic metalaxyl or metalaxyl acid in 10 mM NaCl solutions, making the concentration of *rac*-metalaxyl or *rac*-MX-acid be about 1, 2.5 and 4 mM. To initiate sorption, 1 mL freshly prepared stock solution of *rac*-metalaxyl or *rac*-MX-acid was added into 49 mL mineral suspension. Consequently, the initial concentration of each enantiomer of metalaxyl or MX-acid was approximately 10, 25 and 40 µM. As a control, the experiment was also concurrently performed in aqueous solution. Once the solutions and suspensions were fully mixed by stirring, duplicate samples were taken and measured immediately. For aqueous solution, samples were directly analyzed by HPLC. However, in the case of hectorite and Na-montmorillonite suspension, samples were firstly centrifuged for 10 min at 4000 rpm, and then the supernatant was used for HPLC analysis. The mineral suspensions and aqueous solutions were continuously stirred during the reaction. Suspension or solution pH was monitored and adjusted using 0.1-1 M HCl or NaOH if necessary. Periodically, duplicate samples were taken and measured for sorption of *R*- and *S*-metalaxyl or *R*- and *S*-MX acid.

3.2.5 Chiral HPLC Analysis

Since both the chiral pesticide metalaxyl and its hydrolysis product metalaxyl carboxylic acid have a single pair of enantiomers (i.e., *R*- and *S*-metalaxyl, *R*- and *S*-MX-acid), a chiral column Lux^{TM} Cellulose-1 (chiral stationary phases: cellulose tris(3,5-dimethylphenylcarbamate); column: 3 µm, 150 × 2.0 mm i.d.; Phenomenex, Germany) equipped with a SecurityGuard^{TM} cartridge (Cellulose-1, 3 µm, 4 × 2.0 mm i.d., Phenomenex, Germany) was used for separating the stereoisomers. Analysis for *R*-metalaxyl, *S*-metalaxyl, *R*-MX-acid and *S*-MX-acid was performed by a Shimadzu

HPLC system (Shimadzu, Japan), consisting of an on-line degasser (DGU-20A$_3$), the solvent delivery units (double LC-20AD pumps), a system controller (CBM-20A), an auto-sampler (SIL-20ACHT) and a photodiode array detector (SPD-M20A). The elution of compounds was conducted at an isocratic mode under ambient temperature. The mobile phase contained 65% methanol and 35% formic acid buffer (0.3%, v/v). The flow rate was set to 0.3 mL/min and the wavelength was 266 nm.

External standard calibration was carried out by detecting the standard samples of metalaxyl, MX-acid, enantiopure *R*-metalaxyl and *R*-MX-acid. The enantiomers of metalaxyl were completely baseline separated and those of MX-acid were also well resolved (see Figure 3.2). The elution sequence was MX-acid followed by metalaxyl with *S*-enantiomer before *R*-enantiomer. Enantiomer ratios (ER) can be calculated using the peak area of each enantiomer, i.e. ER = p_S / p_R, where p_S and p_R are the peak areas of the *S*-and *R*-enantiomer, respectively (Buser et al., 2002). As expected, both racemates of metalaxyl and MX-acid gave peak ratios of 1:1 (ER = 1.03 ± 0.03 for *rac*-metalaxyl and ER = 1.02 ± 0.02 for *rac*- MX-acid).

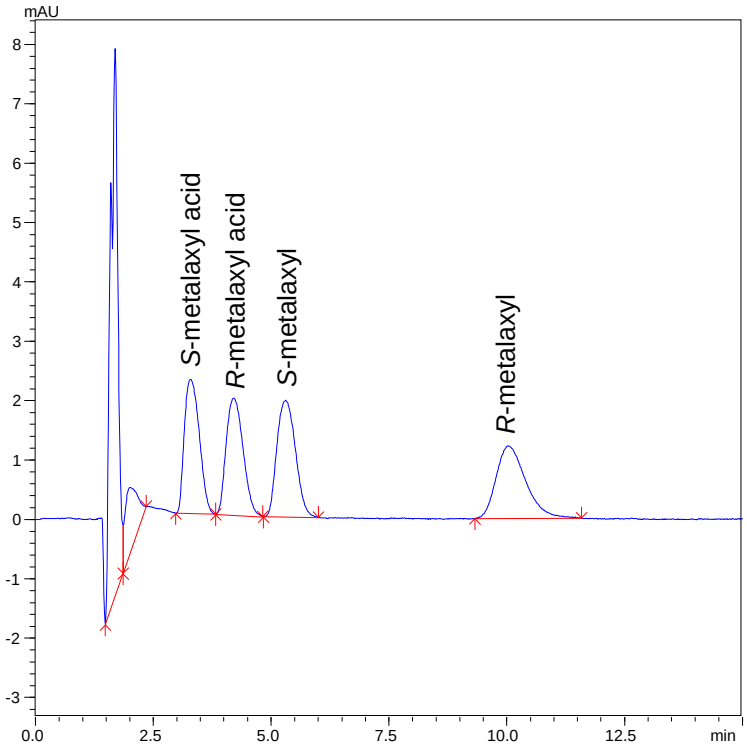

FIGURE 3.2. HPLC chromatograms of racemic metalaxyl and MX-acid (100 µM, in methanol). Chiral column: Lux™ Cellulose-1; mobile phase: 65% methanol and 35% formic acid buffer (0.3%, v/v).

3.2.6 Hydrolysis Kinetics Evaluation

The hydrolysis of metalaxyl was presumed to progress according to pseudo-first-order kinetics, which can be described by the following equation:

$$\ln (C_t / C_0) = - k_{obs} t$$

where C_0 and C_t are the concentrations of reactant at time zero and t, respectively. The observed rate constant (k_{obs}) can be derived by applying linear regression analysis to plot "ln (C_t / C_0) versus t". Then the hydrolysis half-life ($t_{1/2}$) was calculated by:

$$t_{1/2} = \ln 2 / k_{obs}$$

3.3 Results and Discussion

3.3.1 Hydrolysis of Racemic Metalaxyl in Aqueous Solutions

The hydrolysis of *rac*-metalaxyl was investigated in aqueous solutions over pH 2-5 and 9.5-12 under ambient temperature. The results showed that *R*- and *S*-enantiomer of metalaxyl readily hydrolyzed to their respective primary acids over pH 9.5-12, while the two enantiomers were stable over pH 2-5 within a two-month period. For example, Figure 3.3 and 3.4 present the chromatograms of metalaxy for hydrolysis in aqueous solutions at pH 10.47 and pH 3.02, respectively. Additionally, the concentration of each enantiomer of metalaxyl and MX-acid was plotted versus reaction time (Figure 3.5). Both the chromatograms and reaction profiles show that *R*- and *S*-metalaxyl hydrolyzed to *R*- and *S*-MX-acid respectively at pH 10.47 (see Figure 3.3 and 3.5a). Whereas only *R*- and *S*-metalaxyl were eluted by chromatography and their concentrations were stable throughout 55 days at pH 3.02 (see Figure 3.4 and 3.5b), indicating there was almost no hydrolysis occurring at this pH.

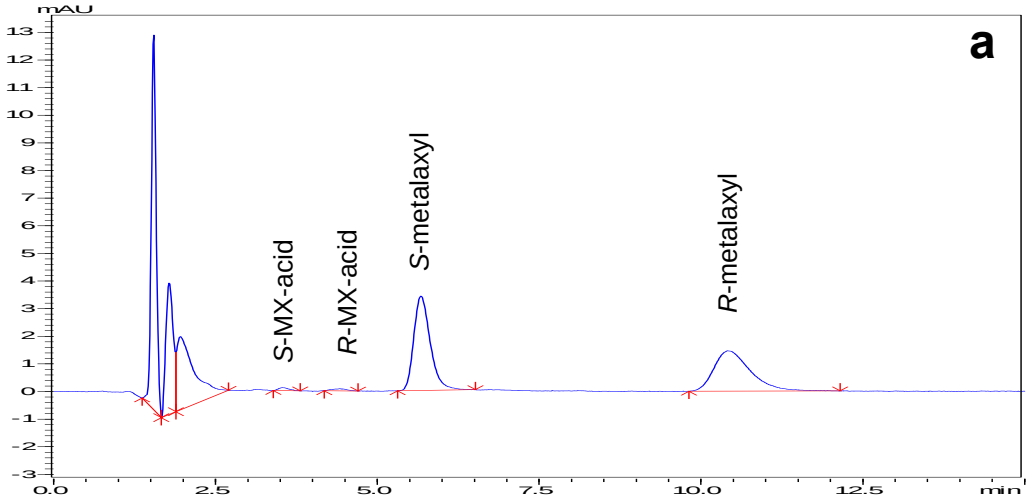

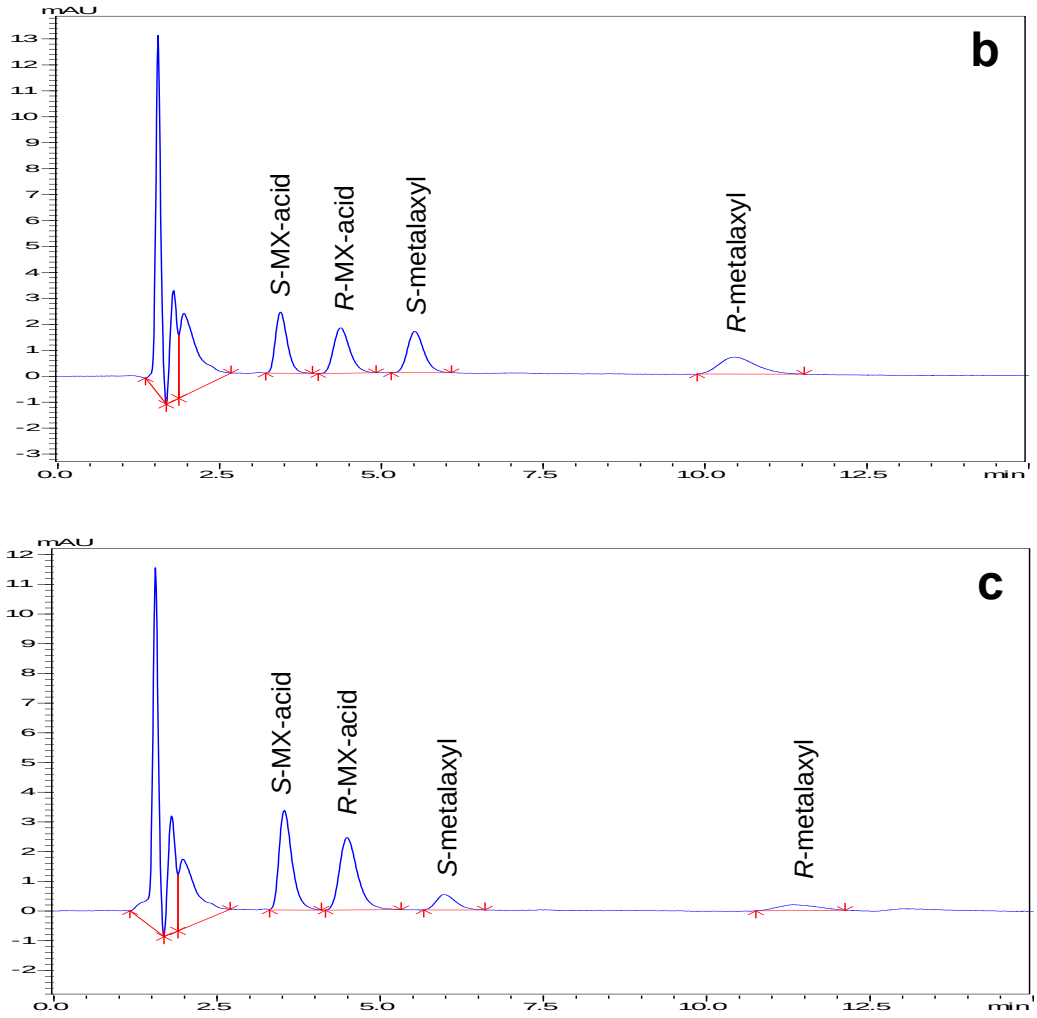

FIGURE 3.3. HPLC chromatograms of reactants and products for metalaxyl hydrolysis in aqueous solution at pH10.47 after (a) 0 h, (b) 116 h, and (c) 305 h, respectively, showing *R*- and *S*-metalaxyl as well as the hydrolysis products *R*- and *S*-MX-acid were eluted.

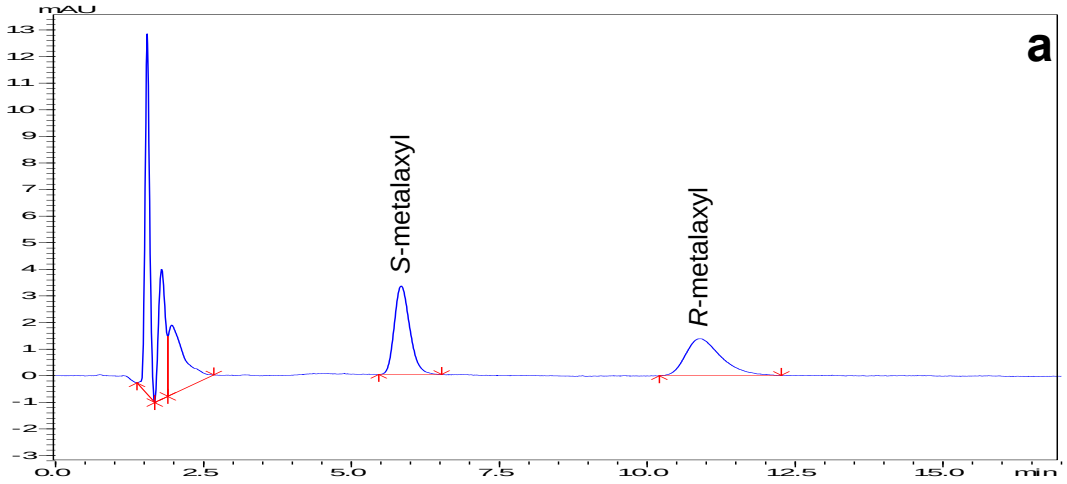

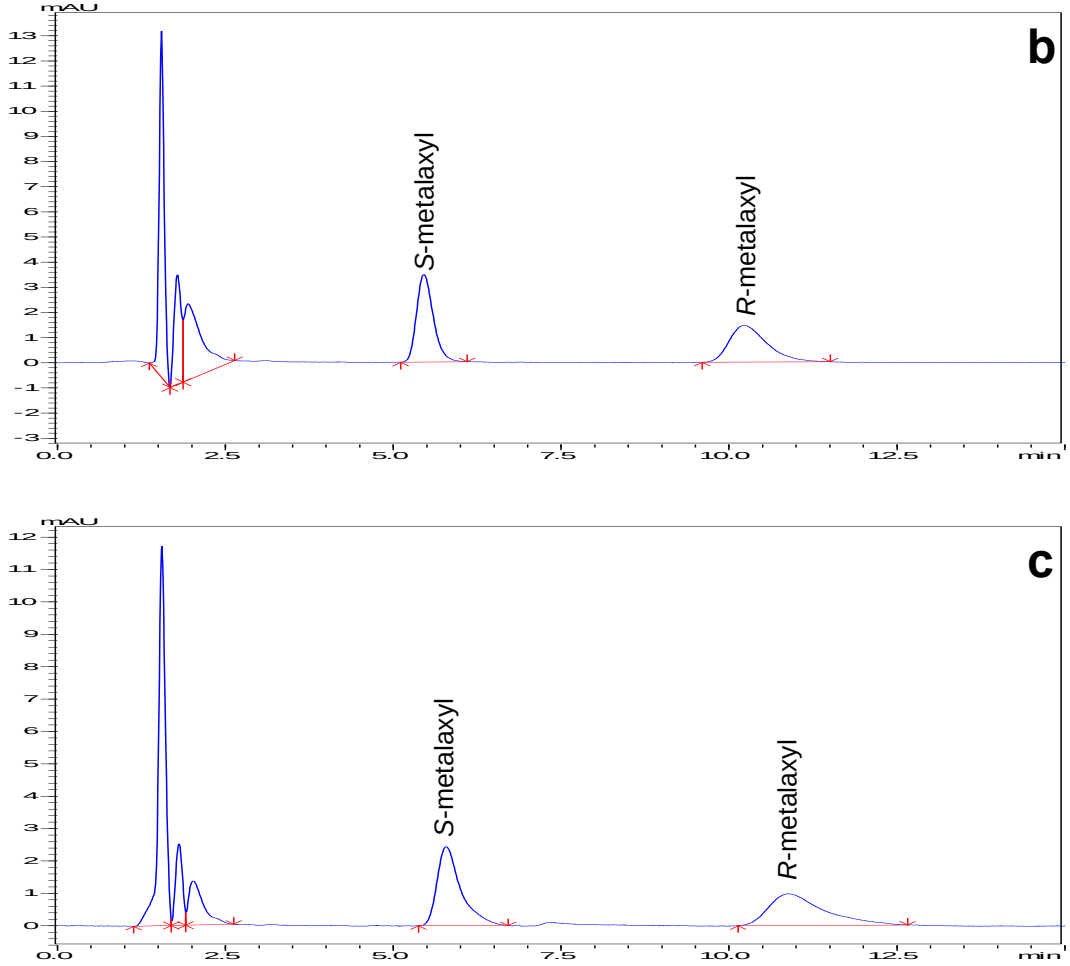

FIGURE 3.4. HPLC chromatograms of reactants and products for metalaxyl hydrolysis in aqueous solution at pH3.02 after (a) 0 h, (b) 120 h, and (c) 1327 h, respectively, showing only *R*- and *S*-metalaxyl were eluted without any product.

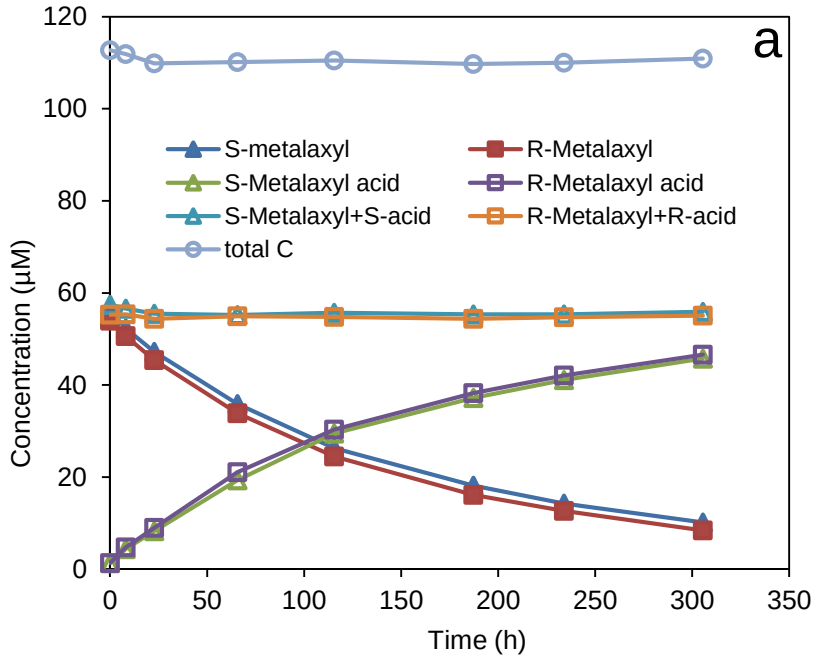

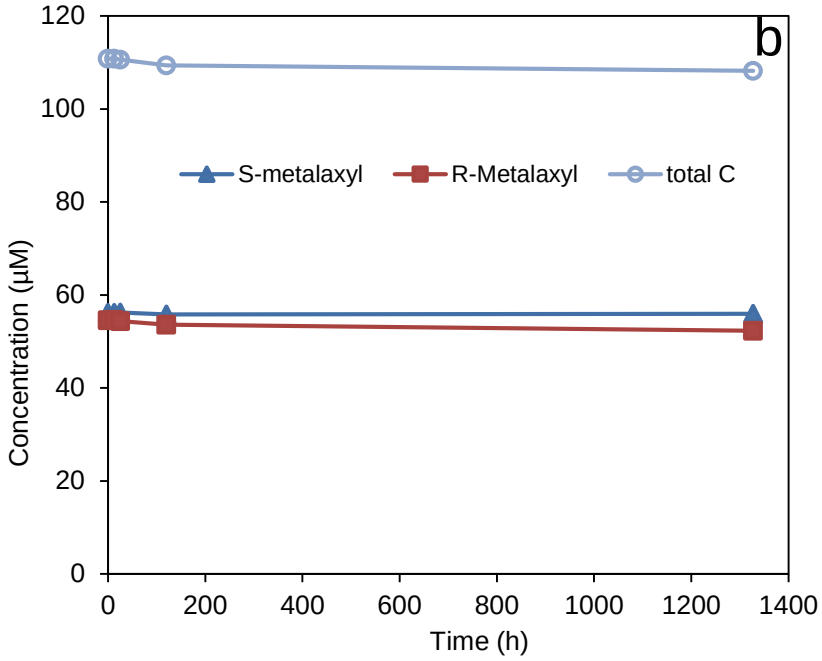

FIGURE 3.5. Hydrolysis of *rac*-metalaxyl in aqueous solution at (a) pH 10.47 and (b) pH 3.02. Concentrations (µM) of reactants and products were plotted versus reaction time (h). Experimental condition: 10 mM formate buffer for pH 3.02, 10 mM carbonate buffer for pH 10.47 and 10 mM NaCl as electrolyte.

For hydrolysis in alkaline solution, the observed rate constants were obtained by performing linear regression analysis on plot of ln (C_t / C_0) versus t. The half-lives were also calculated and listed in Table 3.2. As shown in Table 3.2, the correlation coefficients were >0.99, confirming that metalaxyl hydrolysis in alkaline solutions followed pseudo-first-order kinetics. In addition, hydrolysis rate constants increased significantly as pH increased from 9.52 to 12.01. In Figure 3.6, observed rate constants were plotted against solution pH on the logarithmic scale. The rate-pH profiles show good linearity, and log k_{obs} increases as a function of pH with unit slope, indicating that metalaxyl hydrolysis in aqueous solution is completely base-catalyzed reaction over pH 9.5-12.

TABLE 3.2. Hydrolysis Kinetics of *R*- and *S*-enantiomer of Metalaxyl in Aqueous Solutions[a]

	***S*-metalaxyl**			***R*-metalaxyl**			**ES**
pH	**k_{Robs} (h^{-1})**	**R^2**	**$t_{1/2}$ (h)**	**k_{Sobs} (h^{-1})**	**R^2**	**$t_{1/2}$ (h)**	
9.52	7.28E-04	0.996	952	7.77E-04	0.993	892	0.03
10.01	2.25E-03	0.998	308	2.63E-03	0.996	263	0.08
10.47	5.62E-03	0.996	123	6.08E-03	0.998	114	0.04

10.97	2.07E-02	0.998	33.5	2.30E-02	0.995	30.1	0.05
11.52	6.83E-02	0.993	10.1	7.30E-02	0.995	9.49	0.03
12.01	2.15E-01	0.999	3.22	2.23E-01	0.998	3.11	0.02

[a] k_{Robs} and k_{Sobs}, observed rate constants for hydrolysis of *R*- and *S*-metalaxyl; R^2, correlation coefficients; $t_{1/2}$, half-lives; and ES, enantioselectivity.

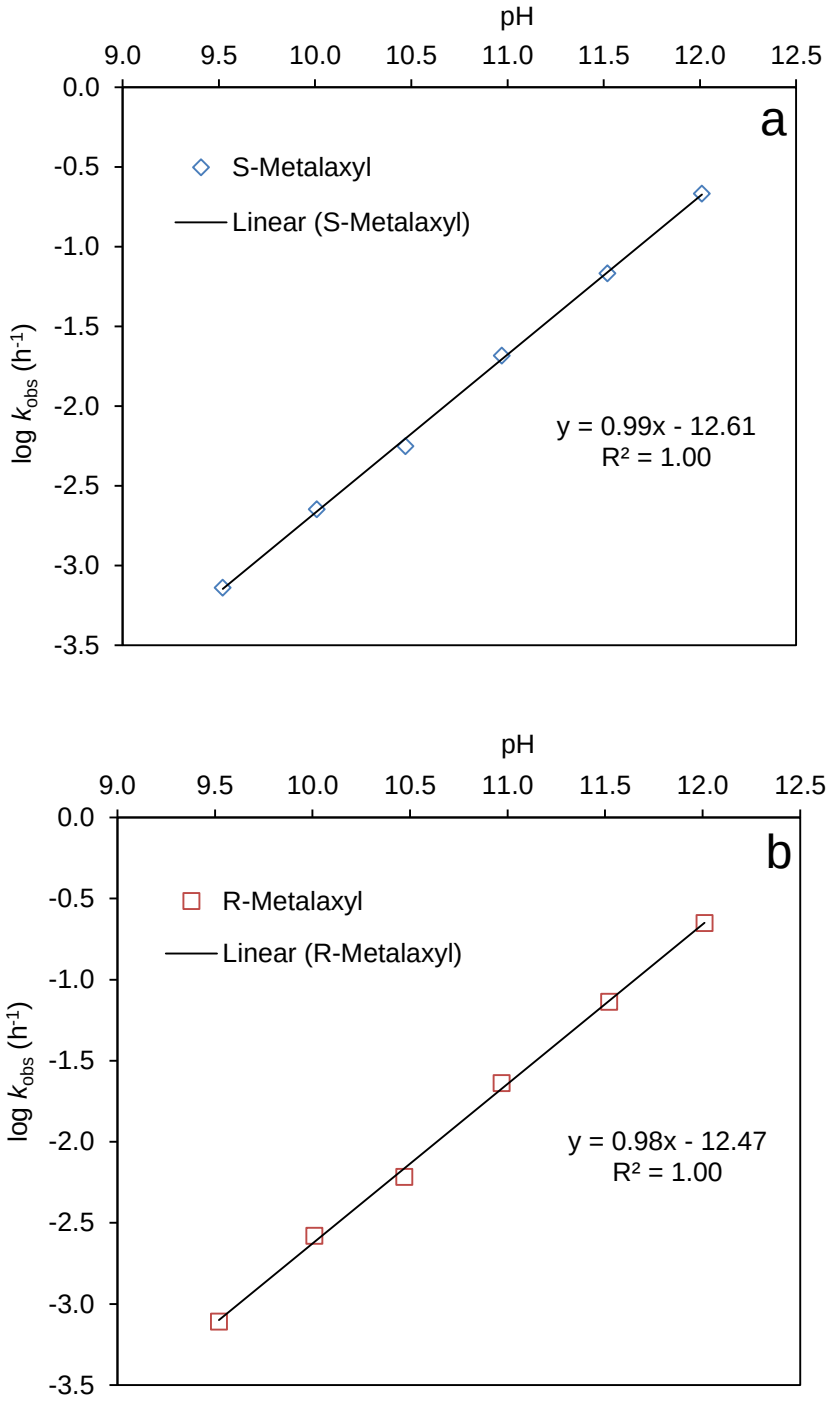

FIGURE 3.6. Plots of log k_{obs} vs pH for *rac*-metalaxyl hydrolysis in alkaline solutions under ambient temperature: (a) *S*-metalaxyl, (b) *R*-metalaxyl.

The rate constants listed in Table 3.2 also showed that *R*-metalaxyl hydrolyzed slightly faster than *S*-metalaxyl. Hence, the enantiomer ratio of metalaxyl may be changed following the reaction. For example, at pH 10.47, the initial enantiomer ratio (ER, defined as the concentration ratio of *S*- and *R*-metalaxyl) was 1.04, whereas at the end of hydrolysis, the enantiomer ratio increased to 1.21. In literature, Müller and Buser (1995) defined the excess of the rate of faster over slower degraded enantiomer as a measure of stereo-/enantioselectivity (ES). Accordingly, the enantioselectivity of *rac*-metalaxyl hydrolysis can be evaluated by the equation ES = (k_R - k_S)/(k_R + k_S), where k_R and k_S are the hydrolysis rate constants of *R*- and *S*-enantiomer, respectively. If *R*-enantiomer hydrolyzes faster than *S*-enantiomer, 0 < ES ≤ 1; when *S*-enantiomer hydrolyzes more rapidly, -1 ≤ ES < 0; and while *R*- and *S*-enantiomer hydrolyze at equal rates (i.e. $k_R = k_S$), ES = 0, the hydrolysis is nonenantioselective. The ES values for metalaxyl hydrolysis were calculated and listed in Table 3.2. The results show that solution pH has insignificant effect on the enantioselectivity of metalaxyl hydrolysis. At most pH, metalaxyl hydrolysis is basically nonenantioselective (ES = 0.02-0.05); while at pH 10.01, the hydrolysis of *R*-enantiomer was slightly preferential (ES = 0.08). However, compared with the high enantioselectivity (ES = 0.37-0.64) for the dissipation of metalaxyl (MX-acid as primary metabolite) in soils (Buser, Müller et al. 2002, Zadra, Marucchini et al. 2002, Buerge, Poiger et al. 2003), the hydrolysis of metalaxyl in alkaline solutions is essentially nonenantioselective. It may be because the dissipation in soil is generally biologically mediated process, whereas the hydrolysis in aqueous solution is chemically mediated reaction (Buser, Müller et al. 2002, Buerge, Poiger et al. 2003).

3.3.2 Metalaxyl Adsorption on Minerals

The stoichiometry of hydrolysis reaction illustrated by Figure 3.7 shows that 1 mol of *S*-metalaxyl or *R*-metalaxyl can hydrolyze to 1 mole of *S*-MX-acid or *R*-MX-acid. To examine the mass balance of metalaxyl hydrolysis in mineral suspensions and aqueous solutions, the total concentrations of *S*-metalaxyl and *S*-MX-acid (or *R*-metalaxyl and *R*-MX-acid) in aqueous phase were plotted versus reaction time. As showed in Figure 3.8, the total concentrations of reactants and products were approximately stable following the hydrolysis in aqueous solutions and some mineral suspensions including SiO_2, Al_2O_3, kaolinite and goethite. Since the total dissolved concentrations of *S*- or *R*-enantiomer in these four mineral suspensions were very

close to those in aqueous solutions, the adsorption of *S*- and *R*-metalaxyl or *S*- and *R*-MX-acid onto SiO_2, Al_2O_3, kaolinite or goethite was insignificant over pH 9.5-11.

However, regarding the other two clay minerals, hectorite and Na-montmorillonite, significant differences were observed for the total dissolved concentrations of *S*-metalaxyl + *S*-MX-acid (or *R*-metalaxyl + *R*-MX-acid) between mineral suspensions and aqueous solutions. For hectorite suspensions, considerable differences were obtained throughout pH 9.5-11. In the case of Na-montmorillonite suspensions, however, major differences were only observed at pH 9.5 and pH 10; while at higher pH of 10.5 and 11, only small differences were measured at the beginning of hydrolysis (Figure 3.8). Furthermore, the less initial dissolved concentrations of reactants (t = 0, almost no hydrolysis product) in mineral suspensions compared with aqueous solutions indicated that metalaxyl adsorbed to hectorite and Na-montmorillonite. It was also illustrated that metalaxyl firmly adsorbed to hectorite and were difficult to be desorbed; whereas in the case of Na-montmorillonite, the adsorbed metalaxyl were much more readily desorbed from the clay except at pH 9.5 (Figure 3.8). In addition, metalaxyl adsorption on hectorite and Na-montmorillonite was dependent on pH.

The sorption of metalaxyl already occurred at the first sampling (marked as t = 0), while no hydrolysis products yielded. Hence, the sorption is a much faster process than hydrolysis, and the concentrations of *R*- and *S*-metalaxyl at t = 0 can be used to evaluate the sorption. The initial enantiomer ratio of metalaxyl in dissolved phase was then calculated. The ER values range from1.04 to 1.06 in hectorite suspensions and from 1.04 to 1.08 in Na-montmorillonite suspensions, indicating that metalaxyl basically remained in racemic form during the sorption. Therefore, the sorption of metalaxyl onto hectorite and Na-montmorillonite over pH 9.5-11 is essentially nonenantioselective. The possible reason is that sorption is a physical and/or chemical process which show an identical affinity for the enantiomers.

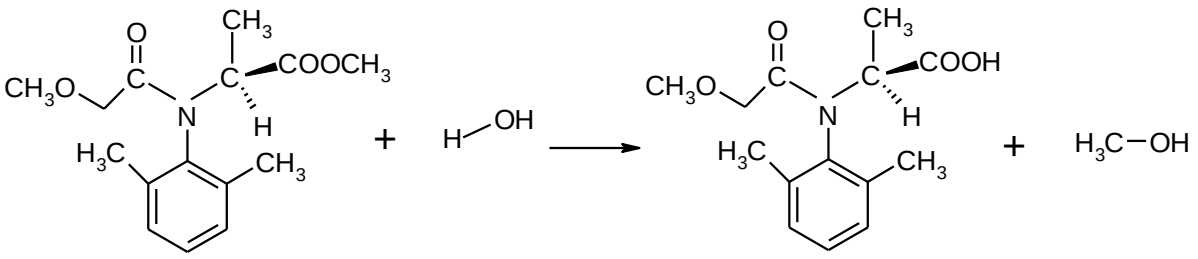

S-metalaxyl *S*-MX-acid

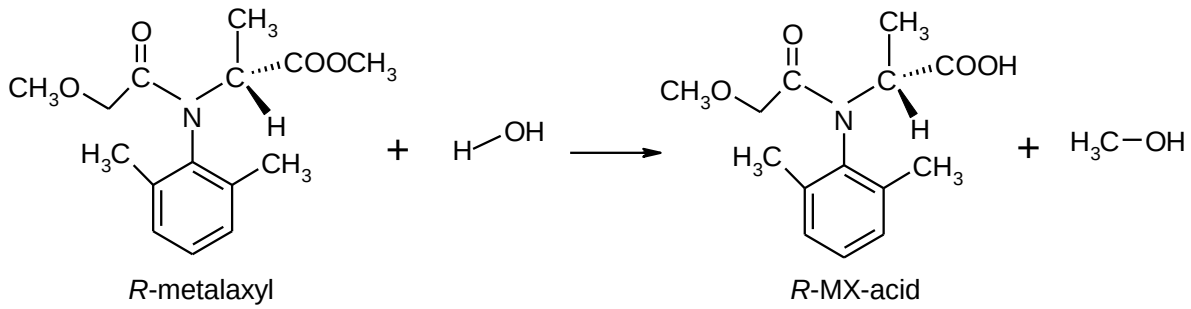

FIGURE 3.7. The equations for metalaxyl hydrolysis.

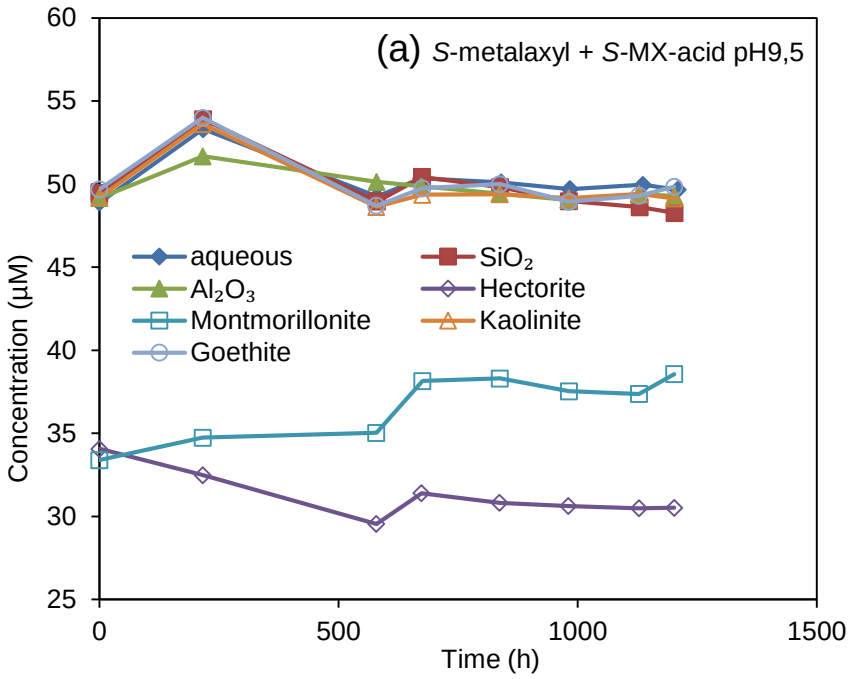

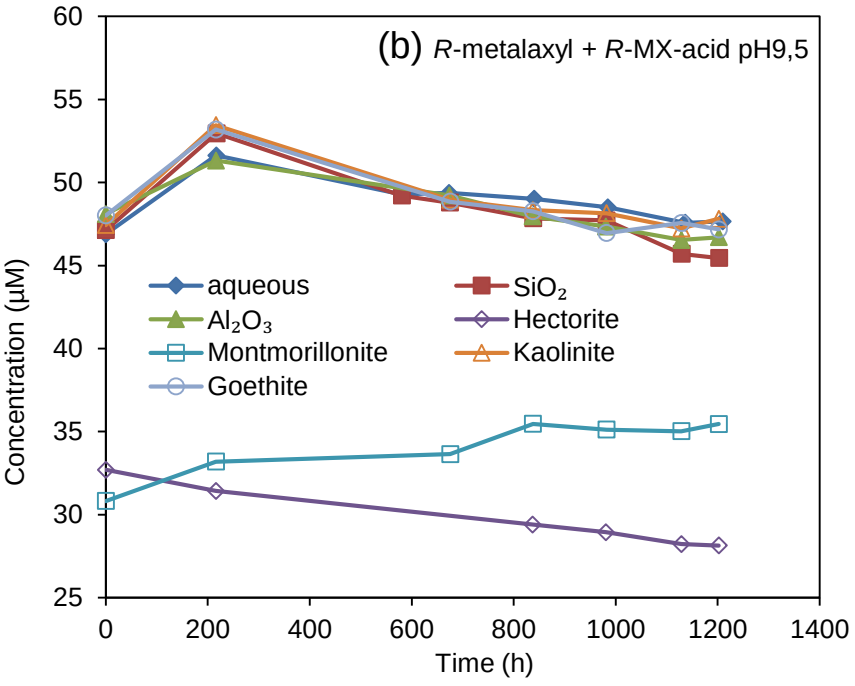

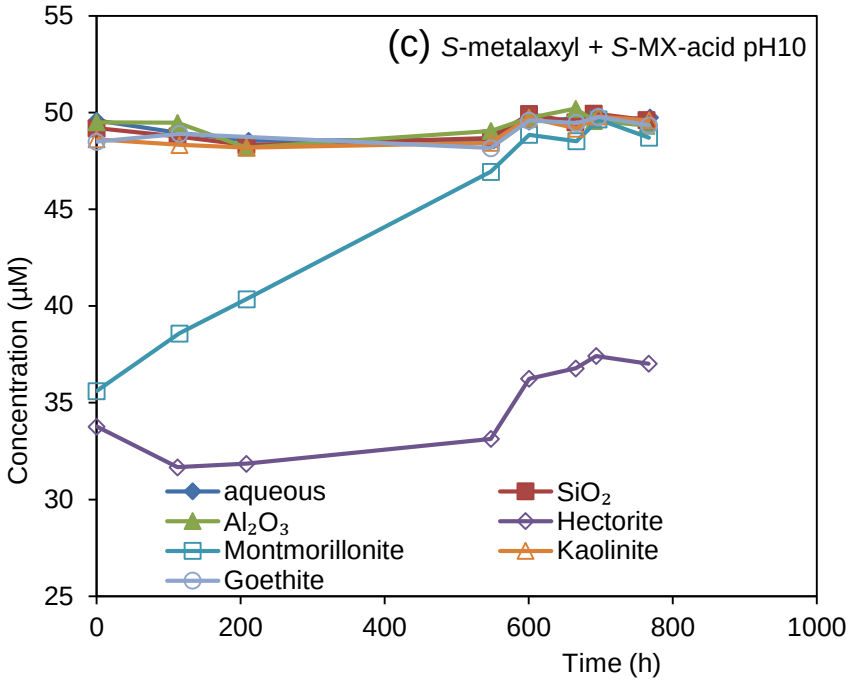
(c) S-metalaxyl + S-MX-acid pH10
Concentration (µM)
Time (h)
aqueous
SiO2
Al2O3
Hectorite
Montmorillonite
Kaolinite
Goethite

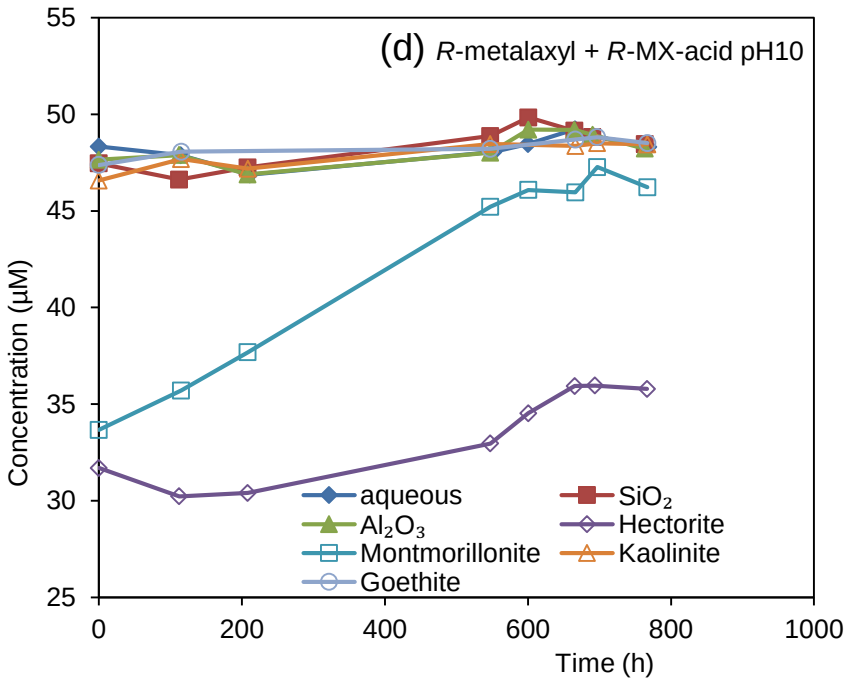
(d) R-metalaxyl + R-MX-acid pH10
Concentration (µM)
Time (h)
aqueous
SiO2
Al2O3
Hectorite
Montmorillonite
Kaolinite
Goethite

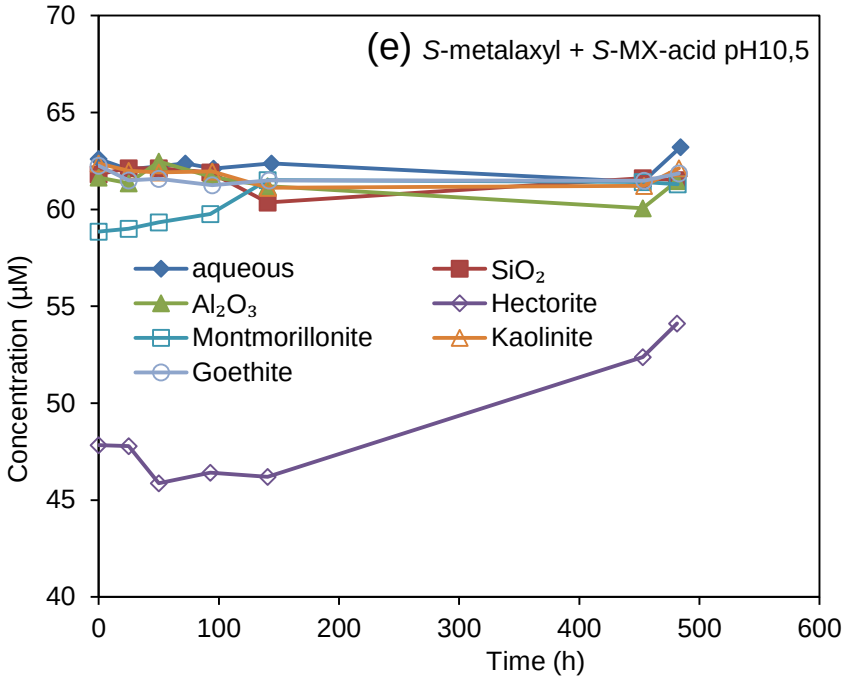
(e) S-metalaxyl + S-MX-acid pH10,5
Concentration (µM)
Time (h)
aqueous
SiO2
Al2O3
Hectorite
Montmorillonite
Kaolinite
Goethite
70
65
60
55
50
45
40
0
100
200
300
400
500
600

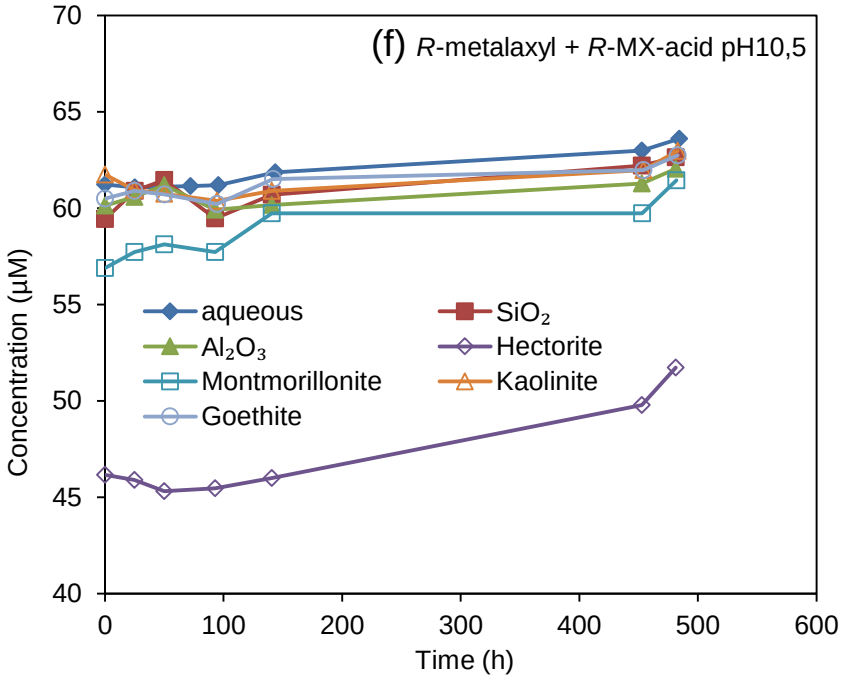
(f) R-metalaxyl + R-MX-acid pH10,5
Concentration (µM)
Time (h)
aqueous
SiO2
Al2O3
Hectorite
Montmorillonite
Kaolinite
Goethite
70
65
60
55
50
45
40
0
100
200
300
400
500
600

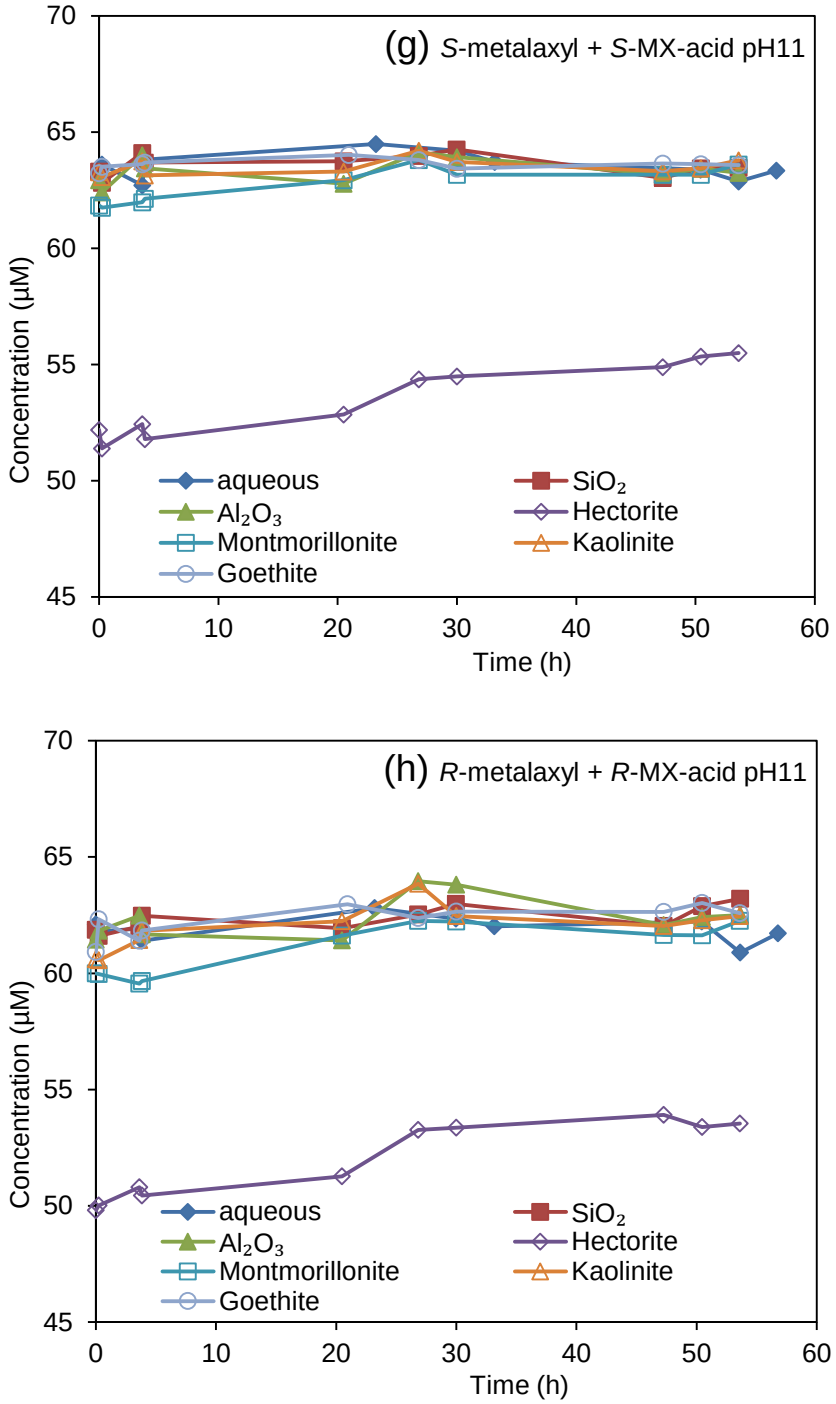

FIGURE 3.8. Mass balance evaluation of metalaxyl hydrolysis in a series of mineral suspensions (SiO_2, Al_2O_3, hectorite, Na-montmorillonite, kaolinite, and goethite) and aqueous solutions at different pH. The total concentrations of *S*-metalaxyl and *S*-MX-acid (or *R*-metalaxyl and *R*-MX-acid) in aqueous phase were plotted versus reaction time. (a), (c), (e), and (g): *S*-metalaxyl and *S*-MX-acid at pH 9.5, 10, 10.5, and 11 respectively; (b), (d), (f), and (h): *R*-metalaxyl and *R*-MX-acid at pH 9.5, 10, 10.5, and 11 respectively.

3.3.3 Metalaxyl Hydrolysis in Mineral Suspensions

As stated above, the measurable kinetics of metalaxyl hydrolysis in aqueous solution only occurred at pH >9.5. Accordingly, batch experiments on metalaxyl hydrolysis in mineral suspensions were conducted at pH 9.5, 10, 10.5, and 11. Meanwhile, the experiments were also carried out in aqueous solutions as a control. The results showed that *R*- and *S*-enantiomer of racemic metalaxyl readily hydrolyzed to their respective acid product in mineral suspensions over pH 9.5-11. For example, Figure 3.9 presents the hydrolysis of metalaxyl in mineral suspensions as well as aqueous solutions at pH 11. Good mass balances were obtained for the hydrolysis in mineral suspensions except for hectorite and Na-montmorillonite (sorption occurred), while good linearity was also shown for the plots of ln (C_t/C_0) versus time. The reaction profiles at the other pH values are similar to those at pH 11. Therefore, the observed rate constants can be calculated using the linear regression analysis, and the correlation coefficients are >0.98 in all cases.

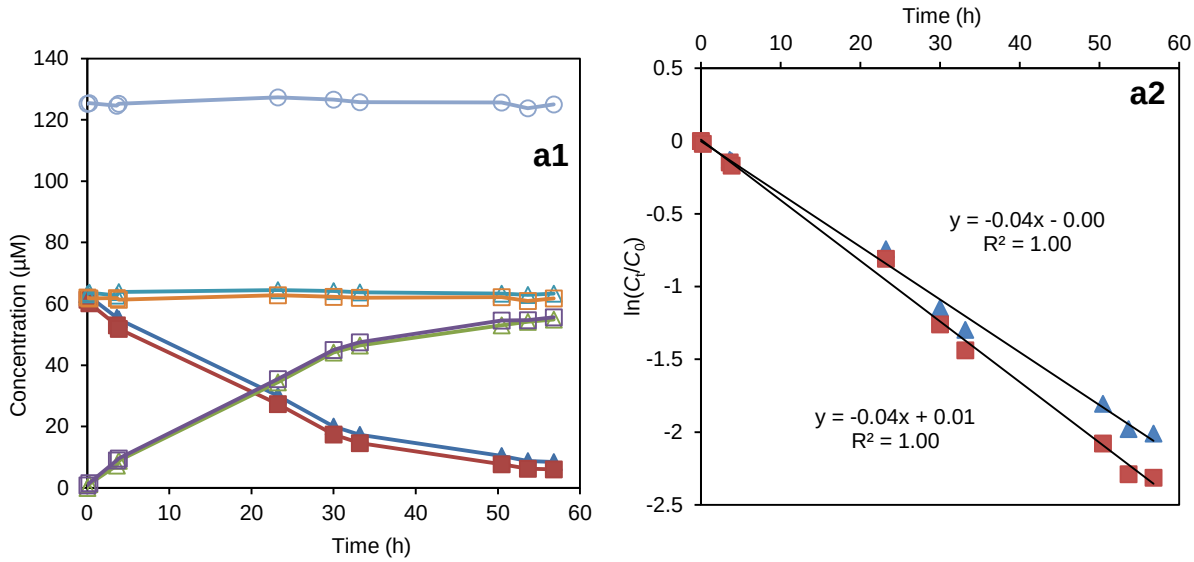

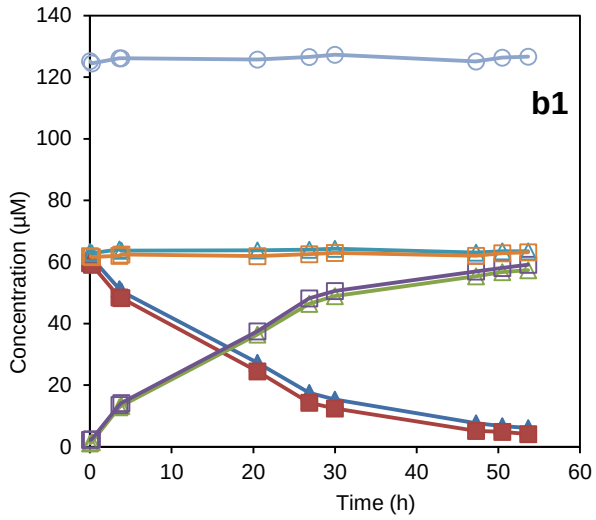
b1
Concentration (µM)
Time (h)

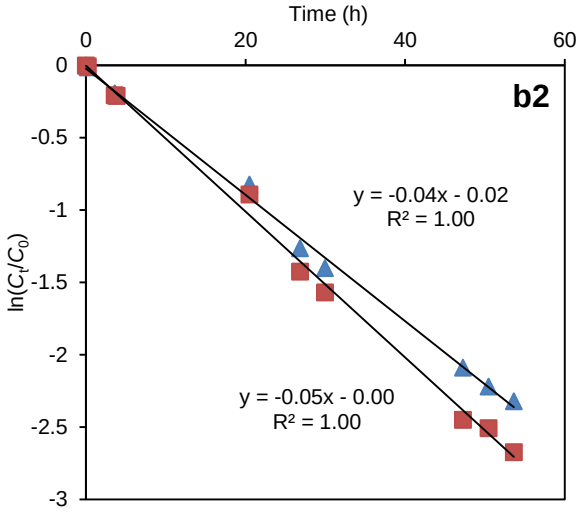
b2
y = -0.04x - 0.02
R² = 1.00
y = -0.05x - 0.00
R² = 1.00
ln(Ct/C0)
Time (h)

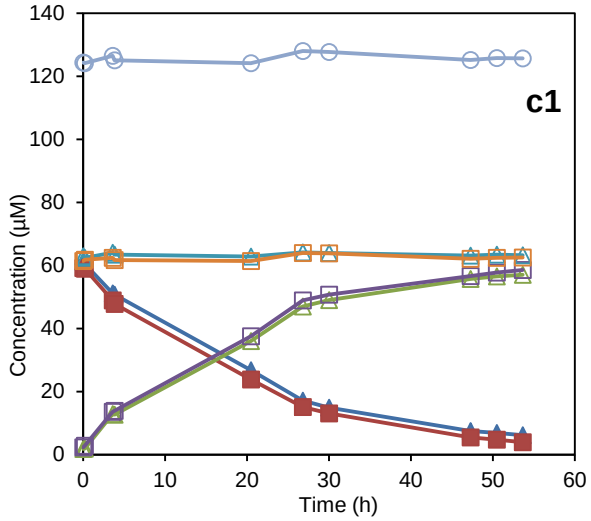
c1
Concentration (µM)
Time (h)

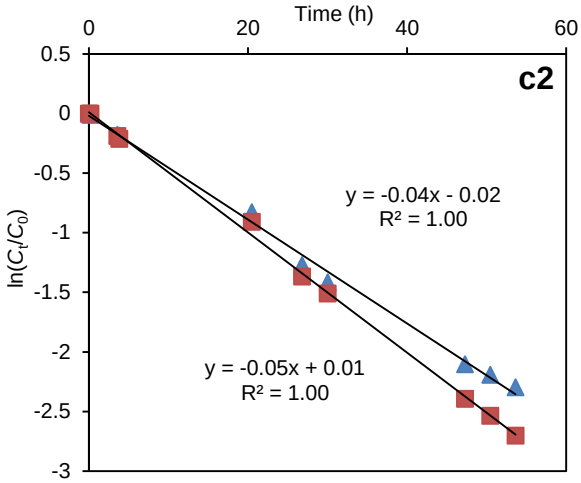
c2
y = -0.04x - 0.02
R² = 1.00
y = -0.05x + 0.01
R² = 1.00
ln(Ct/C0)
Time (h)

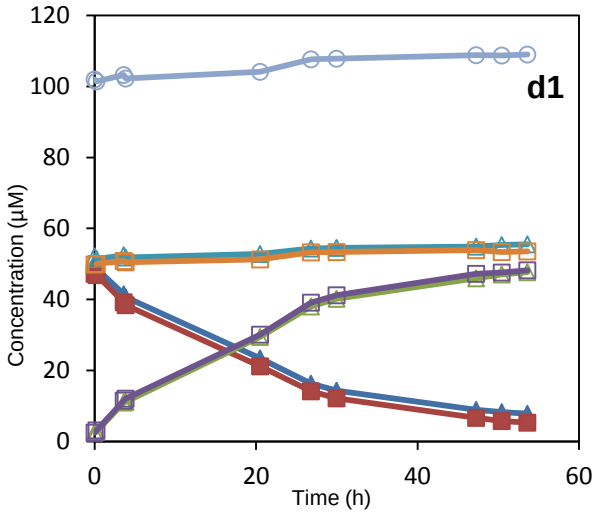
d1
Concentration (µM)
Time (h)

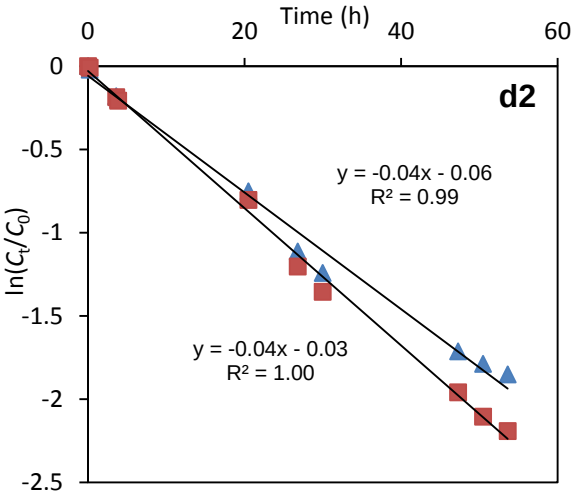
d2
y = -0.04x - 0.06
R² = 0.99
y = -0.04x - 0.03
R² = 1.00
ln(Ct/C0)
Time (h)

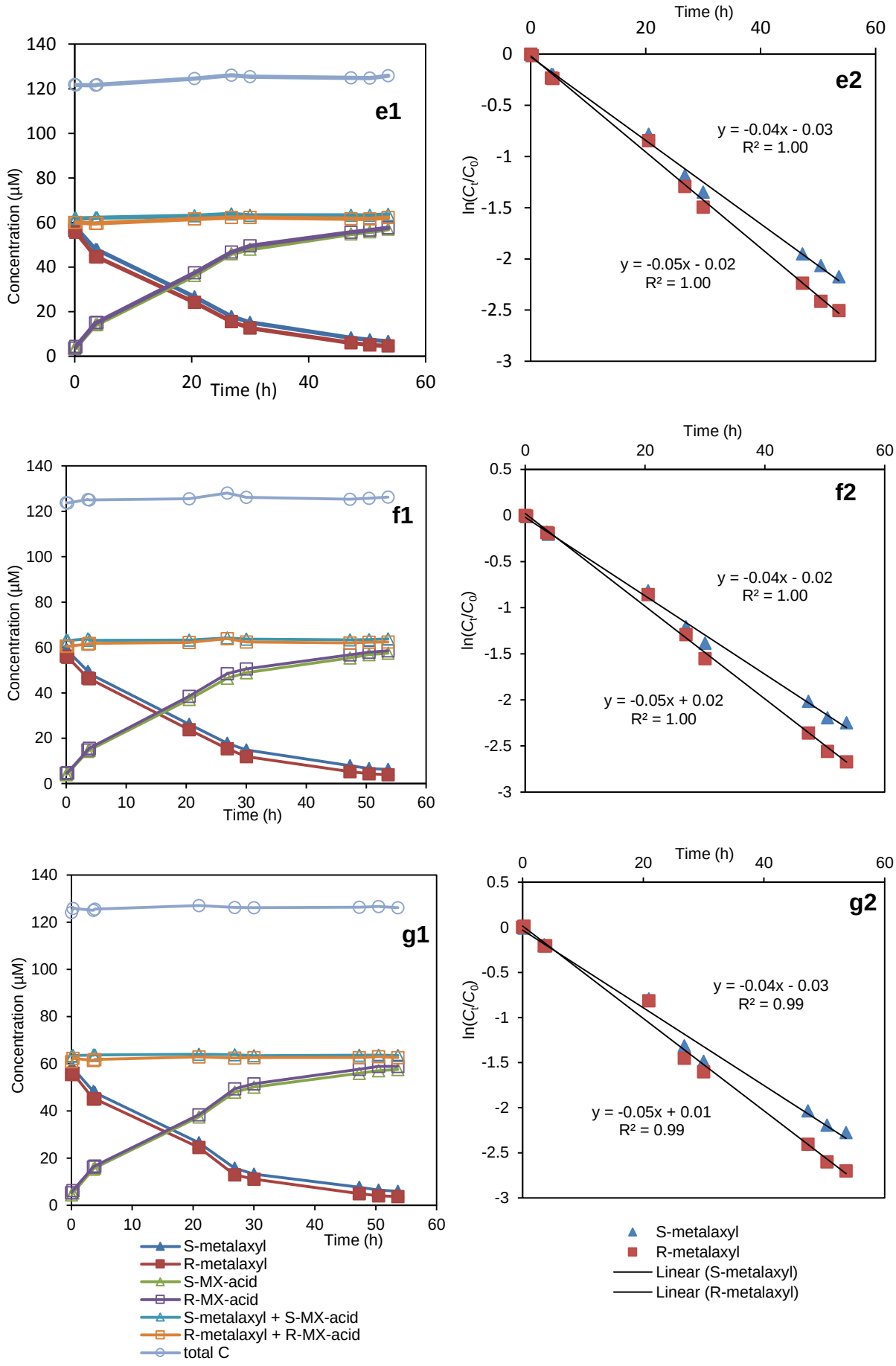
e1
Concentration (µM)
Time (h)
e2
ln(Ct/C0)
y = -0.04x - 0.03
R² = 1.00
y = -0.05x - 0.02
R² = 1.00
f1
f2
y = -0.04x - 0.02
R² = 1.00
y = -0.05x + 0.02
R² = 1.00
g1
g2
y = -0.04x - 0.03
R² = 0.99
y = -0.05x + 0.01
R² = 0.99
S-metalaxyl
R-metalaxyl
S-MX-acid
R-MX-acid
S-metalaxyl + S-MX-acid
R-metalaxyl + R-MX-acid
total C
Linear (S-metalaxyl)
Linear (R-metalaxyl)

FIGURE 3.9. Metalaxyl hydrolysis at pH 11 in (b) SiO_2, (c) Al_2O_3, (d) hectorite, (e) Na-montmorillonite, (f) kaolinite, and (g) goethite suspensions as well as (a) aqueous solution . Concentrations of *R*- and *S*-metalaxyl and their respective acid products *R*- and *S*-MX-acid in aqueous phase plotted versus reaction time (left panel a1-g1). Plots of ln (C_t/C_0) versus time (right panel a2-g2).

Figure 3.10 presents the observed rate constants of R- and S-enantiomer of metalaxyl in different mineral suspensions and aqueous solutions, illustrating that: (i) the hydrolysis of *R*-metalaxyl is slightly faster than that of *S*-metalaxyl, and (ii) the influence of minerals on metalaxyl hydrolysis is not significant. Moreover, the hydrolysis rate constants of *R*- and *S*-metalaxyl were plotted against solution/suspension pH on the logarithmic scale (Figure 3.11). The plots show good linearity for all mineral suspensions and aqueous solutions, and log k_{obs} increases as a function of pH with unit slope. This correlation shows that base-catalyzed hydrolysis is dominant in the range of pH 9.5-11.

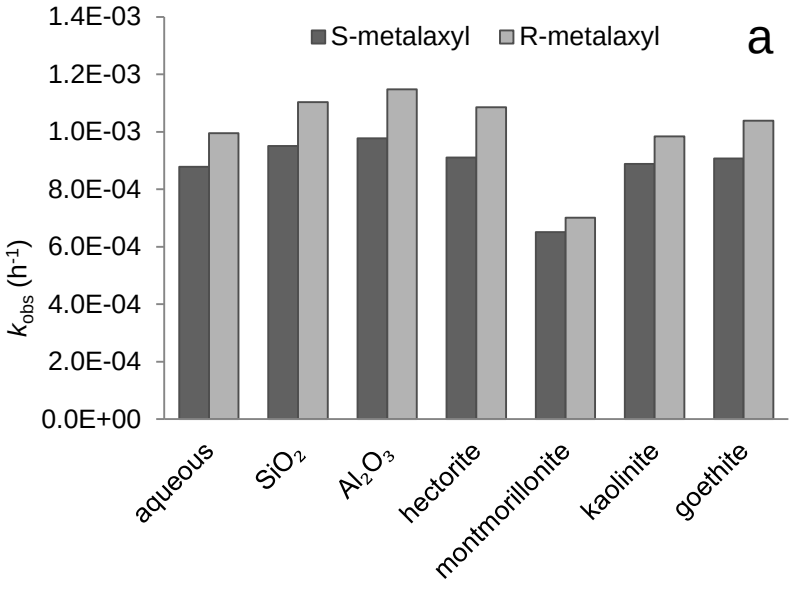

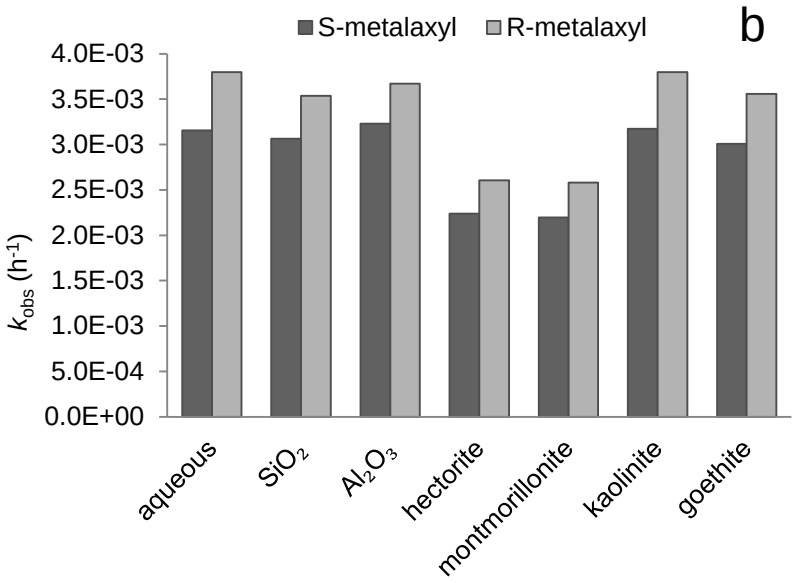
b
S-metalaxyl
R-metalaxyl
k_{obs} (h^{-1})
4.0E-03
3.5E-03
3.0E-03
2.5E-03
2.0E-03
1.5E-03
1.0E-03
5.0E-04
0.0E+00
aqueous
SiO_2
Al_2O_3
hectorite
montmorillonite
kaolinite
goethite

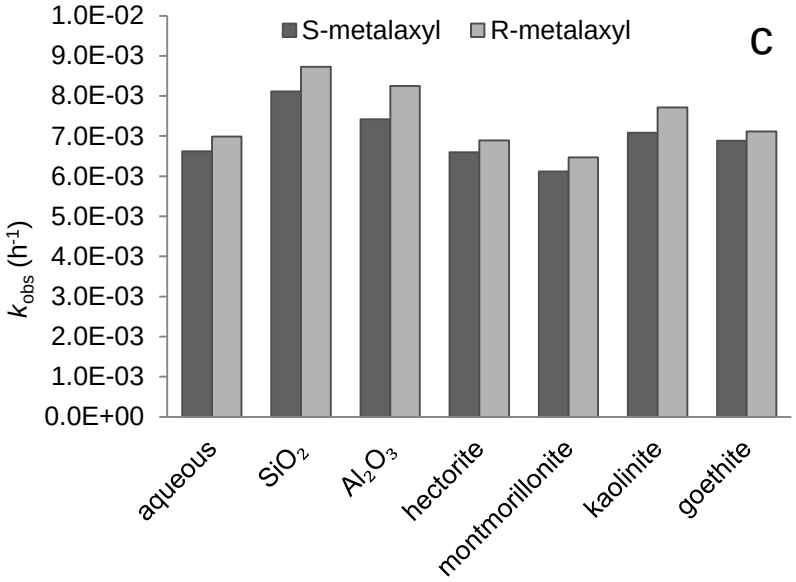
c
S-metalaxyl
R-metalaxyl
k_{obs} (h^{-1})
1.0E-02
9.0E-03
8.0E-03
7.0E-03
6.0E-03
5.0E-03
4.0E-03
3.0E-03
2.0E-03
1.0E-03
0.0E+00
aqueous
SiO_2
Al_2O_3
hectorite
montmorillonite
kaolinite
goethite

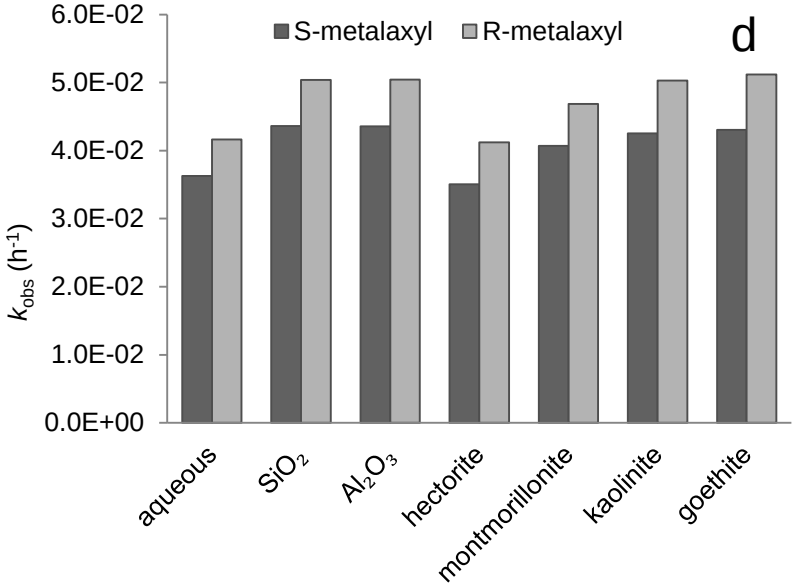
d
S-metalaxyl
R-metalaxyl
k_{obs} (h^{-1})
6.0E-02
5.0E-02
4.0E-02
3.0E-02
2.0E-02
1.0E-02
0.0E+00
aqueous
SiO_2
Al_2O_3
hectorite
montmorillonite
kaolinite
goethite

FIGURE 3.10. The observed rate constants of *S*- and *R*-metalaxyl in a series of mineral suspensions (SiO_2, Al_2O_3, hectorite, Na-montmorillonite, kaolinite and goethite) and aqueous solutions at (a) pH9.5, (b) pH10, (c) pH10.5, and (d) pH11.

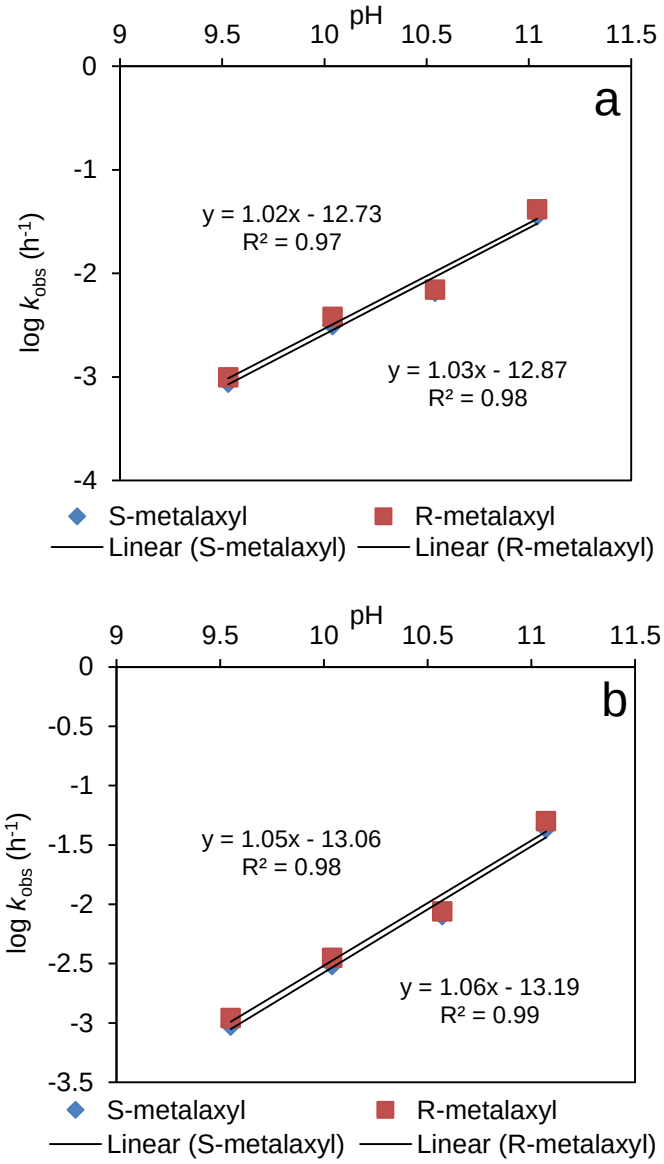

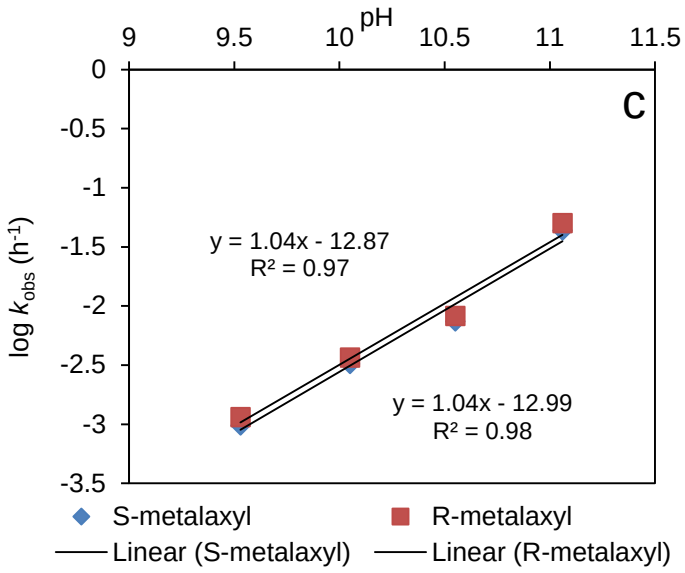
pH
9
9.5
10
10.5
11
11.5
0
-0.5
-1
-1.5
-2
-2.5
-3
-3.5
log k_{obs} (h^{-1})
c
y = 1.04x - 12.87
R² = 0.97
y = 1.04x - 12.99
R² = 0.98
S-metalaxyl
R-metalaxyl
Linear (S-metalaxyl)
Linear (R-metalaxyl)

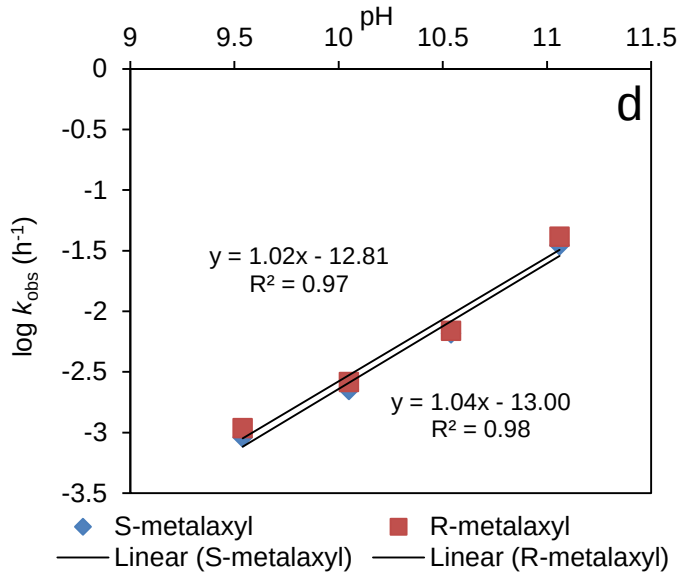
pH
9
9.5
10
10.5
11
11.5
0
-0.5
-1
-1.5
-2
-2.5
-3
-3.5
log k_{obs} (h^{-1})
d
y = 1.02x - 12.81
R² = 0.97
y = 1.04x - 13.00
R² = 0.98
S-metalaxyl
R-metalaxyl
Linear (S-metalaxyl)
Linear (R-metalaxyl)

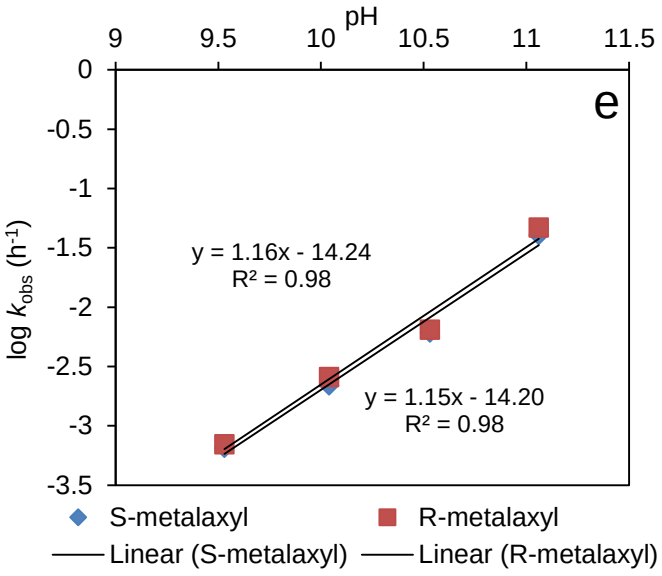
pH
9
9.5
10
10.5
11
11.5
0
-0.5
-1
-1.5
-2
-2.5
-3
-3.5
log k_{obs} (h^{-1})
e
y = 1.16x - 14.24
R² = 0.98
y = 1.15x - 14.20
R² = 0.98
S-metalaxyl
R-metalaxyl
Linear (S-metalaxyl)
Linear (R-metalaxyl)

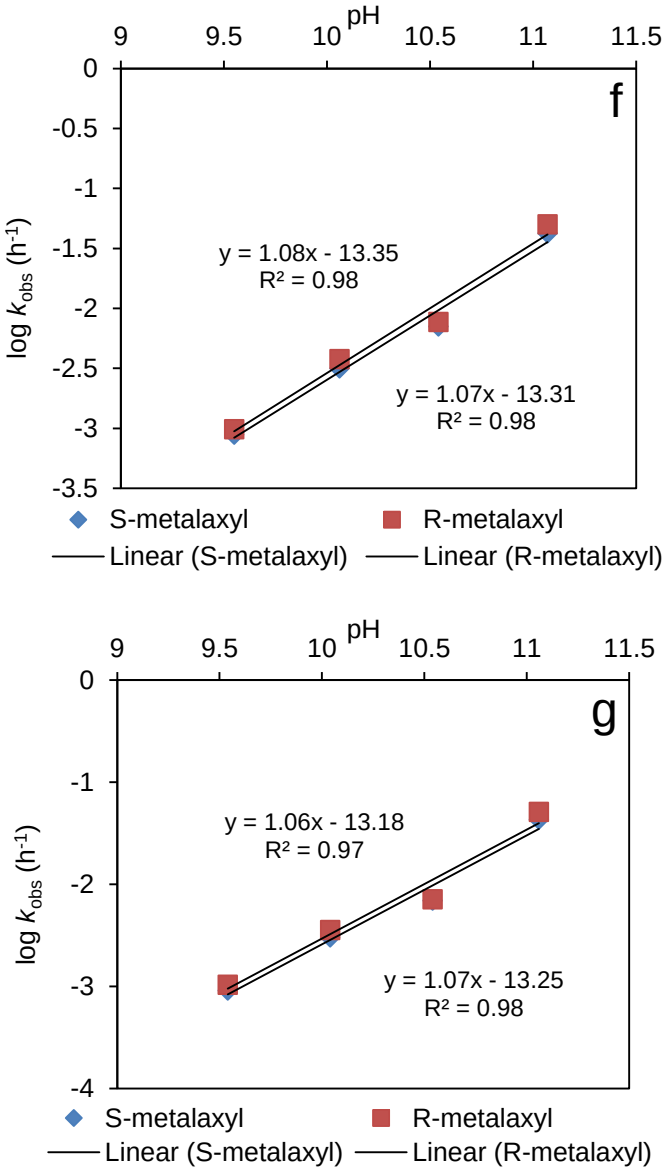

FIGURE 3.11. Effects of pH on hydrolysis of *S*- and *R*-metalaxyl in (b) SiO_2, (c) Al_2O_3, (d) hectorite, (e) Na-montmorillonite, (f) kaolinite, and (g) goethite suspensions as well as (a) aqueous solution. The common logarithms of the observed rate constants (log k_{obs}) plotted versus pH.

The ES values for metalaxyl hydrolysis in mineral suspensions as well as aqueous solutions were calculated and listed in Table 3.3. The results showed that metalaxyl hydrolysis in all mineral suspensions and aqueous solutions is basically nonenantioselective ($0.02 \leq ES \leq 0.09$). Therefore, the influence of minerals on the enantioselectivity of metalaxyl hydrolysis was insignificant. The nonenantioselectivity may be attributed to metalaxyl hydrolysis in mineral suspensions being a chemically mediated process. This is in agreement with the previous reports that the stereo-

selective dissipation of a chiral compound is generally caused by biological reaction; whereas a chemical reaction is not stereo-selective (Buser, Müller et al. 2002, Buerge, Poiger et al. 2003). Furthermore, the reaction profiles in Figure 3.9 also illustrated that hydrolysis of *R*- and *S*-metalaxyl occurred with retention of configuration, which is consistent with the previous studies (Buser, Müller et al. 2002, Buerge, Poiger et al. 2003).

TABLE 3.3. Enantioselectivity for Metalaxyl Hydrolysis in Mineral Suspensions and Aqueous Solutions[a]

	ES			
	pH 9.5	pH 10	pH 10.5	pH 11
aqueous	0.06	0.09	0.03	0.07
SiO_2	0.07	0.07	0.04	0.07
Al_2O_3	0.08	0.06	0.05	0.07
hectorite	0.09	0.08	0.02	0.08
Na-montmorillonite	0.04	0.08	0.03	0.07
kaolinite	0.05	0.09	0.04	0.08
goethite	0.07	0.08	0.02	0.09

[a] ES = $(k_R - k_S)/(k_R + k_S)$, where k_R and k_S are the hydrolysis rate constants of *R*- and *S*-enantiomer respectively.

3.3.4 Metalaxyl-M Hydrolysis in Mineral Suspensions

Batch experiments on the hydrolysis of pesticide metalaxyl-M were also conducted in mineral suspensions as well as aqueous solutions over pH 9.5-11. The results showed that *S*-metalaxyl and *S*-MX-acid were also observed during the reaction besides *R*-metalaxyl and *R*-MX-acid. For instance, the HPLC chromatograms of reactants and products for the reaction of metalaxyl-M in aqueous solution at pH 11.05 were presented in Figure 3.12. At the beginning of reaction highly enantiopure *R*-metalaxyl was eluted (Figure 3.12a); after 29 h, however, significant *S*-metalaxyl as well as *R*- and *S*-MX-acid were also obtained (Figure 3.12b). The reaction profile of metalaxyl-M in aqueous solution at pH 11.05 was plotted in Figure 3.13. The plot showed that the concentration of *R*-metalaxyl gradually decreased, while the concentration of *S*-metalaxyl first increased to a maximum and then decreased. Hence, it was indicated that decomposition of *R*-metalaxyl, formation and subsequent degradation of *S*-metalaxyl, and formation of *R*- and *S*-MX-acid occurred concurrently. Since it has been confirmed above that the ester cleavage of *R*- and *S*-metalaxyl proceeds with retention

of configuration, a series of reaction processes were implied: (i) chiral inversion between *R*-metalaxyl and *S*-metalaxyl; (ii) hydrolysis of *R*-metalaxyl to *R*-MX-acid; (iii) hydrolysis of *S*-metalaxyl to *S*-MX-acid; and (iv) chiral inversion between *R*-MX-acid and *S*-MX-acid (see Figure 3.14). To evaluate the complicated tranformation processes for metalaxyl-M, a computer model was developed using the program MATLAB® (R2010b, The MathWorks, Inc.). The first-order kinetics was applied to each possible reaction, and the preliminary modelling showed *R*- and *S*-metalaxyl hydrolyzed at a similar rate. Therefore, three rate constants were used to describe separate reactions (Figure 3.14), i.e., k_1 was designated the enantiomerization rate constant of *R*- and *S*-metalaxyl, k_2 was designated the hydrolysis rate constant of *R*- and *S*-metalaxyl, and k_3 was designated the enantiomerization rate constant of *R*- and *S*- MX-acid. The modeling results were listed in Table 3.4, showing that almost all k_3 values were zero. Although in some cases k_3 was expressed to be a certain number, it can be neglected compared with k_1 and k_2. Hence, it was indicated that the enantiomerization between *R*- and *S*-MX-acid was insignificant. Figure 3.15 and 3.16 describe the modelling fits for reactions of metalaxyl-M in aqueous solution and goethite suspension (similar figures also obtained for the other minerals), showing that the model fits the experimental data quite well and then can be used to evaluate the reaction processes of metalaxyl-M. In summary, in aqueous solutions and mineral suspensions over pH 9.5-11, the enantiopure *R*-metalaxyl is configurationally labile and can readily enantiomerize to its antipode,*S*-metalaxyl; while both the parent *R*-metalaxyl and the resulting *S*-metalaxyl can hydrolyze to respective acids, *R*- and *S*-MX-acid, which are configurationally stable and do not interconvert to each other.

The rate constants for enantiomerization between *R*- and *S*-metalaxyl (k_1) and hydrolysis of *R*- and *S*-metalaxyl (k_2) were also presented in Figure 3.17. It was shown that the rate constants of enantiomerization are in the range of 22-32% of hydrolysis rate constants. Furthermore, the influence of minerals on hydrolysis and the chiral inversion is insignificnat since the rate constants in different mineral suspensions and aqueous solutions at certain pH are of the same order of magnitude. To evaluate the effects of pH on enantiomerization and hydrolysis, the common logarithms of rate constants were plotted versus pH (Figure 3.18), showing that both hydrolysis and enantiomerization are pH dependent, and the rate constants increase as a function of pH with unit slope. Hence, the enantiomerization is also base-catalyzed reaction over pH 9.5-11.

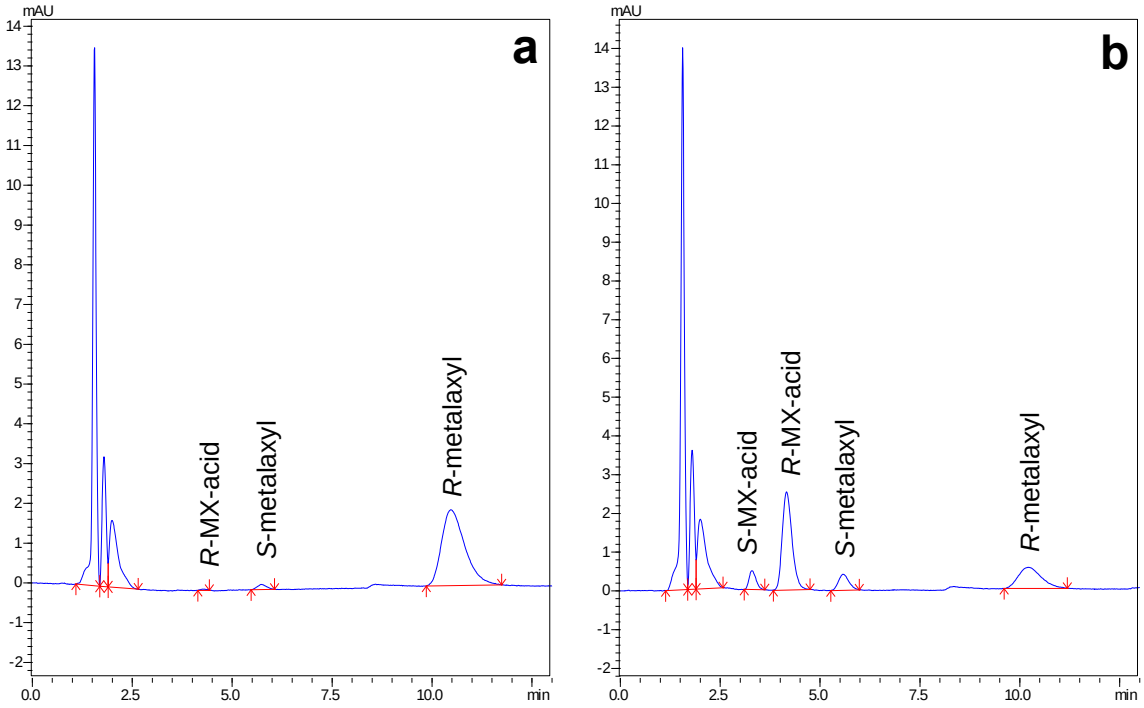

FIGURE 3.12. HPLC chromatograms of reactants and products for hydrolysis of metalaxyl-M in aqueous solution at pH 11.05 after (a) 0 h, and (b) 29 h.

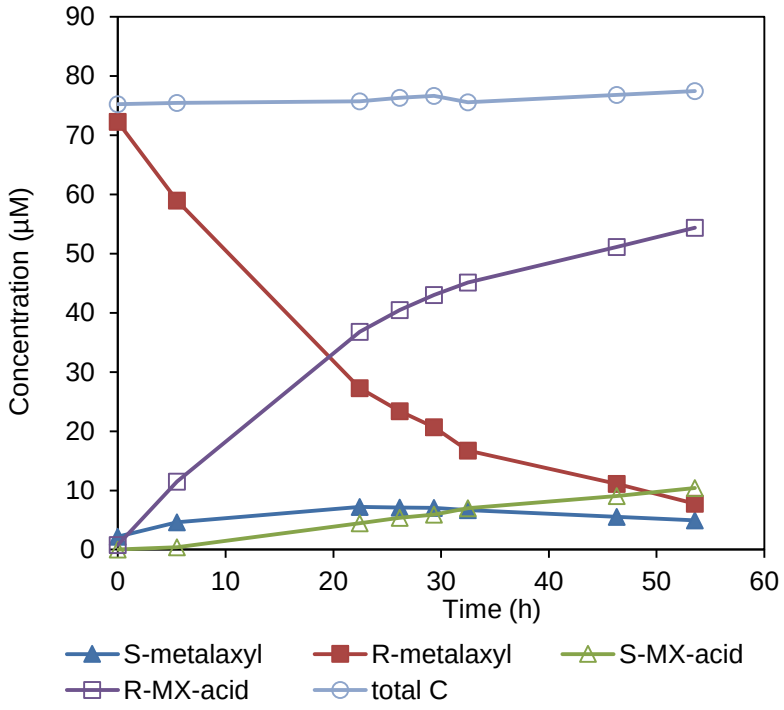

FIGURE 3.13. The reaction profile of metalaxyl-M in aqueous solution at pH 11.05. Concentrations (µM) of reactants and products as well as their total concentrations plotted versus time (h).

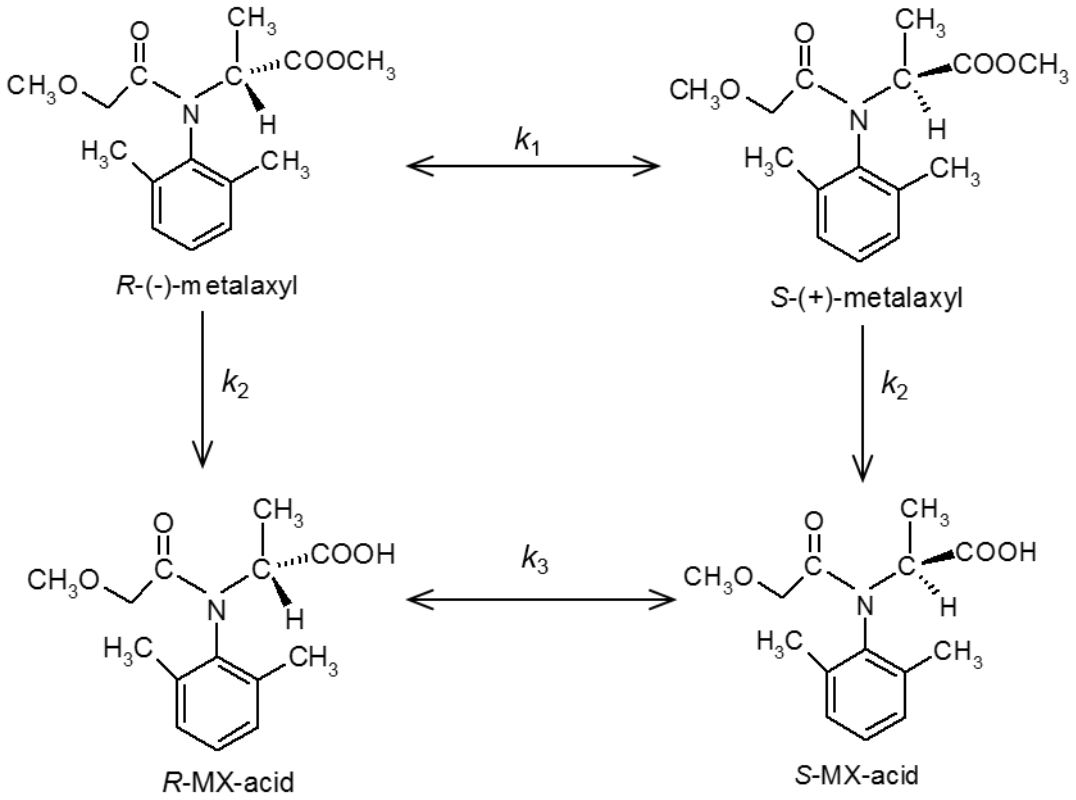

FIGURE 3.14. Reaction scheme for metalaxyl-M in aqueous solutions over pH 9.5-11. k_1, enantiomerization rate constant for *R*- and *S*-metalaxyl; k_2, hydrolysis rate constant for *R*- and *S*-metalaxyl; k_3, enantiomerization rate constant for *R*- and *S*-MX-acid.

TABLE 3.4. Reaction Rate Constants of Metalaxyl-M in Aqueous Solutions and Mineral Suspensions

		Rate Constant		
Mineral	**pH**	k_1 (h^{-1})	k_2 (h^{-1})	k_3 (h^{-1})
aqueous	9.53	2.91E-04 ± 1.86E-05	9.27E-04 ± 1.32E-05	0 ± 0
SiO_2	9.57	3.14E-04 ± 1.79E-05	9.86E-04 ± 1.23E-05	0 ± 0
Al_2O_3	9.54	2.87E-04 ± 1.26E-05	9.19E-04 ± 8.66E-06	0 ± 0
hectorite	9.54	2.12E-04 ± 2.04E-05	8.67E-04 ± 1.61E-05	6.73E-06 ± 2.14E-05
Na-montmorillonite	9.54	1.92E-04 ± 2.28E-05	7.86E-04 ± 2.52E-05	0 ± 0
kaolinite	9.54	2.93E-04 ± 1.22E-05	9.40E-04 ± 8.44E-06	0 ± 0
goethite	9.54	2.81E-04 ± 1.12E-05	9.13E-04 ± 1.00E-05	0 ± 0
Mineral	**pH**	k_1 (h^{-1})	k_2 (h^{-1})	k_3 (h^{-1})
aqueous	10.04	9.60E-04 ± 1.21E-04	3.11E-03 ± 1.09E-04	0 ± 0
SiO_2	10.07	1.00E-03 ± 7.82E-05	3.38E-03 ± 7.98E-05	0 ± 0
Al_2O_3	10.05	9.80E-04 ± 9.07E-05	3.22E-03 ± 8.43E-05	0 ± 0
hectorite	10.04	5.48E-04 ± 1.27E-04	2.50E-03 ± 1.14E-04	0 ± 0
Na-montmorillonite	10.03	8.42E-04 ± 9.29E-05	2.89E-03 ± 8.69E-05	0 ± 0
kaolinite	10.05	8.71E-04 ± 9.34E-05	2.91E-03 ± 9.03E-05	0 ± 0
goethite	10.04	8.65E-04 ±1.17E-04	2.98E-03 ±1.05E-04	0 ± 0
Mineral	**pH**	k_1 (h^{-1})	k_2 (h^{-1})	k_3 (h^{-1})
aqueous	10.53	1.70E-03 ± 2.49E-04	6.62E-03 ± 1.77E-04	7.67E-05 ± 7.54E-05
SiO_2	10.57	2.82E-03 ± 3.66E-04	9.36E-03 ± 3.87E-04	0 ± 0

Al_2O_3	10.57	2.14E-03 ± 2.39E-04	8.00E-03 ± 2.11E-04	5.47E-05 ± 5.51E-05
hectorite	10.58	1.59E-03 ± 3.79E-04	7.18E-03 ± 3.82E-04	9.95E-05 ± 1.11E-04
Na-montmorillonite	10.55	1.94E-03 ± 2.51E-04	7.55E-03 ± 2.57E-04	6.47E-05 ± 6.69E-05
kaolinite	10.56	2.24E-03 ± 2.33E-04	8.11E-03 ± 2.06E-04	1.58E-05 ± 4.65E-05
goethite	10.56	2.79E-03 ± 3.25E-04	9.02E-03 ± 3.42E-04	0 ± 0
Mineral	**pH**	**k_1 (h^{-1})**	**k_2 (h^{-1})**	**k_3 (h^{-1})**
aqueous	11.05	1.07E-02 ± 4.39E-04	3.46E-02 ± 3.82E-04	0 ± 0
SiO_2	11.06	1.29E-02 ± 5.07E-04	4.02E-02 ± 4.38E-04	0 ± 0
Al_2O_3	11.05	1.26E-02 ± 5.69E-04	3.88E-02 ± 4.91E-04	0 ± 0
hectorite	11.05	9.23E-03 ± 7.97E-04	3.25E-02 ± 8.24E-04	0 ± 0
Na-montmorillonite	11.05	1.13E-02 ± 3.27E-04	3.60E-02 ± 3.26E-04	0 ± 0
kaolinite	11.05	1.19E-02 ± 4.20E-04	3.77E-02 ± 3.63E-04	0 ± 0
goethite	11.04	1.10E-02 ± 4.56E-04	3.48E-02 ± 3.94E-04	0 ± 0

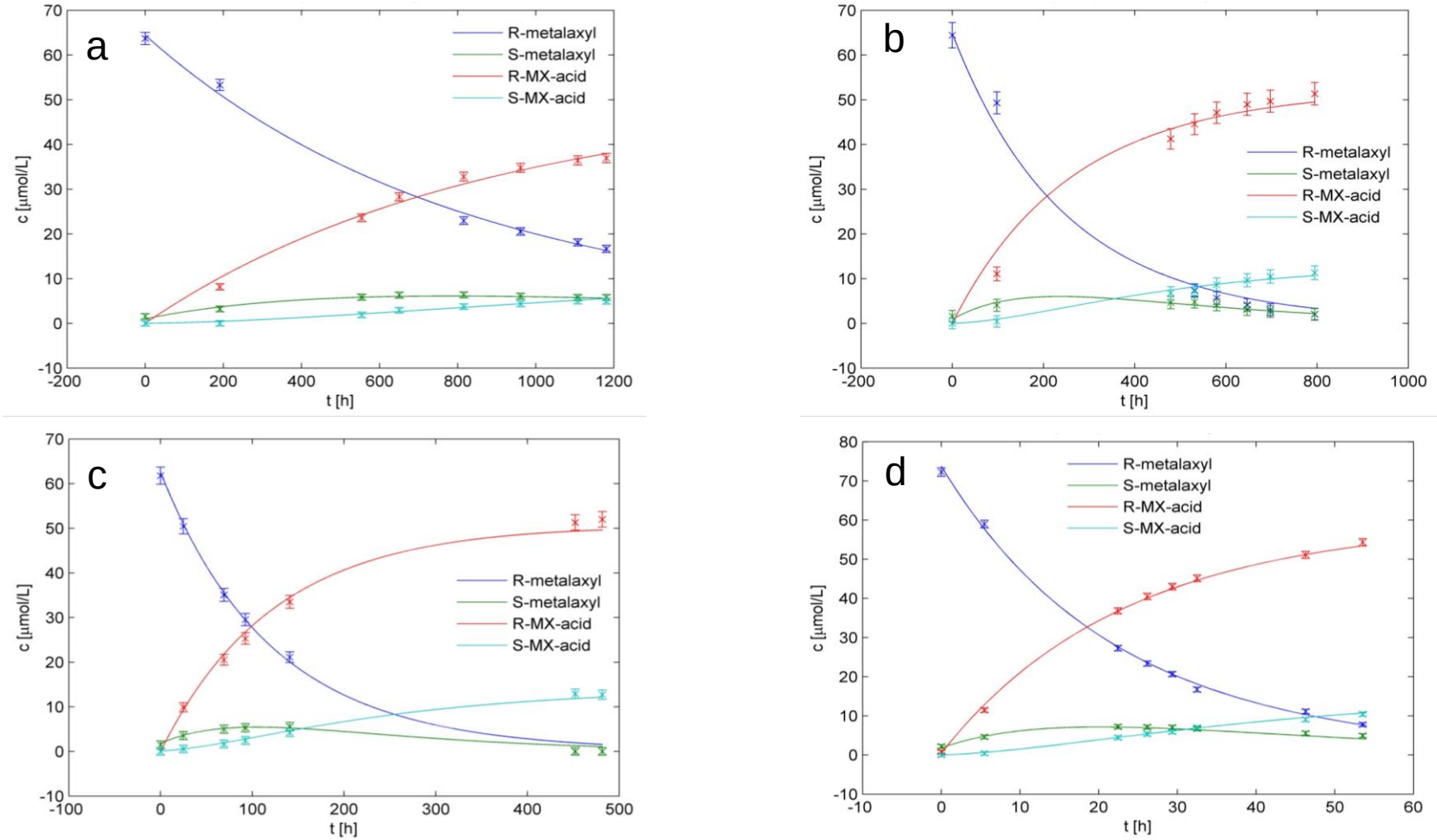

FIGURE 3.15. Reactions of enantiopure *R*-metalaxyl in aqueous solutions at (a) pH 9.53, (b) pH 10.04, (c) pH 10.53, and (d) pH 11.05. Concentrations of reactants and products plotted versus time. Solid lines represent model fits using the rate constants in Table 3.4.

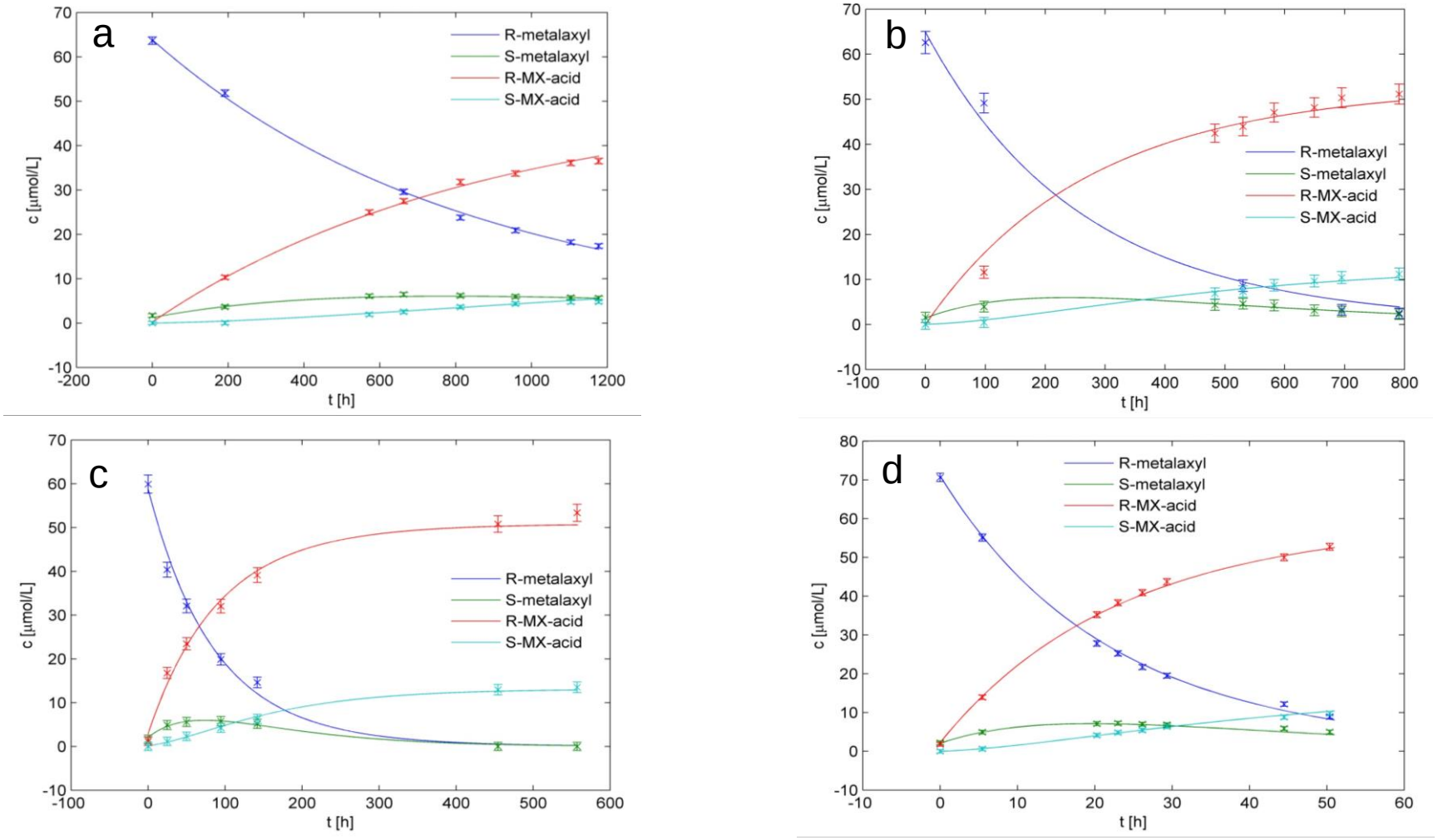

FIGURE 3.16. Reactions of enantiopure *R*-metalaxyl in goethite suspensions at (a) pH 9.54, (b) pH 10.04, (c) pH 10.56, and (d) pH 11.04. Concentrations of reactants and products in dissolved state plotted versus time. Solid lines represent model fits using the rate constants in Table 3.4.

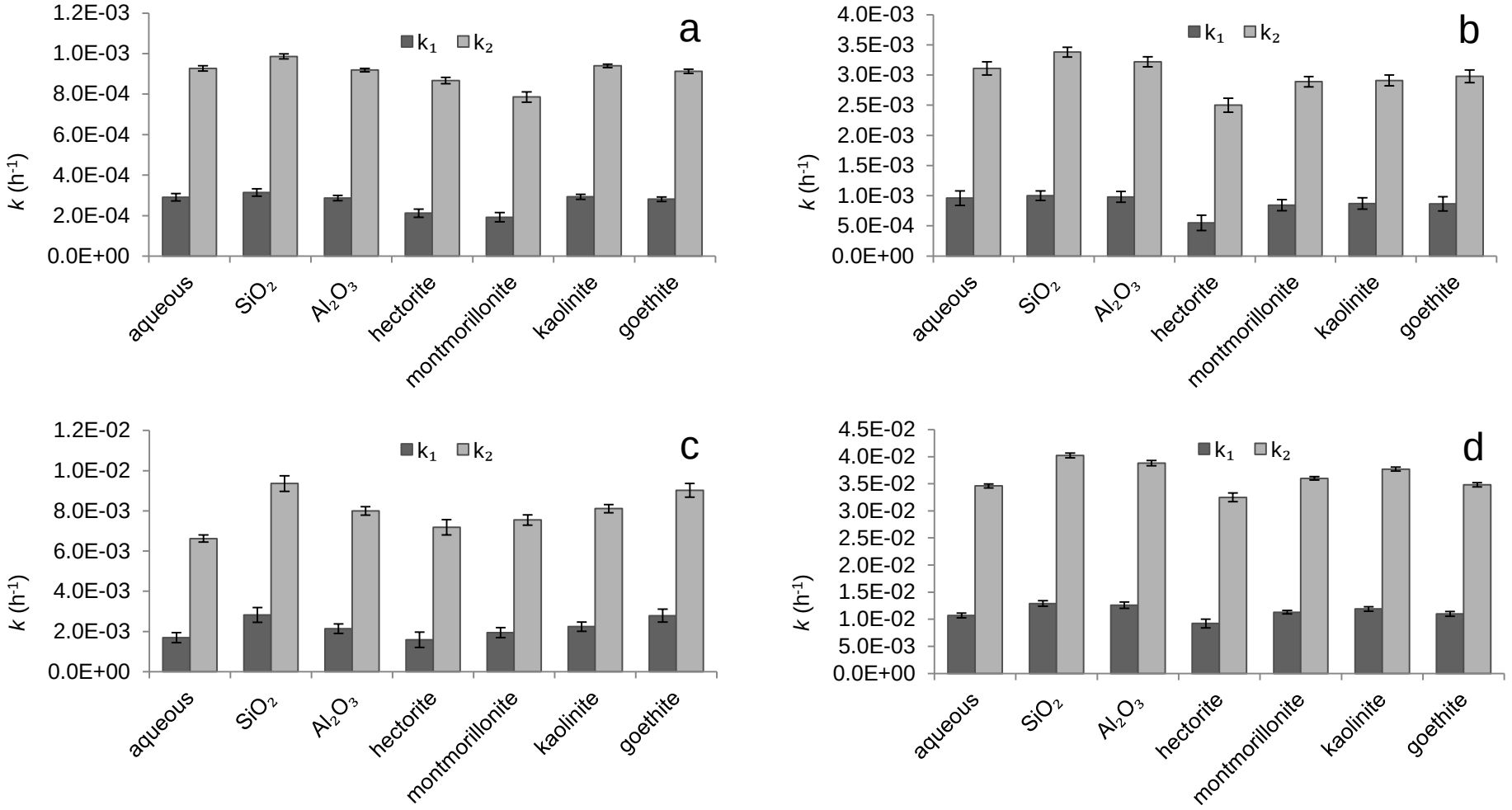

FIGURE 3.17. Rate constants for enantiomerization between *R*- and *S*-metalaxyl (k_1) and hydrolysis of *R*- and *S*-metalaxyl (k_2). Enantiopure *R*-metalaxyl in aqueous solutions and a series of mineral suspensions at (a) pH 9.5, (b) pH 10, (c) pH 10.5, (d) pH 11.

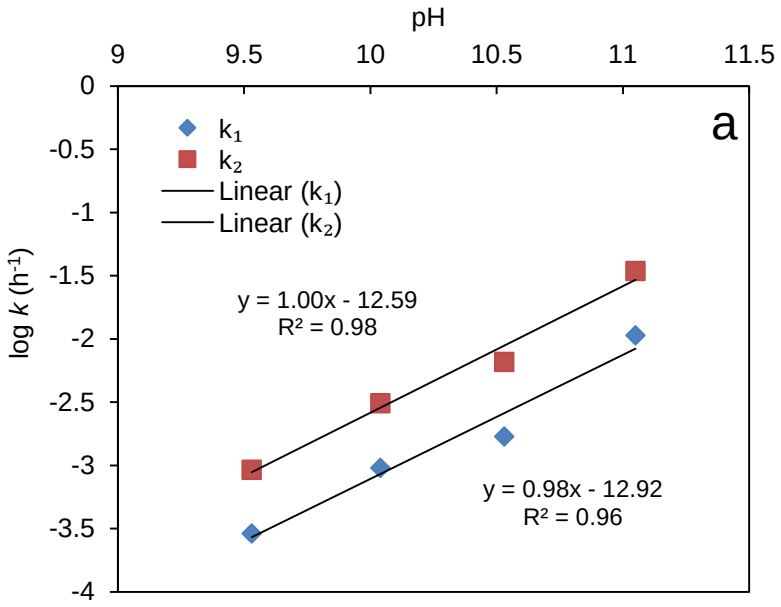
pH
9
9.5
10
10.5
11
11.5
0
-0.5
-1
-1.5
-2
-2.5
-3
-3.5
-4
log k (h-1)
a
k1
k2
Linear (k1)
Linear (k2)
y = 1.00x - 12.59
R² = 0.98
y = 0.98x - 12.92
R² = 0.96

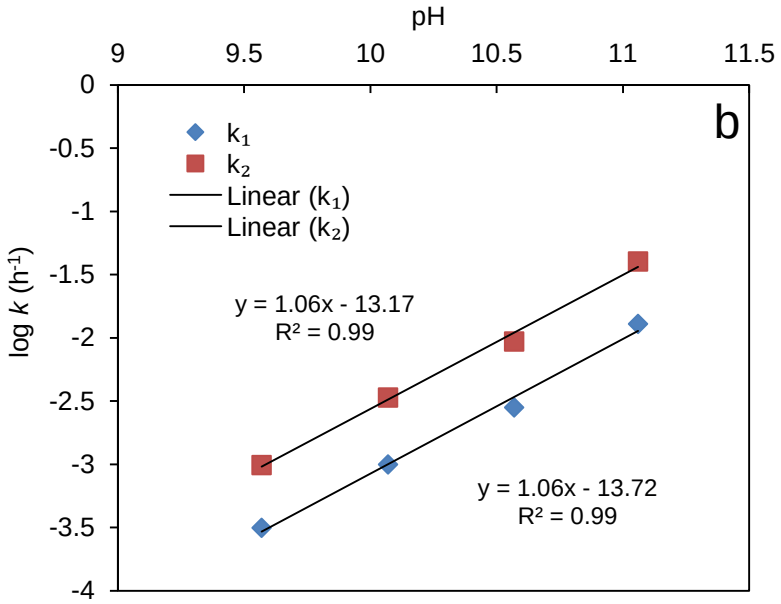
pH
9
9.5
10
10.5
11
11.5
0
-0.5
-1
-1.5
-2
-2.5
-3
-3.5
-4
log k (h-1)
b
k1
k2
Linear (k1)
Linear (k2)
y = 1.06x - 13.17
R² = 0.99
y = 1.06x - 13.72
R² = 0.99

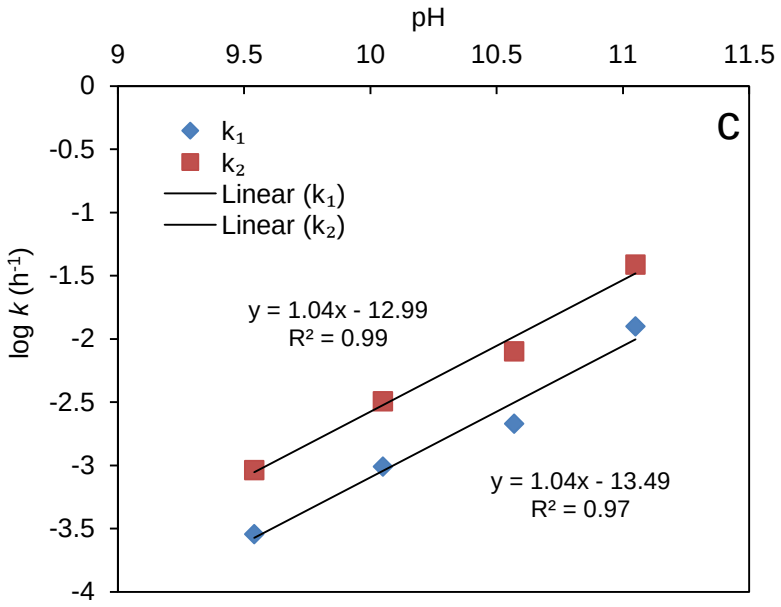
pH
9
9.5
10
10.5
11
11.5
0
-0.5
-1
-1.5
-2
-2.5
-3
-3.5
-4
log k (h-1)
c
k1
k2
Linear (k1)
Linear (k2)
y = 1.04x - 12.99
R² = 0.99
y = 1.04x - 13.49
R² = 0.97

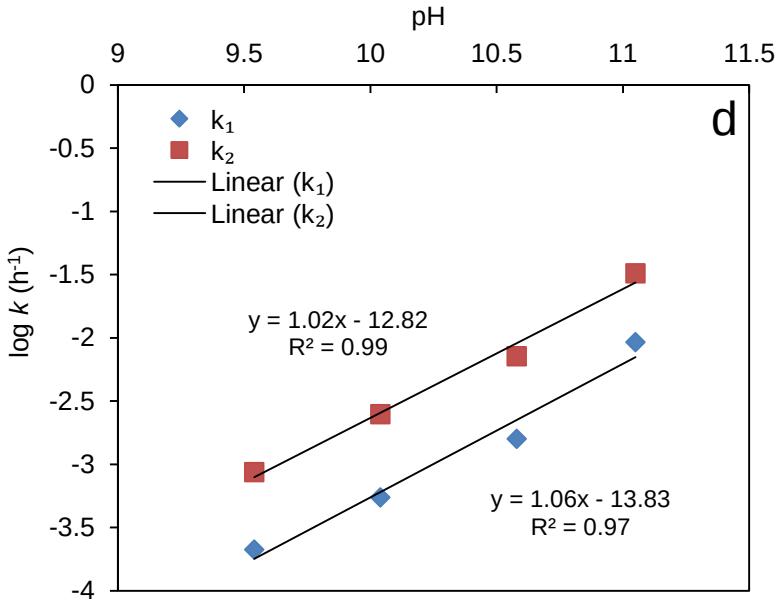
pH
9
9.5
10
10.5
11
11.5
0
-0.5
-1
-1.5
-2
-2.5
-3
-3.5
-4
log k (h-1)
d
k1
k2
Linear (k1)
Linear (k2)
y = 1.02x - 12.82
R² = 0.99
y = 1.06x - 13.83
R² = 0.97

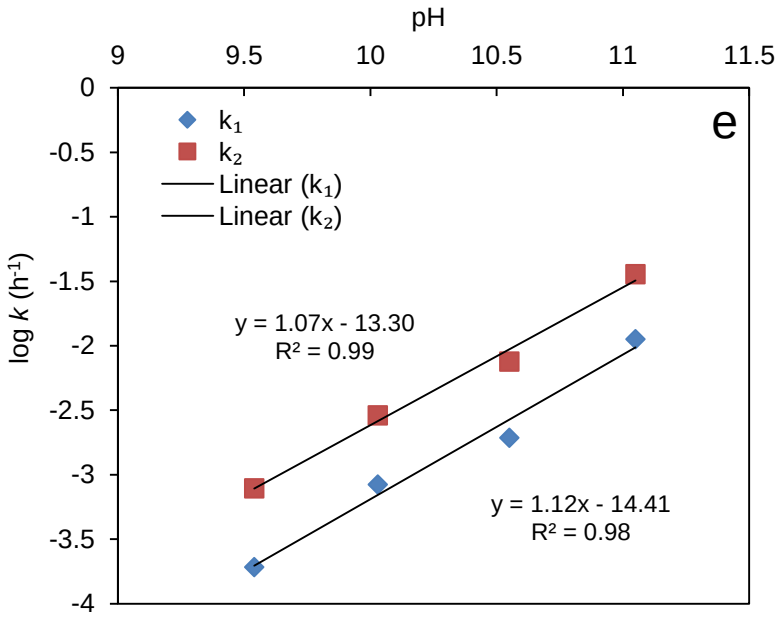
pH
9
9.5
10
10.5
11
11.5
0
-0.5
-1
-1.5
-2
-2.5
-3
-3.5
-4
log k (h-1)
k1
k2
Linear (k1)
Linear (k2)
e
y = 1.07x - 13.30
R² = 0.99
y = 1.12x - 14.41
R² = 0.98

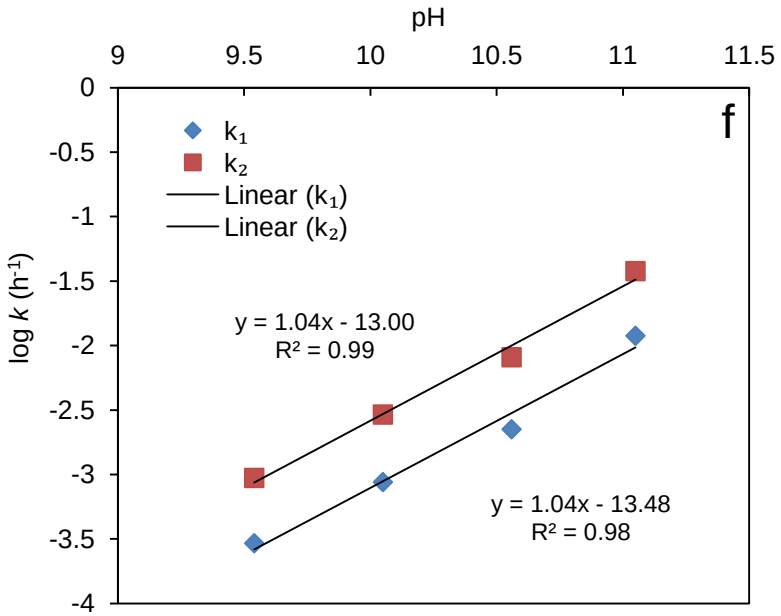
pH
9
9.5
10
10.5
11
11.5
0
-0.5
-1
-1.5
-2
-2.5
-3
-3.5
-4
log k (h-1)
k1
k2
Linear (k1)
Linear (k2)
f
y = 1.04x - 13.00
R² = 0.99
y = 1.04x - 13.48
R² = 0.98

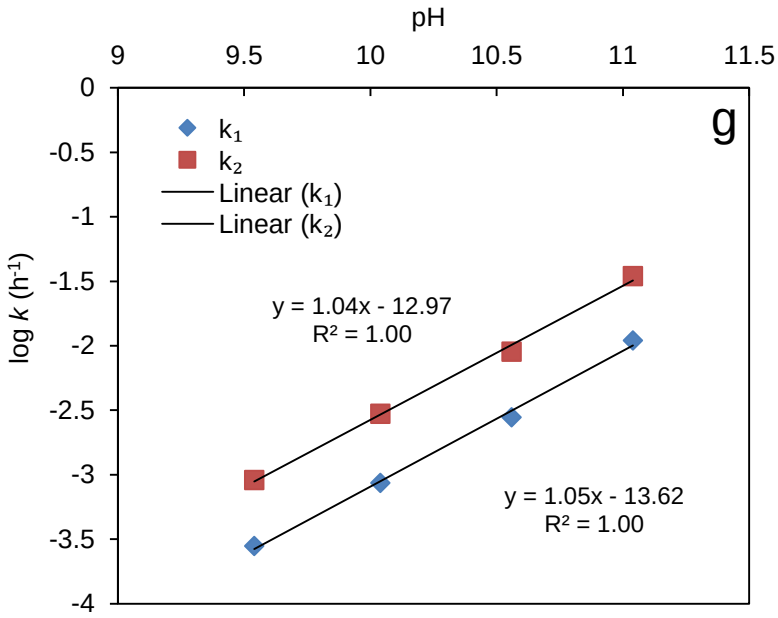

FIGURE 3.18. Effects of pH on enantiomerization of *R*- and *S*-metalaxyl (k_1) and hydrolysis of *R*- and *S*-metalaxyl (k_2) in (a) aqueous solution, (b) SiO_2 suspension, (c) Al_2O_3 suspension, (d) hectorite suspension, (e) Na-montmorillonite suspension, (f) kaolinite suspension, and (g) goethite suspension. The common logarithms of rate constants plotted versus pH.

3.3.5 Chiral Conversion between *R*- and *S*-metalaxyl

Some chiral compounds may be configurationally unstable and undergo enantiomerization or racemization under certain conditions, for example, Müller and Buser (1997) reported two chiral 2-phenoxypropionic acid herbicides (mecoprop and dichlorprop) occurred biologically mediated enantiomerization and degradation in soil. The configurational stability is very important for chiral pesticides, especially for their enantiopure products, since enantiomeriztion may affect the biological activity of pesticides and result in the loss of efficacy. Previous studies have reported both metalaxyl and MX-acid are configurationally stable, and the interconversion between *R*- and *S*-enantiomer is insignificant in soil (Buser, Müller et al. 2002) and sunflowers (Zadra, Marucchini et al. 2002). However, as stated above, chemically mediated enantiomerization between *R*- and *S*-metalaxyl was observed in alkaline aqueous solutions and mineral suspensions. Minerals have insignificant influence on the chiral inversion, while pH has a stronge effect on enantiomerization.

The stereogenic center of metalaxyl is an α-carbon adjacent to the carbonyl group, with one of substituents being hydrogen atom. It was reported that the stereoisomers

of such compounds can undergo acid- or base-catalyzed interconversion via keto-enol tautomerization (Wolf 2008, Mukherjee 2009). For example, in the presence of base, the stereogenic α-carbon is promoted to deprotonate and gives rise to an enolate anion, which is the intermediate during the tautomerization of enol and keto forms. Since the chemically mediated interconversion of *R*- and *S*-metalaxyl was already verified to be base-catalyzed, the reaction scheme can be depicted as Figure 3.19. Although the enantiopure *R*-metalaxyl readily converted to *S*-metalaxyl, the chiral inversion was not observed for their hydrolysis products *R*- and *S*-MX-acids. That may be the result of substituent effects, implying that carboxylic acid group significantly enhanced the configurational stablity compared with the ester group.

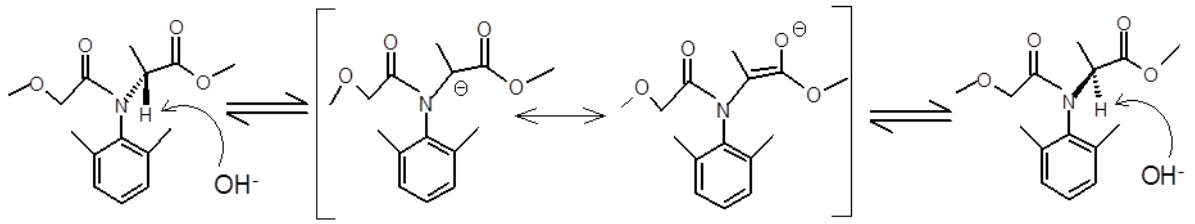

FIGURE 3.19. Possible reaction pathway for base-catalyzed enantiomerization of *R*- and *S*-metalaxyl.

3.4 Conclusions

The hydrolysis of racemic metalaxyl and enantiopure metalaxyl-M in aqueous solutions and mineral suspensions was investigated in this study. The reaction kinetics and enantiomeric ratios of *R*- and *S*-enantiomer of metalaxyl were measured by enantioselective HPLC. For racemic metalaxyl, the hydrolysis of *R*- and *S*-metalaxyl follows pseudo-first-order kinetics and is base-catalyzed reaction over pH 9.5-12 in aqueous solutions and mineral suspensions. Hydrolysis of *R*- and *S*-metalaxyl occurs with retention of configuration. Although *R*-metalaxyl hydrolyzes slightly faster than *S*-metalaxyl, the chemically mediated hydrolysis is basically nonenantioselective. Hydrolysis rate constants in different mineral suspensions approximate to those in aqueous solutions at the same pH, suggesting an insignificant effect of minerals on metalaxyl hydrolysis. In the case of enantiopure metalaxyl-M, a computer model was developed using MATLAB® to describe different reaction processes observed in the experiments. The modeling shows that in mineral suspensions and aqueous solutions over pH 9.5-11 the enantiopure *R*-metalaxyl is configurationally unstable and readily

enantiomerizes to its antipode, *S*-metalaxyl, while the hydrolysis products, *R*- and *S*-MX-acid, are configurationally stable and do not interconvert to each other. The enantiomerization of *R*- and *S*-metalaxyl also follows first-order kinetics and is base-catalyzed reaction. The rate constants of enantiomerization are in the range of 22-32% of the hydrolysis rate constants. In addition, there is not much difference in rate constants of enantiomerization between aqueous solutions and mineral suspensions at the same pH, indicating unimportant influence of minerals on chiral interconversion of metalaxyl enantiomers.

References

Atkins, P. and T. Overton (2010). Shriver and Atkins' Inorganic Chemistry, OUP Oxford.

Bailey, R. A., et al. (2002). 8 - Haloorganics and pesticides. Chemistry of the Environment (Second Edition). R. A. Bailey, H. M. Clark, J. P. Ferris, S. Krause and R. L. Strong. San Diego, Academic Press**:** 223-293.

Bergaya, F. and G. Lagaly (2006). Chapter 1 General Introduction: Clays, Clay Minerals, and Clay Science. Developments in Clay Science. B. K. G. T. Faïza Bergaya and L. Gerhard, Elsevier. **Volume 1:** 1-18.

Brigatti, M. F., et al. (2006). Chapter 2 Structures and Mineralogy of Clay Minerals. Developments in Clay Science. B. K. G. T. Faïza Bergaya and L. Gerhard, Elsevier. **Volume 1:** 19-86.

Büchel, K. H., et al. (2000). Industrial Inorganic Chemistry, 2nd Completely Revised Edition, WILEY-VCH Verlag GmbH.

Buerge, I. J., et al. (2003). "Enantioselective degradation of metalaxyl in soils: Chiral preference changes with soil pH." Environmental Science and Technology **37**(12): 2668-2674.

Buser, H. R., et al. (2002). "Environmental behavior of the chiral acetamide pesticide metalaxyl: Enantioselective degradation and chiral stability in soil." Environmental Science and Technology **36**(2): 221-226.

Carey, F. and R. Sundberg (2007). Stereochemistry, Conformation, and Stereoselectivity. Advanced Organic Chemistry, Springer US**:** 119-251.

Chen, S. and W. Liu (2009). "Enantioselective degradation of metalaxyl in anaerobic activated sewage sludge." Bulletin of Environmental Contamination and Toxicology **82**(3): 327-331.

Churchman, G. J., et al. (2006). Chapter 11.1 Clays and Clay Minerals for Pollution Control. Developments in Clay Science. B. K. G. T. Faïza Bergaya and L. Gerhard, Elsevier. **Volume 1:** 625-675.

Cornejo, J., et al. (2004). Pesticide-clay interactions and formulations. Interface Science and Technology. W. Fernando and S. Kestur Gundappa, Elsevier. **Volume 1:** 247-266.

Cornell, R. M. and U. Schwertmann (2004). Introduction to the Iron Oxides. The Iron Oxides, Wiley-VCH Verlag GmbH & Co. KGaA**:** 1-7.

Cornell, R. M. and U. Schwertmann (2004). Surface Area and Porosity. The Iron Oxides, Wiley-VCH Verlag GmbH & Co. KGaA**:** 95-110.

Cornell, R. M. and U. Schwertmann (2004). Surface Chemistry and Colloidal Stability. The Iron Oxides, Wiley-VCH Verlag GmbH & Co. KGaA**:** 221-252.

Craven, A., et al. (2007). Chapter 2 - Regulatory Aspects of Pesticide Risk Assessment. Pesticide Risk Assessment in Rice Paddies. C. Ettore and K. Dimitrios. Amsterdam, Elsevier**:** 25-253.

EPA. "Types of Pesticides." from http://www.epa.gov/pesticides/about/types.htm.

Estes, T. J. (1988). "Adsorption of low molecular weight halocarbons by montmorillonite." Environmental Science and Technology **22**(4): 377-381.

FAO (2002). International Code of Conduct on the Distribution and Use of Pesticides. Rome, Food and Agriculture Organization of the United Nations.

Fife, T. H. and R. Bembi (1993). "Metal ion promoted hydroxide ion and water catalyzed hydrolysis of amides. Effects of the acyl group and the leaving group." Journal of the American Chemical Society **115**(24): 11358-11363.

Fife, T. H. and V. L. Squillacote (1978). "Metal ion effects on intramolecular nucleophilic carboxyl group participation in amide and ester hydrolysis. Hydrolysis of N-(8-quinolyl)phthalamic acid and 8-quinolyl hydrogen glutarate." Journal of the American Chemical Society **100**(15): 4787-4793.

Fusi, P., et al. (1988). "Interaction of Fluazifop-butyl and Fluazifop with smectites." Applied Clay Science **3**(1): 63-73.

Giles, C. H., et al. (1974). "A general treatment and classification of the solute adsorption isotherm. I. Theoretical." Journal of Colloid and Interface Science **47**(3): 755-765.

Gilliom, R. J., et al. (2006). The Quality of Our Nation's Waters-Pesticides in the Nation's Streams and Ground Water, 1992-2001, U.S. Geological Survey Circular 1291.

Granados, A., et al. (1995). "Kinetic study on the hydrolysis of 1-N-naphthylphthalamic acid (Naptalam)." Journal of Agricultural and Food Chemistry **43**(9): 2493-2496.

Grim, R. E. and N. Güven (1978). Bentonites Geology, Mineralogy, Properties and Uses. Developments in Sedimentology. R. E. Grim and N. Güven, Elsevier. **Volume 24:** 1-256.

Grube, A., et al. (2011). "Pesticides Industry Sales and Usage 2006 and 2007 Market Estimates." from http://www.epa.gov/pesticides/pestsales/07pestsales/market_estimates2007.pdf.

Haderlein, S. B. and R. P. Schwarzenbach (1993). "Adsorption of substituted nitrobenzenes and nitrophenols to mineral surfaces." Environmental Science and Technology **27**(2): 316-326.

Haderlein, S. B., et al. (1996). "Specific adsorption of nitroaromatic explosives and pesticides to clay minerals." Environmental Science and Technology **30**(2): 612-622.

Hawkins, M. D. (1976). "Intramolecular catalysis. Part III.1 hydrolysis of 3′- and 4′-substituted phthalanilic acids [o-(N-Phenylcarbamoyl)benzoic Acids]." Journal of the Chemical Society, Perkin Transactions 2(6): 642-647.

Herwig, U., et al. (2001). "Physicochemical interactions between atrazine and clay minerals." Applied Clay Science **18**(5–6): 211-222.

Huang, C. H. and A. T. Stone (1999). "Hydrolysis of naptalam and structurally related amides: Inhibition by dissolved metal ions and metal (hydr)oxide surfaces." Journal of Agricultural and Food Chemistry **47**(10): 4425-4434.

Huggett, J. M. (2005). CLAY MINERALS. Encyclopedia of Geology. R. C. Selley, L. R. M. Cocks and I. R. Plimer. Oxford, Elsevier**:** 358-365.

Hundal, L. S., et al. (2001). "Sorption of Phenanthrene by Reference Smectites." Environmental Science & Technology **35**(17): 3456-3461.

Hutson, T. R. R. a. D. H. (1999). Phenylamides. Metabolic Pathways of Agrochemicals: Part 2: Insecticides and Fungicides. T. R. Roberts and D. H. Hutson, The Royal Society of Chemistry**:** 1269-1282.

Joo, J. H., et al. (2008). "Imazamethabenz hydrolysis on oxide surfaces at several pH." Journal of Pesticide Science **33**(4): 376-382.

Lagaly, G., et al. (2006). Chapter 7.3 Clay Mineral Organic Interactions. Developments in Clay Science. B. K. G. T. Faïza Bergaya and L. Gerhard, Elsevier. **Volume 1:** 309-377.

Mader, B. T., et al. (1997). "Sorption of nonionic, hydrophobic organic chemicals to mineral surfaces." Environmental Science and Technology **31**(4): 1079-1086.

McBride, M. B. (1994). Environmental Chemistry of Soils, Oxford University Press, Incorporated.

Miller, G. T. (2004). Sustaining the Earth, 6th edition, Thompson Learning, Inc. Pacific Grove, California.

Monkiedje, A., et al. (2003). "Degradation of racemic and enantiopure metalaxyl in tropical and temperate soils." Environmental Science and Technology **37**(4): 707-712.

Monkiedje, A., et al. (2007). "Elimination of racemic and enantioenriched metalaxyl based fungicides under tropical conditions in the field." Chemosphere **69**(4): 655-663.

Mukherjee, P. S. (2009). "Chiral interconversion monitoring of a drug candidate by supercritical fluid chromatography (SFC)." Journal of Pharmaceutical and Biomedical Analysis **50**(3): 349-355.

Müller, M. D. and H. R. Buser (1995). "Environmental behavior of acetamide pesticide stereoisomers. 2. Stereo- and enantioselective degradation in sewage sludge and soil." Environmental Science and Technology **29**(8): 2031-2037.

Müller, M. D. and H. R. Buser (1997). "Conversion reactions of various phenoxyalkanoic acid herbicides in soil. 1. Enantiomerization and enantioselective degradation of the chiral 2-phenoxypropionic acid herbicides." Environmental Science and Technology **31**(7): 1953-1959.

Müller, U. and U. Gisi (2008). Newest Aspects of Nucleic Acid Synthesis Inhibitors — Metalaxyl-M. Modern Crop Protection Compounds, Wiley-VCH Verlag GmbH**:** 739-746.

Murray, H. H. (2006). Chapter 2 Structure and Composition of the Clay Minerals and their Physical and Chemical Properties. Developments in Clay Science. H. M. Haydn, Elsevier. **Volume 2:** 7-31.

Nasser, A., et al. (1997). "Adsorption of alachlor by montmorillonites." Journal of Thermal Analysis **50**(1-2): 257-268.

Patnaik, P. (2003). Handbook of Inorganic Chemicals, McGraw-Hill.

Plastourgou, M. and M. R. Hoffmann (1984). "Transformation and fate of organic esters in layered-flow systems: The role of trace metal catalysis." Environmental Science and Technology **18**(10): 756-764.

Pleština, R. (2003). PESTICIDES AND HERBICIDES | Types of Pesticide. Encyclopedia of Food Sciences and Nutrition (Second Edition). C. Editor-in-Chief: Benjamin. Oxford, Academic Press**:** 4473-4483.

Przystas, T. J. and T. H. Fife (1990). "The metal-ion-promoted water- and hydroxide-ion-catalysed hydrolysis of amides." Journal of the Chemical Society, Perkin Transactions 2(3): 393-399.

Pusino, A., et al. (1996). "Montmorillonite Surface-Catalyzed Hydrolysis of Fenoxaprop-ethyl." Journal of Agricultural and Food Chemistry **44**(4): 1150-1154.

Reddy, K. V., et al. (1991). "Divalent metal ion catalyzed hydrolysis of picolinanilides." Inorganic Chemistry **30**(18): 3520-3525.

Rosenfeld, P. E. and L. G. H. Feng (2011). 11 - Pesticides. Risks of Hazardous Wastes. Boston, William Andrew Publishing**:** 127-154.

Sayre, L. M., et al. (1992). "Metal ion catalysis of amide hydrolysis. Very large rate enhancements by copper(II) in the hydrolysis of simple ligand-functionalized tertiary amides." Inorganic Chemistry **31**(6): 935-937.

Scheinost, A. C. (2005). METAL OXIDES. Encyclopedia of Soils in the Environment. H. Editor-in-Chief: Daniel. Oxford, Elsevier**:** 428-438.

Schlautman, M. A. and J. J. Morgan (1994). "Sorption of perylene on a nonporous inorganic silica surface: Effects of aqueous chemistry on sorption rates." Environmental Science and Technology **28**(12): 2184-2190.

Schulze, D. G. (2005). CLAY MINERALS. Encyclopedia of Soils in the Environment. H. Editor-in-Chief: Daniel. Oxford, Elsevier**:** 246-254.

Schwarzenbach, R. P., et al. (2005). Chemical Transformations I: Hydrolysis and Reactions Involving Other Nucleophilic Species. Environmental Organic Chemistry, John Wiley & Sons, Inc.**:** 489-554.

Schwarzenbach, R. P., et al. (2005). Sorption III: Sorption Processes Involving Inorganic Surfaces. Environmental Organic Chemistry, John Wiley & Sons, Inc.**:** 387-458.

Schwarzenbach, R. P. and J. Westall (1981). "Transport of nonpolar organic compounds from surface water to groundwater. Laboratory sorption studies." Environmental Science and Technology **15**(11): 1360-1367.

Shin, J. Y. and M. A. Cheney (2004). "Abiotic transformation of atrazine in aqueous suspension of four synthetic manganese oxides." Colloids and Surfaces A: Physicochemical and Engineering Aspects **242**(1–3): 85-92.

Smolen, J. M. and A. T. Stone (1997). "Divalent metal ion-catalyzed hydrolysis of phosphorothionate ester pesticides and their corresponding oxonates." Environmental Science and Technology **31**(6): 1664-1673.

Smolen, J. M. and A. T. Stone (1998). "Metal (hydr)oxide surface-catalyzed hydrolysis of chlorpyrifos-methyl, chlorpyrifos-methyl oxon, and paraoxon." Soil Science Society of America Journal **62**(3): 636-643.

Sparks, D. L. (2003). 2 - Inorganic Soil Components. Environmental Soil Chemistry (Second Edition). Burlington, Academic Press**:** 43-73.

Tang, W. and L. M. Sayre (1993). "Divalent metal ion catalyzed hydrolysis of N-methyl-4′-nitro-6-carboxypicolinanilide. pH-Rate profile transitions and buffer inhibition." Inorganic Chemistry **32**(25): 5785-5791.

Theng, B. K. G. (2012). Chapter 1 - The Clay Minerals. Developments in Clay Science. B. K. G. Theng, Elsevier. **Volume 4:** 3-45.

Torrents, A. and A. T. Stone (1991). "Hydrolysis of phenyl picolinate at the mineral/water interface." Environmental Science and Technology **25**(1): 143-149.

Torrents, A. and A. T. Stone (1993). "Catalysis of picolinate ester hydrolysis at the oxide/water interface: inhibition by adsorbed natural organic matter." Environmental Science and Technology **27**(12): 2381-2386.

Torrents, A. and A. T. Stone (1993). "Catalysis of picolinate ester hydrolysis at the oxide/water interface: Inhibition by coadsorbed species." Environmental Science and Technology **27**(6): 1060-1067.

Torrents, A. and A. T. Stone (1994). "Oxide surface-catalyzed hydrolysis of carboxylate esters and phosphorothioate esters." Soil Science Society of America Journal **58**(3): 738-745.

United States. Environmental Protection Agency. Prevention, P. and T. Substances (1994). Reregistration Eligibility Decision (RED): Metalaxyl, U.S. Environmental Protection Agency, Prevention, Pesticides and Toxic Substances.

Vallero, D. A. (2004). Chapter 7 - Chemical Reactions in the Environment. Environmental Contaminants. Burlington, Academic Press**:** 333-388.

Wei, J., et al. (2001). "Influence of Clay Minerals on the Hydrolysis of Carbamate Pesticides." Environmental Science & Technology **35**(11): 2226-2232.

Weidenhaupt, A., et al. (1997). "Sorption of Organotin Biocides to Mineral Surfaces." Environmental Science & Technology **31**(9): 2603-2609.

Wolf, C. (2008). Chapter 3 Racemization, Enantiomerization and Diastereomerization. Dynamic Stereochemistry of Chiral Compounds: Principles and Applications, The Royal Society of Chemistry**:** 29-135.

Zadra, C., et al. (2002). "Behavior of metalaxyl and its pure R-Enantiomer in sunflower plants (Helianthus annus)." Journal of Agricultural and Food Chemistry **50**(19): 5373-5377.

4. Conclusions and Outlook

4.1 Conclusions

The overall goal of this thesis is to elucidate the influence of minerals on surface mediated hydrolysis. A series of minerals were selected, including SiO_2, Al_2O_3, goethite, kaolinite, hectorite and Na-rich montmorillonite. Batch experiments on the hydrolysis of pesticides or pesticide-like amides were performed at the mineral-water interface.

With respect to the amides, the major objective is to investigate if the hydrolysis of amides with adjacent functional groups can be promoted or inhibited by mineral surfaces. First, for 4'- and 2'-NPTA, hydrolysis is intramolecular catalyzed reaction in acidic solutions (pH < 4.3). A side reaction occurred besides hydrolysis, and a by-product *N*-phenylphthalimide may be formed due to the nucleophilic attack of the amide nitrogen on the carboxylic carbonyl carbon followed by water elimination. Furthermore, the observed rate constants of 4'- and 2'-NPTA in acidic mineral suspensions decrease with increasing pH and are of the same order of magnitude as those in the corresponding aqueous solutions. Consequently, the investigated minerals have little influence on the intramolecular catalyzed hydrolysis of 4'- and 2'-NPTA. In addition, no measurable adsorption on mineral surfaces was observed for 4'- and 2'-NPTA as well as the products 4- and 2-nitroaniline. Second, for N-Me-PCA, hydrolysis in aqueous solutions and mineral suspensions is general base-catalyzed reaction over pH 9.5-11. Mineral surfaces have no significant effect on N-Me-PCA hydrolysis, the observed rate constants at certain pH are only slightly lower in hectorite and Na-montmorillonite suspensions compared with aqueous solutions and the other mineral suspensions. Moreover, adsorption of N-Me-PCA occurred on hectorite and Na-montmorillonite to different extent depending on suspension pH.

Regarding the chiral pesticides, the main objective is to study the stereo-selectivity of hydrolysis as well as the influence of minerals on hydrolysis. Batch experiments with racemic metalaxyl and enantiopure metalaxyl-M were conducted in aqueous solutions and mineral suspensions. The reaction kinetics and enantiomeric ratios of *R*- and *S*-enantiomer of metalaxyl were measured by enantioselective HPLC. For racemic metalaxyl, the hydrolysis of *R*- and *S*-metalaxyl follows pseudo-first-order kinetics and is base-catalyzed reaction over pH 9.5-12 in aqueous solutions and mineral suspensions. Hydrolysis of *R*- and *S*-metalaxyl occurs with retention of configuration.

Although *R*-metalaxyl hydrolyzes slightly faster than *S*-metalaxyl, the chemically mediated hydrolysis is basically nonenantioselective. Hydrolysis rate constants in different mineral suspensions approximate to those in aqueous solutions at the same pH, suggesting an insignificant effect of minerals on metalaxyl hydrolysis. In the case of enantiopure metalaxyl-M, a computer model was developed using MATLAB® to describe different reaction processes observed in the experiments. The modeling shows that in mineral suspensions and aqueous solutions over pH 9.5-11 the enantiopure *R*-metalaxyl is configurationally unstable and readily enantiomerizes to its antipode,*S*-metalaxyl, while the hydrolysis products, *R*- and *S*-MX-acid, are configurationally stable and do not interconvert to each other. The enantiomerization of *R*- and *S*-metalaxyl also follows first-order kinetics and is base-catalyzed reaction. The rate constants of enantiomerization are in the range of 22-32% of the hydrolysis rate constants. In addition, there is not much difference in rate constants of enantiomerization between aqueous solutions and mineral suspensions at the same pH, indicating unimportant influence of minerals on chiral interconversion of metalaxyl enantiomers.

In summary, besides sorption on two types of clay minerals, no significant influence of mineral surfaces were found on the hydrolysis of the examined amides and phenylamide pesticides in this study. Hence, even though metal oxides and/or clay minerals played an important role in the hydrolysis of some agrochemicals (Torrents and Stone 1994, Wei, Furrer et al. 2001), the surface mediated reactions should be individually evaluated for each type of pesticide and mineral.

4.2 Outlook

The surface catalyzed or inhibited transformation of pesticides was mainly investigated and observed with pure mineral. However, in natural soils, there will be a variety of inorganic and organic species (e.g. natural organic matter) that may compete with organic pollutants for the reactive surface sites. For example, FeOOH- and TiO_2-catalyzed hydrolysis of phenyl picolinate and methyl picolinate were found to be inhibited by adsorbed inorganic ions (calcium and phosphate) and organic acids (benzoate, salicylate and picolinate) due to the occupation of surface sites (Torrents and Stone 1993). Furthermore, TiO_2-catalyzed hydrolysis of methyl picolinate was also inhibited by adsorbed natural organic matter (NOM) (Torrents and Stone 1993). Moreover, humic acid-coated goethite was reported to reduce the sorption capacity of

goethite for phenoxyacetic acid pesticide MCPA since the organic coating decreased the number of surface sites accessible to pesticide (Iglesias, López et al. 2010). In addition, such association may also facilitate the interaction of pesticide with mineral. For instance, ferrihydrite coatings on Ca-saturated montmorillonite increased sorption of herbicides atrazine and simazine on the clay, and the humic acid association with Ca-montmorillonite also increased the sorption of both herbicides (Celis, Cornejo et al. 1998).

Moreover, many organic contaminants bear redox sensitive functional groups such as nitro-, amino-, thio-, azo, nitrile, quinone or sulfoxy. It was shown that such compounds may undergo abiotic transformation through interactions with redox sensitive metals in natural porous media. Through sorption to and/or precipitation at iron oxides the reactivity of surface-bound Fe(II) considerably increased compared with freely dissolved form, and the adsorbed Fe(II) was found to significantly promote the reaction of many reducible compounds, such as halogenated methanes (Amonette, Workman et al. 2000, Pecher, Haderlein et al. 2002) and nitroaromatic compounds (Klausen, Trober et al. 1995, Elsner, Schwarzenbach et al. 2004). Furthermore, reactive ferrous iron species at clay mineral surfaces can be structural Fe(II) or Fe(II) bound by surface complexation, while Fe(II) bound by ion exchange at basal siloxane surfaces was found to be unreactive for acetyl nitrobenzenes (Hofstetter, Schwarzenbach et al. 2003). In addition, surface complexes or surface coatings of ferrous iron at inert minerals such as Al_2O_3 or SiO_2 may also serve as redox reactive sites at the solid matrix of soils for organic pollutants. For example, the reduction of oxime carbamate pesticides was catalyzed by adsorbed Fe(II) on different minerals including SiO_2, Al_2O_3, TiO_2, hematite, kaolinite and goethite (Strathmann and Stone 2003).

Hence, the interaction of pesticides with soil mineral fraction can be significantly influenced by other soil components, e.g., the association of ferrous iron species and other reducing agents with mineral surfaces may play an important role in redox reactions of agrochemicals. Assessing surface-mediated reaction of pesticides at different mineral surfaces with or without other soil components will improve the understanding of organic contaminants transformation in natural environments.

References

Amonette, J. E., et al. (2000). "Dechlorination of carbon tetrachloride by Fe(II) associated with goethite." Environmental Science and Technology **34**(21): 4606-4613.

Celis, R., et al. (1998). "Sorption of atrazine and simazine by model associations of soil colloids." Soil Science Society of America Journal **62**(1): 165-171.

Elsner, M., et al. (2004). "Reactivity of Fe(II)-Bearing Minerals toward Reductive Transformation of Organic Contaminants." Environmental Science and Technology **38**(3): 799-807.

Hofstetter, T. B., et al. (2003). "Reactivity of Fe(II) species associated with clay minerals." Environmental Science and Technology **37**(3): 519-528.

Iglesias, A., et al. (2010). "Adsorption of MCPA on goethite and humic acid-coated goethite." Chemosphere **78**(11): 1403-1408.

Klausen, J., et al. (1995). "Reduction of substituted nitrobenzenes by Fe(II) in aqueous mineral suspensions." Environmental Science and Technology **29**(9): 2396-2404.

Pecher, K., et al. (2002). "Reduction of polyhalogenated methanes by surface-bound Fe(II) in aqueous suspensions of iron oxides." Environmental Science and Technology **36**(8): 1734-1741.

Strathmann, T. J. and A. T. Stone (2003). "Mineral surface catalysis of reactions between FeII and oxime carbamate pesticides." Geochimica et Cosmochimica Acta **67**(15): 2775-2791.

Torrents, A. and A. T. Stone (1993). "Catalysis of picolinate ester hydrolysis at the oxide/water interface: inhibition by adsorbed natural organic matter." Environmental Science and Technology **27**(12): 2381-2386.

Torrents, A. and A. T. Stone (1993). "Catalysis of picolinate ester hydrolysis at the oxide/water interface: Inhibition by coadsorbed species." Environmental Science and Technology **27**(6): 1060-1067.

Torrents, A. and A. T. Stone (1994). "Oxide surface-catalyzed hydrolysis of carboxylate esters and phosphorothioate esters." Soil Science Society of America Journal **58**(3): 738-745.

Wei, J., et al. (2001). "Influence of Clay Minerals on the Hydrolysis of Carbamate Pesticides." Environmental Science & Technology **35**(11): 2226-2232.